UNIVERSITY OF
LINCOLN

Effects of non-invasive electrical brain stimulation and modulated neural mechanisms: a combined behavioural, computational and electrophysiological approach

F Ghin

Doctor of Philosophy

2019

UNIVERSITY OF
LINCOLN

Effects of non-invasive electrical brain stimulation and modulated neural mechanisms: a combined behavioural, computational and electrophysiological approach

Filippo Ghin

A thesis submitted in partial fulfilment of the requirements of the University of Lincoln for the degree of Doctor of Philosophy

School of Psychology

College of Social Science

September 2019

Abstract

Transcranial electrical stimulation (tES) is a non-invasive neuromodulatory techniques used to induce transient alterations of the normal cortical activity and to study the related behavioural and physiological outcomes. Transcranial direct current stimulation (tDCS) delivers low intensity direct electrical current and its effects are influenced by the polarity used (anodal or cathodal). High-frequency transcranial random noise stimulation (hf-tRNS) is a tES regime that delivers alternating current at random intensity and random frequencies and its underlying mechanisms are still unclear. The aim of this research is to investigate the effects and mechanisms of action of different tES regimes on the visual cortex probed using well-known paradigms of visual motion perception.

In a first series of experiments (Chapter 2) we explored the effects of anodal and cathodal tDCS and hf-tRNS over the left hMT^+ on a global motion direction discrimination task. The results showed that hf-tRNS reduced the motion coherence threshold, whereas anodal and cathodal tDCS did not have any effect. To further investigate hf-tRNS effects on global motion processing, we measured observers' performance in estimating local motion directions and the number of estimates that can be polled together (Chapter 3). The results showed that hf-tRNS only increased the integration of local motion direction cues, suggesting an effect on the pooling of directional signals rather than an alteration of the selectivity for specific directions.

To further explore hf-tRNS mechanisms of action on the visual cortex, we investigated whether its modulatory effects could be explained within the stochastic resonance framework, whereby the addition of an optimal level of stimulation-induced noise could increase the discrimination of weak stimuli (Chapter 4). Hf-tRNS was administered at five different intensities while observers performed a motion direction discrimination task. Significant improvements in performance for hf-tRNS at 1.5 mA were found, whereas further increments of the intensity (2.25 mA) significantly impaired the performance. These results indicate that hf-tRNS modulates motion direction discrimination in a way that is compatible with the stochastic resonance phenomenon. In Chapter 5, we explored if hf-tRNS is able to induce behavioural and electrophysiological aftereffects. Before and after 20 minutes of bilateral hf-tRNS, EEG activity was recorded during a period of resting state and during the execution of a motion direction discrimination task. The results showed that offline hf-tRNS did not affect post-stimulation direction discrimination accuracy and VEPs measure of amplitude and latency elicited by the moving stimulus. Moreover, mean power spectra density for alpha

and beta oscillations at rest increased between pre and post-stimulation, but not specifically for the hf-tRNS. Overall, these results suggest that offline hf-tRNS has limited behavioural and electrophysiological long term effects on the visual cortex.

In conclusion, the results presented here show that online hf-tRNS is able to improve motion direction discrimination performance in agreement with the stochastic resonance framework when delivered over hMT^{+}. We suggested that this could be the results of an increased probability of weak neurons coding for the signal direction to generate an action potential consequently increasing the overall signal-to-noise ratio.

Table of Contents

List of Tables

List of Figures

Acknowledgments

I would like to thank my supervisor Andrea Pavan for all the support and guidance throughout all these years that has never fall short even in difficult moments.

Thanks to Prof George Mather, Dr Adriano Contillo and Dr Louise O'Hare for their useful comments and insights.

Most importantly, thanks to my family that gave me the possibility to study all these years and without which I would have never achieved this goal. Thanks to Charlotte that has been on my side for the last two years and supported me in everyday struggle and influenced my life with positivity and happiness.

Finally, thanks to my friends and colleagues for all the good laughs, jokes and shenanigans.

List of contributions

The author Filippo Ghin is principal investigator in all the work presented in this thesis. Experimental chapters are presented in style of journal articles each at various stage of publication. Contributions include experimental design (Pavan Andrea and Adriano Contillo), data analysis (Pavan Andrea, Adriano Contillo and Louise O'Hare), data interpretation (Pavan Andrea and Adriano Contillo) and manuscript corrections (Pavan Andrea, Adriano Contillo, George Mather and Louise O'Hare). Additional contributions include data collection and participant recruitment (Rita Donato, Chiara Milesi and Emily Hird).

Chapter 1: General Introduction

The ability to visually perceive the world that surround us is probably one of the most important functions of our sensory systems. The capability to elaborate static and dynamic visual images is crucial to execute from simple to extremely complex tasks and to direct our decisions in everyday life. Thus, it is not surprising that the visual system and the cerebral structures involved in the formation of visual stimuli has received an extensive psychological, physiological and biological investigation by the scientific community. Early studies on the animal visual cortex (Hubel & Wiesel, 1968a, 1968b) dramatically increased our understanding on the development and functioning of the visual system, not only of those animals being subject of the examination, but also of the human visual cortex itself. Among the many visual functions, perception of motion is probably one of the most important. The ability to perceive dynamic images determines our interaction with the world and allows to elaborate spatial and time inferences about moving objects that surround us.

An extensive approach to study the visual cortex and its mechanisms is to produce a transient alteration of normal neural activity in observers prior or while performing a visual task. To this purpose, in the last decades, researchers developed a number of non-invasive brain stimulation techniques (NIBS; Miniussi, Harris, & Ruzzoli, 2013). The basic assumption in using such techniques is that by temporarily manipulating the ongoing neural activity, one can derive hypothesis of the altered state of the system comparing the manipulated outcome with respect to a control condition. Furthermore, the result of this comparison allows to make assumption on what are the mechanisms for which the stimulation technique operates.

Transcranial electric stimulation (tES) is one of most used NIBS. The considerable use of this technique arise from several and important advantages. For example, one advantage is the relative simple usability that allow its applications by researchers from many research areas. Moreover, tES has very limited risk of side effects for the participants being stimulated. Another advantage is the “contained” cost that permits many laboratories to purchase this equipment for their research. All these factors promoted a fast application of this technique in combination of rehabilitative trainings with the ultimate goal to improve impaired sensory and cognitive abilities due to pre-existing conditions. Furthermore, tES in combination with rehabilitative trainings might have the potential to be established as a promising approach in many visual deficits and

impairments connected to visual abilities. For example a recently introduced tES protocol, the transcranial random noise stimulation (tRNS), has demonstrated to be effective in improving contrast sensitivity and visual acuity in amblyopic observers (Campana, Camilleri, Pavan, Veronese, & Giudice, 2014; Moret, Camilleri, Pavan, & Lo Giudice, 2018). Moreover, recent evidences showed that when compared to other stimulation protocols like transcranial direct current stimulation (tDCS), tRNS resulted in better performance modulation in visual perception tasks (Fertonani, Pirulli, & Miniussi, 2011; Pirulli, Fertonani, & Miniussi, 2013; Pobric et al., 2018).

So far application of tES protocols on the visual cortex has particularly focused on exploring stimulation effects of visual static stimuli (Antal & Paulus, 2008; Antal, Nitsche, & Paulus, 2006). More interestingly, investigation of tES effects on visual motion perception has received relative less attention and fewer studies attempted to explain the underlying mechanism of different stimulation protocols (Battaglini, Noventa, & Casco, 2017). As aforementioned, visual motion perception is a crucial function of the visual system, thus the lack of evidences should be addressed. The application of tES in combination with visual motion paradigms might increase our understanding on motion perception, but also about the underlying stimulation mechanisms in the visual cortex.

Considering these premises, the general intent of this Thesis is to extend our knowledge on the modulatory effects of non-invasive electrical brain stimulation techniques on the visual cortex. In order to do this, we used established visual motion paradigms to probe and investigate the effects of non-invasive electrical brain stimulation on the visual cortex. Moreover, since its promising results in the recent literature, this Thesis also aims to assess the extent of tRNS behavioural effects in comparison to other stimulation protocols, to investigate its possible mechanisms of action on the visual cortex.

This chapter gives a general introduction about non-invasive transcranial electrical stimulation techniques and visual motion perception. For this purpose, the first part of the chapter is dedicated to a brief review of the most used transcranial electrical brain stimulation protocols such as transcranial direct current stimulation (tDCS) and transcranial alternating current stimulation (tACS) and transcranial random noise stimulation (tRNS). In the second part of this Chapter, a brief summary is also dedicated to how the visual system processes visual motion information, which cortical areas are involved in this perceptual function and previous studies assessing the effects of tES on visual motion perception. In the last part of the chapter, aims and the main research questions addressed in this Thesis are reported.

1.1 Transcranial Electrical Stimulation (tES)

Transcranial electric stimulation (tES) belongs, together with transcranial magnetic stimulation (TMS) and several other methodologies, to the so-called non-invasive brain stimulation (NIBS) techniques. tES is a battery powered device which is able to deliver a low intensity electrical current through one or more electrodes placed over the scalp for several minutes (Figure 1.1). The intensity of the current stimulation is measured in Ampere (A), which represents current that flows with electric charge of one Coulomb (C) per second (s) $A = \frac{C}{s}$. Nowadays, different electrical stimulation protocols are used. The most known protocols are the transcranial direct current stimulation (tDCS), and transcranial alternating current stimulation (tACS). Relatively new protocols, such as the random noise stimulation (tRNS) have been investigated just in the last decade. The details of the proposed mechanisms of action and effects of these stimulation protocols will be the focus of the following paragraphs (paragraphs 1.1.1 to 1.1.3). Overall, application of electrical current on the brain and its behavioural, physiological and clinical outcomes have been extensively studied in the last twenty years (Nitsche et al., 2008). However, such technique has its roots way back in the human history. Sarimento, San-Juan, and Prasath (2016) reported the history of transcranial electric stimulation throughout the centuries. Early evidence of use of electrical current for a clinical purpose arrives from ancient Greece. Aristoteles and Plato described how torpedo fish, which is able to generate electrical discharges, was used for curatives purposes. During the Roman Empire, positioning a torpedo fish on the scalp was described as practice in order to alleviate headache. However, with the progress of civilization and advance of technologies, electric current started to be applied with mechanical devices (for a review see Sarmiento et al., 2016). A substantial step forward into brain stimulation was made in the 18th century by Luigi Galvani and his nephew Giovanni Aldini. Galvani's invention, the galvanic battery, able to deliver direct electrical current was used by Aldini to treat a man affected from depression. According to the records, after several weeks of application the patient benefited from the experimental treatment (Parent, 2004). Late in the 18th century, the treatment of patients using electrical stimulation became prominent in German psychiatry. However, even if at that time electrical brain stimulation was going through a period of popularity, discontinuity in clinical evidence and in the procedures applied, led inevitably to a disuse of this technique around the 1930 (Steinberg, 2013). In the 20th century, interest around brain stimulation moved back and forth until the last decade when new technologies and advancements in experimental

procedures (Merton & Morton, 1980) produced a new wave of interest. Brain stimulation was not limited to clinical applications, but was also used as a tool to study the brain and its functions. Nowadays, transcranial electrical stimulation is established and recognized, even if with cautions, as a technique that is able to modulate brain cognitive and sensory functions and helpful in specific treatments.

As aforementioned, the most used protocol are tDCS, tACS and tRNS. In the following paragraphs, a short summary covering evidence and proposed mechanism of action are exposed for these stimulation regimes.

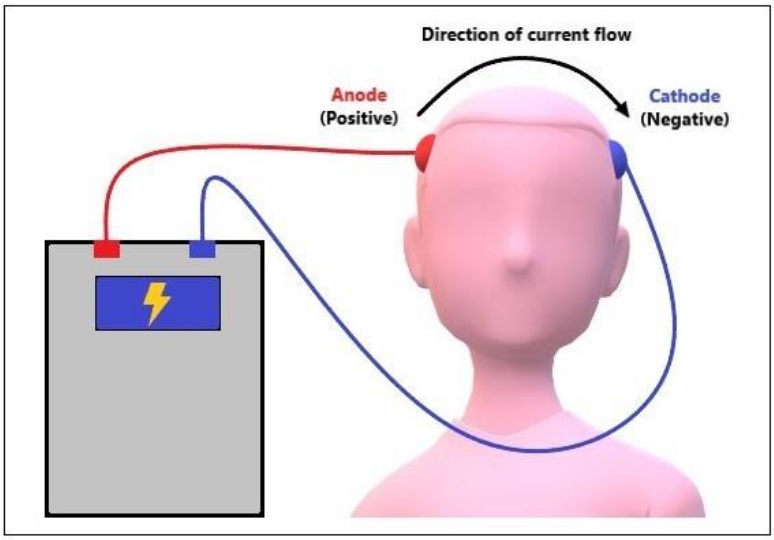

Figure 1.1. Representation of a transcranial electrical current stimulation (tES). A Battery driven device deliver low intensity current (mA) through a pair of electrodes positioned on the scalp. In a transcranial direct current stimulation (tDCS), the current flows constantly from the anode to the cathode electrode. In a transcranial alternating stimulation (tACS) and in the transcranial random noise stimulation (tRNS) the polarity, and consequently the current flow, shift depending the frequency/s selected. Adapted from Higgins & George (2008).

1.1.1 Transcranial Direct Current Stimulation (tDCS)

tDCS is so far the most used and studied type of non-invasive transcranial electrical stimulation delivering direct current troughs two or more electrodes. The characteristic of tDCS is the possibility to deliver anodal (positive charge) or cathodal (negative charge) current. When applying a stimulation protocol with two electrodes, usually the electrode delivering the polarity of interest (active electrode) is placed over a target area, while the second electrode is placed over a "neutral area" and is addressed as reference electrode. It was early discovered that the effects of the direct current over the cortex depend from its polarity. For example Bindiman and Lippold (1964) found that in anesthetized rodents cerebral cortex, anodal stimulation increased the spontaneous firing rate of active neurons

close to the electrode, while cathodal stimulation decreased the neural firing rate. Overall, it has been proposed that anodal stimulation depolarizes the resting membrane potential (increasing firing rate), while cathodal stimulation hyperpolarizes it (decreasing firing rate). Even if it has been shown that stimulation in deep brain structure can lead to opposite outcomes (Purpura & McMurtry, 1965), physiological results seemed to confirm this modulatory effects in human studies over the motor cortex (for a review see Nitsche et al., 2008). For instance, Nitsche and Paulus (2000) found that application of direct current over healthy participants resulted in excitability changes over the motor cortex up to 40%. The direction of such excitability resulted from the polarity of the stimulation, with anodal-tDCS increasing the excitability, whereas cathodal-tDCS produced the opposite effect.

1.1.1.1 Physiological and electrophysiological modulation of tDCS

The modulatory effects that anodal and cathodal tDCS have in altering the ongoing neural activity have been early addressed by researchers. For example, to study the different outcomes depending on stimulation polarity and to investigate cortical excitability in the visual cortex a practical and fast method is by measuring phosphene thresholds (Antal, Kincses, Nitsche, & Paulus, 2003; Lang et al., 2007). Usually phosphenes can be described as spots lights or blurred light perceptions. Phospene can be elicited by mechanical, electrical or magnetic stimuli applied along the visual pathway. A common way to elicit phosphene is to deliver Transcranial Magnetic Stimulation (TMS) pulses over the occipital cortex. TMS is a non-invasive brain stimulation technique that permits the alteration of normal electric brain functioning by delivering magnetic impulses at selected intensities and frequencies over the scalp of an observer. The minimum TMS intensity that is able to elicit a phosepene is referred to as the phosphene threshold and it is often used as an indirect measure to assess excitability of the visual cortex. Thus, Antal et al. (2003) studied specific changes in neural excitability of the striate cortex (V1) resulting from anodal and cathodal tDCS. The authors measured phosphene threshold before, immediately after and 12, 20 and 30 min after 10 min of tDCS. Results showed that phosphene threshold was reduced (i.e., increased cortical excitability), immediately after and 10 min after the end of anodal simulation. On the other hand, cathodal stimulation resulted in increased phosephene threshold (i.e., decreased cortical excitability).

An electrophysiological validation of excitatory modulation of tDCS on the visual cortex was investigated shortly after by Antal, Kincses, Nitsche, Bartfai, & Paulus, (2004a). The authors found that tDCS modulated the amplitude of the visual evoked potentials (VEPs) depending on the polarity of the stimulation. Specifically, while observers were asked to look at sinusoidal luminance gratings concurrent application of cathodal tDCS over the primary visual cortex decreased the amplitude of an early negative VEP, N70 component, caused by activation of neurons in the visual cortex, whereas the anodal stimulations increased its amplitude. Moreover the results showed that a positive VEP, the P100 showed a tendency to increase after the cathodal stimulation, while anodal stimulation did not affect its amplitude. The modulation was more efficient for the cathodal stimulation and only when applying the specific Oz-Cz (active and reference electrode, respectively) montage for the stimulation electrodes and when presenting low contrast stimuli rather than high contrast stimuli. However, polarity effects of anodal and cathodal tDCS in modulating VEPs show some discrepancies between different studies which have been explained to be the result of the type of visual stimuli used and electrodes positions (Antal & Paulus, 2008). For example, a later study showed that in response to a pattern-reversal checkboards and a stimulation protocol using an extra-cephalic reference electrode, P100 amplitude significantly increased during cathodal stimulation, whereas P100 amplitude decreased during anodal stimulation (Accornero, Li, Maurizio, & Riccia, 2007). Along with VEP modulation also changes in oscillatory activity by tDCS have also been investigated (Antal, Edina, Kincses, Nitsche, & Paulus, 2004b; Mangia, Pirini, & Cappello, 2014; Spitoni, Cimmino, Bozzacchi, Pizzamiglio, & Di Russo, 2013). Overall, results show that tDCS is able to induce modulation of the oscillatory activity in different frequency bands. However, the type of alteration carried by the polarity of the stimulation and their aftereffects are still ambiguous.

Nowadays, it is still very popular to refer to the anodal tDCS has an excitatory stimulation and to cathodal tDCS as an inhibitory stimulation. However, it is also true that several studies found that the excitatory and inhibitory effects tDCS are not solely polarity dependent, but also count on the type of neurons effectively stimulated, the depth and their location in the brain, and the axonal and dendritic orientation on the cortex with respect to the direction of the stimulation (Das, Holland, Frens, & Donchin, 2016). Moreover, several studies showed that the inhibitory and excitatory effects of tDCS might be dependent from the experimental parameters of the stimulation as time of application, duration and stimulation intensity (Pirulli, Fertonani, & Miniussi, 2014). For example it has been found that cathodal tDCS delivered at 1mA reduced the motor evoked potentials

(MEP) excitability, whereas cathodal tDCS at 2mA resulted in the opposite effect as it increased cortical excitability, demonstrating that increased intensity of the stimulation does not necessarily correspond to further excitability enhancement (Batsikadze, Moliadze, Paulus, Kuo, & Nitsche, 2013). The authors speculated that opposite effects of the stimulation intensity might be explained as the result of the dependency of the direction of plasticity (i.e. long-term depression or long-term potentiation) from the level of amount of calcium influx throughout the neural membrane altered by the stimulation. Specifically, they suggested that low calcium postsynaptic increments resulting from the 1mA cathodal tDCS could induce long-term depression plasticity, whereas higher calcium enhancement induced by the 2mA cathodal tDCS could lead to long-term potentiation mechanisms (Cho, Aggleton, Brown, & Bashir, 2001; Lisman, 2001).

1.1.1.2 Behavioural modulation of tDCS

tDCS behavioural effects over the visual cortex showed also a precarious level of stability, the polarity dependent predictions based on the physiological results showed to be not always applicable and different assumptions have been proposed to explain discrepancies between studies. For example, a study investigating tDCS effects when stimulation was applied over the visual cortex (Antal, Nitsche, & Paulus, 2001) found that visual functions like contrast perception could be temporarily affected by tDCS. They applied anodal and cathodal tDCS for seven minutes over the occipital cortex and estimated contrast thresholds. The results showed that while cathodal stimulation increased contrast threshold during and 10 minutes after stimulation, anodal stimulation did not influence the performance. However, a subsequent study showed that contrast sensitivity was increased by anodal tDCS, whereas cathodal tDCS did not produce any significant effect (Kraft et al., 2010). Spiegel, Hansen, Byblow, & Thompson (2012) tested anodal and cathodal tDCS effects to reduce inhibitory interaction on the visual cortex by measuring contrast threshold in a surround suppression visual paradigm. Surround suppression occurs when a target stimulus is surrounded by a mask stimulus producing an increment of contrast detection threshold and seems to originate in V1. Results demonstrated that anodal stimulation over the occipital cortex reduced surround suppression since the masking no longer showed any effects on contrast detection thresholds. On the other hand, cathodal stimulation did not show any significant effect in reducing surround suppression.

With the intent to increasing knowledge on what parameters in stimulations studies can affects their outcomes, Pirulli, Fertonani, & Miniussi (2014) carried out a series of experiments in which they tested the effects of cathodal tDCS applied over V1 in different conditions while observers were asked to perform an orientation discrimination task. Specifically the authors tested cathodal tDCS effects in modulating task performance by testing different timing of stimulation (online and offline stimulation), duration of the stimulation (9 and 22min), intensities of stimulation (1.5 and 0.75 mA) and they also tested the introduction of pauses (2min) during the stimulation period. Results showed that stimulation delivered prior to the task (offline) induced facilitation effects while the same improvement was not detected when stimulation was delivered during the execution of the task (online). Duration of stimulation was slightly correlated with the facilitation boost, and intensity of the stimulation was demonstrated to be a critical factor in inducing facilitation effects. Specifically, they found that across block of the experimental task, the rate at which the performance improved was higher when stimulation was delivered for 22 min with respect to the 9 min condition. Moreover, they also found that when delivering stimulation at 1.5 mA for 22 min, it significantly increased the performance with respect to the control condition. On the other hand, when the stimulation was delivered only for 9 min it did not induce any significant modulation of the performance with respect to the control condition.

Moreover, the introduction of short pauses did not introduce any significant difference with respect to a continuous stimulation. To explain their results, especially the discrepancy between offline and online stimulation, the authors suggested that the online tDCS mechanism of action might rely on the hyperpolarization and depolarization of the neural membrane actively influenced by the task of interest. On the other hand offline effects might rely on the change of neural state in the stimulated area and lowering the signal strength to produce a response (Miniussi et al., 2013).

1.1.1.3 Proposed tDCS mechanisms of action

Alongside investigating behavioural and physiological effects, early studies started looking at the mechanism of action upon which tDCS relies. A proposed mechanism behind the ability of tDCS to alter the resting membrane potential and impact the firing rate, is the possibility to alter the concentration of intracellular calcium ions (Ca^{2+}; Bikson et al., 2004). This mechanism could be crucial in determining tDCS effects as it has been found that increments in Ca^{2+} concentration can promote short and long-

term plasticity (Greer & Greenberg, 2008). Pharmacological studies on humans found that blockade of voltage dependent sodium (Na^+) channels and Ca^{2+} have the ability to cancel excitatory effects of anodal tDCS, while they do not affect cathodal inhibitory effects (Nitsche et al., 2003). Moreover, it has been found that while N-methyl-D-aspartate (NMDA) receptor do not have much responsibility for effects after short application of tDCS, they seems critical in formation of post stimulation after-effects. In fact, it has been found that partial NDMA receptor agonist d-cycloserine prolongs the effects of anodal tDCS (Nitsche et al., 2004). Inhibitory neurotransmitter GABA also seems to play a role on the tDCS mechanism of action. It has been shown that anodal tDCS caused a reduction in GABA concentration, while cathodal tDCS decreased glutamatergic neuronal activity with a correlated reduction in GABA concentration. However, differently form the anodal stimulation, the authors suggested that the decrease in GABA following cathodal stimulation could be attributable to the biochemical relationship between the glutamate and the GABA, as the glutamate is a substrate of the enzyme GAB-67 responsible of GABA synthetization (Stagg et al., 2009).

Taken together these and other studies (for a review see Nitsche & Paulus, 2011) extend our knowledge on tDCS mechanism at the neural level. However, caution has to be taken extending these results to a more macroscopic level, when multiple neural structures are influenced by the electric field in standardized tDCS protocol, especially in clinical settings (Flöel, 2014).

1.1.2 Transcranial Alternating Current Stimulation (tACS)

This stimulation technique has not been used in the Thesis, but for sake of completeness a short overview of its usage and effects is reported. Transcranial alternating current stimulation (tACS), as the name indicates, is a type of tES that delivers alternating current at a given frequency. tACS deploys a current waveform that periodically change its direction, thus the polarity of the electrodes shift from anodal to cathodal at a given frequency. For example, at one instant in time the voltage difference between its electrodes is +100 V, then 0.01 seconds later the voltage difference is -100 V, then another 0.01 seconds after that it is back to +100 V again and so on. The period of such a signal is the amount of time it takes to complete one cycle. For the example given above, the period (T) is 0.02 seconds. Frequency (f) is the inverse of the period (T) ($f = 1/T$). The frequency is the number of cycles that occur per unit time (e.g., number of cycles in one second). Moreover, always for the example given above that would be 50

cycles/second (1s / 0.02s = 50 Hz). The unit for frequency is "hertz" (Hz). tACS has the advantage to be well suited to modulate brain oscillation in a frequency-specific manner (Herrmann, Rach, Neuling, & Strüber, 2013). Because of the continuing shifts of polarity every half cycle of the period, tACS is suggested to not affect the resting membrane potential, so having an excitatory or an inhibitory action like tDCS. However, the short depolarization and hyperpolarization could be enough to induce entrainment effect in the cortex (Antal & Herrmann, 2016). Similarly to tDCS, tACS has been explored in several sensory and cognitive functions (for a complete review see Antal & Herrmann, 2016; Herrmann et al., 2013; Tavakoli & Yun, 2017). Kanai et al. (2008) showed that tACS is able to induce phosphene sensations in both light (eyes open) and dark conditions (eyes closed). Specifically, they tested tACS applied at different frequency (4Hz, 8Hz, 10Hz, 12Hz, 14Hz, 16Hz, 18Hz, 20Hz, 22Hz, 24Hz, 30Hz and 40Hz in a randomized order). When applied within the alpha frequency range (8-14Hz), tACS over the occipital cortex induced phosephene perception in the dark condition, whereas tACS delivered within beta frequency range (14-22Hz) induced phosphene more effectively in light condition. Since alpha activity is generally dominant in an eye closed condition and beta activity is more dominant in eyes open condition, the authors suggested that the selectivity showed by the stimulation frequency in each condition its caused by an interaction with the ongoing oscillatory activity in the stimulated cortex (Kanai, Chaieb, Antal, Walsh, & Paulus, 2008). These findings were challenged shortly after in a commentary article by Schwiedrzik (2009) in which it was questioned if the phosphene perceived by the participants in Kanai et al. (2009) were not the result of a cortical activation, but actually the result of the current spreading over the scalp reaching the neural populations in the retina. This critique was partially supported by the results obtained by Schutter & Hortensius (2010) demonstrating that a similar phosphene perception could be found using different tACS montages (i.e., occiput– vertex, frontalis–vertex, and occiput-right shoulder) and suggesting a modulation of retinal cells and not only a cortical activation in the occipital cortex. Interestingly, in a follow up study, Kanai, Paulus, & Walsh (2010), although not excluding the activations of retinal cells, demonstrated that tACS was able to modulate TMS induced phosphene threshold and therefore confirming the ability of this stimulation protocol to alter the cortical excitability on the occipital cortex.

It has been proposed that tACS entrainment of cortical brain oscillation is achieved when the exogenous frequency matches the neural rhythm (Romei, Thut, & Silvanto, 2016). Kanai, Paulus and Walsh (2010) examined cortical excitability modulation during tACS over the visual cortex at different frequencies (ranging from 5 to 40Hz) by

measuring phosphene thresholds elicited via single pulse TMS. The results showed that tACS at 20 Hz decreased phosphene threshold during the stimulation, thus increased cortical excitability. However, tACS delivered at different frequencies did not modulate cortical threshold, so the author suggested that tACS has the ability to modulate cortical excitability in a frequency dependent manner. Electrophysiological evidence that tACS can entrain brain oscillation has also been investigated (Cecere, Rees, & Romei, 2015; Helfrich et al., 2014; Minami & Amano, 2017; Neuling et al., 2015; Zaehle, Rach, & Herrmann, 2010). Zaehle et al. (2010) devised a protocol in which tACS was delivered over the occipital cortex at the individual alpha frequency (IAF) and measured alpha power levels through EEG recording. Results showed that with respect to a Sham control group, tACS increased alpha power in parieto-central electrodes. However, it should be noted that in this study, the stimulation was not delivered concurrently with the EEG recording, but it was delivered in an offline protocol (i.e. between EEG registrations). Therefore, the alpha power increments shown in this specific paradigm might have been also the results of specific plastic changes of cortical activity that have been shown to be responsible of alpha power enhancements (Vossen, Gross, & Thut, 2015).

Moreover, tACS delivered at IAF or close to the IAF has been used to study perceptual audio-visual integration (Cecere et al., 2015). In their study, Cecere et al. (2015) investigated the effects of tACS delivered at the IAF or at IAF±2 Hz in a sound-induced double-flash illusion. In this illusion when two beep are presented in a short time (e.g. 100 ms) together with one flash, a second illusory flash is perceived. The authors suggested that alpha oscillation might played an important role in this audio-visual stimuli integration since they found a correlation between IAF peak and the size of the temporal illusion. tACS was fundamental to confirm this hypothesis because when delivered at the IAF + 2HZ the temporal window of the illusion shrunk, whereas when stimulation was delivered at IAF + 2Hz it was enlarged when stimulation was delivered at IAF – 2Hz, providing an indirect confirmation of the ability of tACS to entrain brain oscillations. More recently, direct evidence that tACS can entrain brain oscillations have been found. For example Minami & Amano (2017) demonstrated that tACS was able to modulate individual peak alpha frequency (PAF) depending on the frequency of stimulation. Specifically, the authors measured inter-participant variation of PAF concurrent with tACS stimulation. The results showed that PAF was specifically modulated by the frequency of stimulation, as its frequency was higher when tACS was delivered at PAF + 1Hz and lower when tACS was delivered at PAF -1 Hz, therefore providing a direct demonstration of the ability of this stimulation protocol to entrain brain oscillations.

1.1.3 Transcranial Random Noise Stimulation (tRNS)

Transcranial random noise stimulation (tRNS) delivers alternating current at random intensities and frequencies within specific ranges. Random frequencies are usually produced within the range of 0.1 Hz - 600/640 Hz (depending on the device). The characteristic of this stimulation technique is that a random level of current is generated for every sample (sampling rate usually around 1200/1300 sample/s) with no overall DC offset, and following a Gaussian distribution, which means that if a current amplitude of 1.5 mA is selected, 99% of the generated currents will have an amplitude between – 0.75 mA and + 0.75 mA. The frequency of the current is limited to half of the sampling rate with all coefficients having a similar amplitude (i.e., "white noise"). Unlikely the tDCS, tRNS does not have a polarization effect, since the polarity switches continuously. Also unlike tACS, it does not have entrainment effects of endogenous oscillatory activities as it is delivered in a broad range of frequencies. tRNS has been applied at different frequency ranges, the full spectrum range (0.1 Hz - 600/640 Hz), low-frequency range (usually between 0.1 Hz -100 Hz) and high-frequency range (usually between 101 Hz - 600/640 Hz). The following paragraphs present an overview of the relevant literature reporting electrophysiological and behavioural findings using tRNS. Moreover, proposed mechanisms of action of tRNS are also discussed.

1.1.3.1 Physiological and electrophysiological modulation of tRNS

The first tRNS effects on humans have been assessed on the motor cortex (Terney, Chaieb, Moliadze, Antal, & Paulus, 2008). In their study Terney et al. (2008), assessed cortical spinal excitability modulated after 10 min of tRNS at 1 mA. A method to measure modulations on corticospinal excitability caused by an experimental manipulation (i.e. tES protocol) is to assess the change in occurrence or amplitude of motor evoked potentials (MEP) triggered via TMS. Specifically, MEP amplitude were estimated by delivering single pulse TMS and paired pulse TMS over the motor cortex and the premotor cortex. The authors found that when assessed via single pulse TMS, if tRNS was delivered over left M1 (reference over the contralateral orbit) it significantly increased the intensity of motor evoked potential (MEP) up to 20-50% and up to 60 min after the stimulation, while no significant difference with respect to the control condition was found when tRNS was delivered over the premotor cortex. Moreover they assessed specific tRNS effects on cortical excitability when delivered at low (0.1-100 Hz) and high

(101-640 Hz) frequency and found that excitability measures after high-frequency tRNS (hf-tRNS) were significantly higher with respect to low frequency tRNS (lf-tRNS). Paired pulse TMS also showed that tRNS over M1 selectively increased short interval intracortical facilitation (ICF) compared to the Sham control condition. In another study, Chaieb et al. (2011) investigated if MEP measures after tRNS were modulated as a function of stimulation duration. In particular, the authors measured corticospinal excitability after 4, 5 and 6 minutes of full spectrum tRNS (i.e., 0.1-640 Hz) over the left M1 (reference electrode over the contralateral orbit). The results showed that when delivered for 5 and 6 minutes, tRNS increased excitability up to 30 minutes, in line with their previous study (Terney et al., 2008). However, 4 minutes of stimulation did not show any significant effect in modulating cortical excitability. The author concluded that in order to establish significant after-effects application time is a crucial parameter. Importance of duration of stimulation and electrodes position (unilateral or bilateral montage) have also been investigated in a recent study which demonstrated the non-linearity in stimulation duration with the duration of aftereffects on MEP levels (Parkin, Bhandari, Glen, & Walsh, 2019). Parkin et al. (2018) found that 10 min of unilateral hf-tRNS stimulation (active electrode over the left M1 and reference electrode over the right contralateral orbit), increased MEP amplitude, but the same stimulation duration with a bilateral montage in which electrodes were placed over the left and right M1 did not showed any significant effect. Moreover, increasing the duration of the unilateral hf-tRNS to 20min also did not produce any significant effect.

Transient alteration of cortical excitability has also been investigated by measuring changing in blood oxygenation level dependent (BOLD) level via fMRI after tRNS was delivered over the sensorimotor cortex (Chaieb et al., 2009). The results showed that tRNS produced a decrease in BOLD levels on the sensorimotor cortex with respect to the control Sham condition (a control condition where stimulation is delivered for just few seconds). The authors argued that, if considered tRNS as an excitatory stimulation, the decrease of BOLD level does not necessarily work against previous results on MEP modulation. In fact the authors suggested that the decrement could be the results of a homeostatic response of the system against the stimulation interference according to the regulatory mechanism of the postsynaptic activity levels that gives long-term potentiation and long-term depression (Bienenstock, Cooper, & Munro, 1982). Thus, low overall cortical activity level might increase the synaptic strength of operating neuronal connections, whereas a high level of activity might decrease it. Moreover, Chaieb et al. (2009) suggested that, since BOLD signal has been linked to synaptic

activity rather than spiking activity (Logothetis, Pauls, Augath, Trinath, & Oeltermann, 2001), tRNS might alter synaptic activity, rather than modulate spike rates in a tDCS manner. These findings have also been partially replicated in a subsequent study aiming at investigating whether brain stimulation over the left M1(reference over the contralateral orbit) could modulate visual motor learning by measuring changes in BOLD signal (Saiote, Polanía, Rosenberger, Paulus, & Antal, 2013). Specifically the study compared effects of anodal tDCS, cathodal tDCS, low and high frequency tRNS delivered for 10 min at 1 mA. The results showed that at the behavioural level, none of the stimulation protocols produced a significant change in learning performance. However, BOLD signal measurements showed a reduction in the hf-tRNS condition with respect to the lf-tRNS condition and with respect to the Sham stimulation. The authors suggested that the reduction in BOLD activity registered in the hf-tRNS session could be the results of the experimental paradigm used. In particular, basing on to the assumption that hf-tRNS could modulate ongoing neural oscillations (Chaieb et al., 2009), hf-tRNS could have increased the neural synchronization during the learning paradigm. This would have improved the efficiency of the neural activity leading to a higher specificity of the metabolic activation of the cerebral area of interest and in turn a lower BOLD signal.

Modulation of cortical activity induced by tRNS has also been investigated in other sensory systems like visual and auditory systems. Recently, hf-tRNS modulation of visual cortical excitability has been investigated by measuring phosphene threshold (Herpich, Contò, van Koningsbruggen, & Battelli, 2018). Results showed that 20 min of hf-tRNS at 1 mA decreased phosphene threshold, thus increasing cortical excitability, lasting up to 90 minutes. Few studies also looked at electrophysiological modulation of tRNS on the auditory cortex (Rufener, Geyer, Janitzky, Heinze, & Zaehle, 2018; Rufener, Ruhnau, Heinze, & Zaehle, 2017; Van Doren, Langguth, & Schecklmann, 2014). Van Doren et al. (2014) assessed hf-tRNS modulatory effects in a resting state activity period and in auditory steady state responses (ASSRs). Baseline measure were taken with the EEG, followed by 20 min of hf-tRNS at 2 mA after which post stimulation EEG measures were taken again. The results showed an increment in band power for the ASSRs responses in the post with respect to the pre hf-tRNS condition. In the resting state, the authors registered a general increment in power for different frequency bands between pre and post stimulation, but no significant difference between the real and the control stimulation condition. Moreover, Rufener et al. (2017), always in the auditory system, found that bilateral tRNS over the auditory cortex increased performance in an auditory gap detection task (to measure temporal resolution), but no significant difference on a

pitch discrimination task (to measure spectral resolution). The results also showed that hf-tRNS was able to reduce latency of the N1 component and it showed a trend for the P50 component but only during the gap detection task. No significant difference in peak amplitude was reported either for the N1 or for the P50 components.

Overall, these results show that tRNS could produce physiological and electrophysiological modulation of cortical activity. However, though there are more evidence for modulatory effects of tRNS on the motor cortex and auditory system, its modulatory effects on the visual system and underlying mechanisms have been scarcely investigated. Therefore, more studies are necessary in order to assess the effects of tRNS when delivered over the visual cortex.

1.1.3.2 Behavioural modulation of tRNS

Since its first introduction, tRNS has been employed in several perceptual and cognitive domains. Evidence shows that tRNS can modulate behavioural performance in visual perceptual learning (Camilleri, Pavan, & Campana, 2016; Camilleri, Pavan, Ghin, Battaglini, & Campana, 2014; Campana et al., 2014; Fertonani et al., 2011; Moret et al., 2018; Pirulli et al., 2013), in face discrimination (Prete, Malatesta, & Tommasi, 2017; Romanska, Rezlescu, Susilo, Duchaine, & Banissy, 2015), in motion adaptation (Campana, Camilleri, Moret, Ghin, & Pavan, 2016), attentional functions (Tyler, Contò, & Battelli, 2018; van Koningsbruggen, Ficarella, Battelli, & Hickey, 2016) and arithmetic and numerosity abilities (Dormal, Javadi, Pesenti, Walsh, & Cappelletti, 2016; Karolis et al., 2018; Pasqualotto, 2016; Popescu et al., 2016; Snowball et al., 2013). Despite its application in many contexts, this section focuses on the applications of tRNS on the visual system. A closer look is given to studies that compared the effects of tRNS with other stimulation protocols, time of application, implementation of different parameters (such as frequency range and stimulation intensity) and outcomes on visual performance in myopic and amblyopic populations.

Fertonani et al.'s (2011) study on visual perceptual learning in an orientation discrimination task compared effects of performance between lf- and hf-tRNS, anodal and cathodal tDCS. The results showed that while hf-tRNS increased performance at the task, anodal stimulation initially boosted the learning, but was followed by a reduction of the performance. Moreover, cathodal tDCS was also significantly different with respect to the Sham stimulation. The authors also reported that lf-tRNS results were less clear, because even if performance showed a certain level of improvement it was not

significantly different from both Sham stimulation and hf-tRNS. This study also demonstrated that tRNS and tDCS do not necessarily lead to equivalent behavioural outcomes when applied to the visual system. Shortly after, the same research group also investigated the role of timing of stimulation in modulating learning performance. In this second study, Pirulli, Fertonani and Miniussi (2013) examined whether different stimulations (hf-tRNS and anodal tDCS) delivered before (i.e., offline) or during the task (i.e., online) lead to a different performance. The findings showed that, when hf-tRNS was delivered in the online condition the stimulation increased the performance, whereas when the stimulation was delivered in the offline condition it was not significantly different from the Sham. Noteworthy, anodal tDCS showed the opposite trend, with an increase of the performance in the offline condition, but not for the online condition. The authors concluded that these results highlight the importance of the state of activation (Silvanto & Muggleton, 2008) when delivering tES protocols and showed how tRNS and tDCS might relay on different mechanisms of action.

Discrepancies between high and low frequencies tRNS effects on the visual cortex have also been investigated using the motion after-effect (MAE) (Campana et al., 2016). MAE is a phenomenon in which a stationary or flickering stimulus is seen to move in an opposite direction with respect to a previously presented stimulus (often called adapter) presented for several seconds. This perceptual illusion has been explained as the result of imbalanced activity between the adaptation of neurons tuned to a specific direction (activated by the moving adapter stimulus) and the neurons tuned to the other directions (Mather, Pavan, Campana, & Casco, 2008). In the study, effects of hf and lf-tRNS delivered bilaterally over the hMT^{+} were assessed on the duration of the MAE, specifically to determine a reduction or an increment of the visual illusion. The results showed that when hf-tRNS was delivered a reduction of the MAE duration was observed, whereas when lf-tRNS was applied it resulted in an increment of MAE duration. The authors speculated that the discrepancy between low and high frequency tRNS outcomes could be the results of distinctive modulation of the high and low frequency ranges applied over the stimulated area. Physiological evidence on rabbit's retinal neurons showed that sinusoidal stimulation between 5 and 25Hz produced strong responses only near the soma of the ganglion cell limiting the modulation to a more "focal activity". On the other hand, higher frequencies (i.e. 100Hz) modulated responses both on the soma and over distal axons (Freeman, Eddington, Rizzo, & Fried, 2010). Campana et al. (2016) speculated that a similar mechanism might happen using hf-tRNS, which might lead to opposite effects when neurons are in an adapted state of activation.

Other stimulation parameters, such as intensity of the stimulation, have been investigated to assess modulatory outcomes of tRNS. In this instance, van der Groen and Wenderoth (2016) studied the effects of different hf-tRNS intensities (ranging from 0 to 1.5 mA) in a visual detection task. The authors devised a stimulation protocol where stimulation was delivered over the occipital cortex (i.e. Oz). What the authors reported is that performance on a contrast detection task was increased according to the stimulation intensity, especially around 1 mA. These results pointed out the importance of the relationship between the task in examination and the intensity at which the stimulation is delivered.

Promising applications of tRNS in improve behavioural performance in healthy observers (Fertonani et al., 2011; Pirulli et al., 2013), motivated researchers to investigate the possibility of boosting performance when coupling perceptual learning regimes with tRNS on populations with visual deficits. Perceptual learning trainings have been established as a promising tool to improve visual abilities such as visual acuity and contrast sensitivity in amblyopic observers (Polat, 2009). Amblyopia is a developmental deficit in spatial vision, impairing visual functions such as visual acuity and contrast sensitivity. However, this impairment does not arise from defects of the organic eye, but is linked to disrupted functional connectivity within the primary visual cortex (Polat, 1999). Short perceptual learning paradigms (8 sessions) coupled with hf-tRNS demonstrated to increase visual acuity and contrast sensitivity with respect to the perceptual learning alone. Authors suggested that the improvement could be the results of neural plasticity changes in the primary visual cortex boosted by hf-tRNS (Campana et al., 2014; Moret et al., 2018).

Overall, evidence in most of the studies support the idea that tRNS can improve behavioural performance and modulate physiological activity of the cortex. However, since this technique has been much less investigated with respect to the tDCS and tACS, its underlying mechanisms are still debated.

1.1.3.3 Proposed tRNS mechanisms of action

Since the first study applying tRNS, suggestions about its mechanisms of action in altering the brain activity have been made. Terney and colleagues (2008) speculate that the mechanism of action of tRNS is to modulate the activity of sodium ions (Na^+) channels. Bromm (1968) argued that depolarization of the neural membrane allows the Na^+ channel to open, and increase the influx of ions. However if the concentration of Na^+

is insufficient there is no further depolarization to undermine the possibility generate an action potential. Terney et al. (2008) speculated that time for the repolarization of the membrane takes longer with respect to the time to complete another entry of Na^+ ions. If stimulation is applied in this condition then another influx of Na^+ can occur (before the repolarization of the membrane), increasing the depolarization of the membrane and in turn increasing the chance for the cell to generate an action potential. This hypothesis was supported by a study in which repetitive extracellular high frequency stimulation applied in cultured rat neurons promoted an influx of sodium ions incrementing depolarization levels (Schoen & Fromherz, 2008). Thus, Terney and colleagues (2008) suggested that a similar mechanism of action could develop using tRNS. Additionally, Fertonani and colleagues (2011) hypothesised, that being a subthreshold and repetitive stimulation, tRNS could induce a temporal summation of neural activity when the time constant (i.e. the velocity at which neuron's voltage level decays to its resting state after it receives an input signal), is longer enough to let the summation of two input presented in close sequence. Moreover, the authors suggested that tRNS could have an impairment effect in the natural drive for homeostasis for the system. Specifically, they argued that the summation of depolarizing current caused by the tRNS inputs would particularly affect those neurons engaged by the task, thus inducing an increase in the behavioural performance measured in their studies (Fertonani et al., 2011; Pirulli et al., 2013). In support of the hypothesis that tRNS alters normal activity of sodium channels of engaged neurons, a pharmacological study (Chaieb, Antal, & Paulus, 2015) measured MEP excitability while participants were administer pharmacological interventions. Specifically, the study tested tRNS interaction with Lorazepam (a $GABA_A$ receptor agonist), rapinirol (a dopamine receptor agonist), carbamazepine (a sodium channel blocker), dextromethorphan (a NDMA receptor agonist), and D-cycloserine (a partial NDMA receptor agonist). Results supported the hypothesis of sodium channel mechanism related to tRNS effects, since MEP excitability significantly decreased after carbamazepine administration up to 60 min. Moreover, lorazepam showed a trend in reducing excitability effects of tRNS.

An additional proposed mechanism of action is based on a phenomenon named stochastic resonance (McDonnell & Abbott, 2009; Moss, Ward, & Sannita, 2004; Ward, 2009). Stochastic resonance is a phenomenon whereby the randomness of a signal (i.e. noise) can have a positive role in signal processing (McDonnell & Abbott, 2009). Stochastic resonance phenomenon has been applied in several contexts spacing form engineering, climate models and biological systems. The general idea behind this theory

is that, in a system like the brain which is not linear, if an "optimal" amount of noise is applied to the system it can lead to an enhanced output signal or information content. In its simplest description, stochastic resonance results from the combination of a threshold, a subthreshold stimulus and noise (Figure 1.2). In this paradigm, a signal/stimulus can be encoded or perceived when a threshold crossing happens and if the stimulus/signal is by definition subthreshold, the chance of this to cross the threshold is limited. However, according to the stochastic resonance phenomenon, if noise is added to the stimulus/signal the probability of a threshold crossing to happen increase substantially (Moss et al., 2004). Stochastic resonance phenomenon has been successfully tested in animal (Douglass, Wilkens, Pantazelou, & Moss, 1993; Levin & Miller, 1996) and human sensory systems (Collins, Imhoff, & Grigg, 1996; Cordo et al., 1996; Simonotto et al., 1997). For example, stochastic resonance has been investigated in the human visual system and it has been demonstrated that noise can profoundly change the quality at which an image is perceived. When a certain amount of visual noise was added to visual stimuli participants could perceive better details by increasing contrast sensitivity and motion direction discrimination (Riani & Simonotto, 1994; Simonotto et al., 1999; Simonotto et al., 1997; Treviño, Torre-Valdovinos, & Manjarrez, 2016). Being a random frequency stimulation, tRNS has been proposed to induce random activity (i.e. noise) in the system (Miniussi et al., 2013). Neural noise induced by non-invasive brain stimulations such as TMS in fact has been suggested as a mechanism to explain the efficiency of stimulation in improving behavioural performance (Miniussi, Ruzzoli, & Walsh, 2010; Ruzzoli et al., 2011; Schwarzkopf, Silvanto, & Rees, 2011). tRNS is a non-focal stimulation that might increase neural noise. According to the stochastic resonance phenomenon this increment in neural noise could boost the activity of those units in which the signal is too weak to generate an output (Fertonani & Miniussi, 2017; Miniussi et al., 2013). Although stochastic resonance has been suggested as a possible explanation of the results observed in studies investigating tRNS effects in different cognitive and sensory systems (Fertonani et al., 2011; Pirulli et al., 2013; Terney et al., 2008), few studies have directly tested it (van der Groen, Tang, Wenderoth, & Mattingley, 2018; van der Groen & Wenderoth, 2016). Van der Groen and Wenderoth (2016) argued that the intensity at which tRNS is applied could control the level of neural noise that could be injected in the system, and so control the optimum amount of noise needed to improve behavioural performance. Effectively, they reported that depending on the relationship between stimulus level (sub or supra-threshold), performance was affected by mean of tRNS intensity and that this was comparable to a condition where visual noise was added to the

stimulus. The authors suggested that their study showed that tRNS effects can be linked to a stochastic resonance mechanism.

Despite the promising results regarding how tRNS operates at the neural levels, further investigations are needed to better understand this non-invasive modulatory technique. This necessity is driven by the large amount of discrepancies between different studies, and the possibility to employ tRNS (and tES in general) as a safe and reliable technique that can be applied in rehabilitative and training regimes.

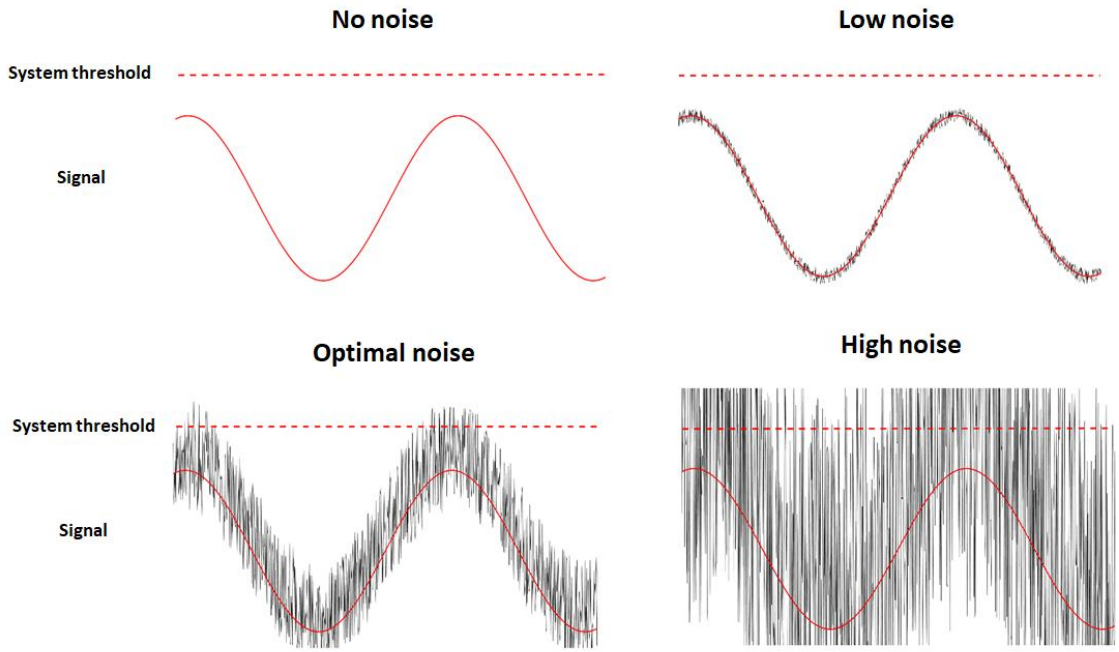

Figure 1.2. Stochastic resonance phenomenon.
A periodic subthreshold signal is depicted below the threshold (top-left panel) and the consequences of different levels of noise are represented in each box. When the noise is absent or it is too weak, the signal is maintained below the threshold (top-left and top-right panels). However, if an "optimal" amount of noise is added (bottom-left panel) signal can cross the threshold level and be detected or processed. When an excessive amount of noise is added (bottom-right panel) the signal is covered by the noise and the information content is degraded. Adapted from van der Groen et al. (2018)

1.2 Visual Motion Perception

Motion perception is the mechanism through which we infer environmental features such as speed and direction of moving objects. The elaboration of motion perception begins from the projection of a moving image on the eye's retina and is further processed along a series of more complex structures on the visual pathways. To form a complete and detailed perception of a moving object, information are transferred from the retinal

cells to the lateral geniculate nucleus (LGN) and then towards the primary visual cortex area and motion specialized temporal-occipital areas like V2, V3A and V5/hMT^{+} (Aaen-Stockdale & Thompson, 2012). Among the sensory abilities, perception of visual motion has been one of the most studied in the last decades, thanks to the several physiological studies carried on primates and humans observers (Albright & Stoner, 1995; Burr & Thompson, 2011).

As above mentioned, processing of visual motion starts early in the retina. In particular, in addition to basic operation like contrast processing, it has been found that retinal structures can also respond to speed, suggesting that even these early stages can have consequences on motion perception (Billino, Bremmer, & Gegenfurtner, 2008). For example, it has been shown that the velocity of moving objects is differently analysed by rod and cones cells in the retina, where the cone system seems to be 20% better in detecting stimulus velocity when moving stimuli are presented at low temporal frequency (< 4 Hz) (Gegenfurtner, Mayser, & Sharpe, 2000). Interneurons like amacrine cells also play an important role in transmission of the visual motion signal. Amacrine cells selectively respond to different motion directions depending on their receptive fields (Kim, Soto, & Kerschensteiner, 2015). Visual motion information is carried from these early units through ganglion's axons to the LGN. Ganglion cells can be divided in magnocellular neurons and parvocellular neurons. Each type has different morphological and functional characteristics. Magnocellular neurons have larger receptive fields and are specialized in elaborate motion information, they are more sensitive to high temporal frequency stimuli and able to process faster and transient responses. On the other hand, the parvocellular neurons have smaller receptive fields and seems to be more sensitive to constant stimuli and colours (Livingstone & Hubel, 1988). Magnocellular and parvocellular neurons projects their axons in two separate layers of the LGN. While the first two layers (beginning from the ventromedial region) are categorized as magnocellular layers, the remaining four layers are categorized as parvocellular layers. The topographical organization of the LGN is also maintained in the primary visual cortex. However, it is noteworthy to mention that the segregation between magnocellular and parvocellular elaboration of the visual motion information is not complete. Studies investigating elaboration of motion after permanent impairment of the magnocellular pathways found that monkeys could still process visual motion information of direction and speed when the signal was solely conveyed by the parvocellular pathways. These findings highlight the notion that visual motion information can reach primary visual cortex in multiple ways (Merigan, Byrne, & Maunsell, 1991). In the primary visual cortex

(V1), neurons have larger receptive fields than in LGN. This means that neurons in V1 can respond to orientated lines and are sensible to direction of motion when a luminous stimulus is moved across their receptive fields (Hubel & Wiesel, 1968a, 1968b). However, at this stage of elaboration, processing of visual motion stimuli is still considered limited and ambiguous and there is still debate on how information about local motions from single neurons are combined across space to form perception of moving edges and objects.

Integration of many motion detectors responding to motion stimuli has been allocated in higher areas of visual analysis such as V3A and V5/hMT$^+$ (Aaen-Stockdale & Thompson, 2012) that receive most of their inputs from V1. These areas, compared to V1, integrate signal outputs from of larger portion of the visual field and accurately extract direction and velocity of moving objects. At this stage of elaboration extrapolation of coherent global motion can also be achieved (Braddick et al., 2001; Thompson, Aaen-Stockdale, Koski, & Hess, 2009). Perception of global motion results from the integration of many local motion vectors in order to form a global percept with a specific direction. Studies investigating global motion integration and the physical parameters that can modulate global motion perception, often rely on a test paradigm where a random dot kinematogram (RDK) is presented to an observer which has to detect the correct motion direction (Newsome & Paré, 1988). In a RDK task, in its simplest form, a certain amount of dots are presented in random locations evenly spaced with respect to each other, across the size of the stimulus. Usually some of these dots move coherently in a specific direction, while the rest of the presented dots move in random directions. The ratio between the coherently moving dots and the random moving dots determines the difficulty of the task. If a small number of coherent moving dots (i.e., signal) is presented together with a high number of random moving dots (i.e., noise) the probability to detect the correct direction are low (low signal-to-noise ratio). However, if the number of coherent moving dots presented is increased the probability to detect the correct direction is higher (high signal-to-noise ratio). Sensitivity to coherent global motion (or coherence threshold) is often measured by performing a task were the coherence of the stimulus is changed across several presentations.

Evidence that temporal-occipital areas are essential in global motion processing comes from both animal and human studies. The MT area, the primates counterpart of the human hMT$^+$, has been shown to be essential in processing visual global motion (Albright, 1984; Newsome & Pare, 1988; Rodman & Albright, 1989; Rodman & Albright, 1987). For instance, Albright (1984) investigated neural responses for direction

and orientation selectivity in macaque monkey over the MT with three types of moving stimuli: slits, single spot and random dot fields. On average, responses were similar for all the three kind of stimuli and they were higher with respect to the same stimuli tested on V1, but also with respect to static stimuli. MT neurons showed a high range of direction-tuning bandwidths and 83% percent responded selectively to orientation. Moreover, results showed that 61% of the tested neurons had an orientation preference perpendicular to the motion direction preference, while another 29% had an orientation preference parallel to the preferred motion direction. The author concluded that these results demonstrated the higher specialization of MT in process global motion stimuli than V1.

In humans, areas like V5 and V3A or the hMT^+ complex have been investigated to understand their role in process visual motion. The possibility to induce a virtual lesion or transient alteration of the neural functioning via TMS has demonstrated to be a promising paradigm for this purpose in both healthy and observer with visual deficits (Beckers & Zeki, 1995; Campana, Cowey, & Walsh, 2006; Cowey, Campana, Walsh, & Vaina, 2006; Pavan, Alexander, Campana, & Cowey, 2011; Thompson et al., 2009). For example, by delivering a 1 Hz offline repetitive transcranial magnetic stimulation (rTMS), Thompson et al. (2009) demonstrated a double dissociation between V1 and hMT^+ in their role to perform motion integration. Their results showed that rTMS over V1 increased coherent motion stimuli, whereas rTMS over hMT^+ cortex had the opposite effect.

Most of the afferent input in temporal-occipital areas like the hMT+ complex seems to origin in the early visual cortex V1. To explain the relationship between the V1 and the hMT^+ it has been suggested to investigate the neural responses to global motion in patients where V1 has been permanently damaged. If the V1 is unilaterally damaged information of motion coherence processed in hMT^+ could be carried by interhemispheric pathways or directly from subcortical structures, bypassing the primary visual area (Ajina, Kennard, Rees, & Bridge, 2015). Ajina et al. (2015) tested this possibility in participants with unilateral V1 lesion presenting moving dots to both the left and right hemi-field separately. fMRI BOLD activity level showed that when the sighted hemi-field was stimulated (thus activating contralateral hemisphere), a significant activation of the contralateral hMT^+ was reported. Moreover, BOLD levels were positively correlated with the level of stimulus coherence. On the other hand, when the blind hemi-field was stimulated the correlation between the hMT^+ activity and the stimulus coherence was disrupted. However, when stimuli where presented in the sighted hemi-field, ipsilateral

activity in hMT^+ (the same hemisphere of the damaged V1) reported similar activity with respect to a control group. The authors suggest that these results showed a complex system in which the motion signals are carried to hMT^+ not just along the same hemisphere but also originating from the opposite hemisphere structures form which the signal is transferred across the corpus callosum.

These findings demonstrate the central role of temporal-occipital cortex in processing global motion. NIBS can be helpful to improve our understanding of the visual functions involved in motion perception. However, to date only few studies addressed these research issues by using specific tES protocols and investigated the role of different stimulation parameters like current polarity, current intensity or stimulation duration. In the next paragraph, a summary of the current evidence on tES and visual motion is outlined.

1.2.1 tES effects on visual motion

Since its first application to investigate the human sensory system, few studies investigated tES effects on perception of visual motion. However, up to date there are several discrepancies between findings, making it problematic to draw firm conclusions on the effects of electrical brain stimulation on motion perception.

In an early tES study, Antal et al. (2003) showed that 10 min of anodal and cathodal tDCS over the V1 was able to alter moving phosphene threshold elicited via biphasic TMS pulse over the hMT^+ area. The authors argued that moving phophenes threshold depended also from the excitability state of the V1 area. Shortly later, Antal et al. (2004c) found that cathodal tDCS over hMT^+ improved motion direction discrimination performance when coherent motion was presented among random moving dots. Whereas, when coherent motion was solely presented anodal stimulation improve performance at the task. These results have been partially replicated in a recent studies (Battaglini et al., 2017; Zito et al., 2015). In particular, Battaglini et al. (2017) investigated effects of anodal and cathodal tDCS as a function of noise reduction and signal enhancement. The authors speculated that cathodal and anodal tDCS effects on visual motion might rely on different mechanisms. While cathodal stimulation could enhance discriminability by modulate incoherent motion or stimuli with a low signal-to noise ratio, anodal stimulation would be effective only in modulating coherent motion or stimuli with a high signal-to-noise ratio.

However, as previously mentioned, depending on the paradigm applied, discrepancies have been found among studies on the effective tDCS outcomes in visual motion. For example another study, (Antal, Chaieb, Cziraki, Paulus, & Greenlee, 2012) failed to replicate a previous finding (Antal et al., 2004c). In this study, participants performed a motion discrimination task at three fixed levels of coherence. The observers performed the task after cathodal tDCS or Sham stimulation. The results showed no differences in the accuracy or reaction times between cathodal tDCS and control condition. Nonetheless, brain image fMRI showed that the cathodal tDCS increased motion-evoked BOLD signal in the area MT+ independently of the level of coherence of the visual stimulus.

Plasticity effects of tES on motion perception have also been investigated (Olma et al., 2013). In this study, participants with unilateral visual cortex lesions performed a 5-day perceptual training regime with anodal tDCS or Sham stimulation to examine the long-term neuroplasticity in the V5/MT brain area using the same motion paradigm of Antal et al. (2004c). Measurements of the motion sensitivity threshold were taken before and immediately after the stimulation session, and after 2 and 4 weeks (follow-up). Results show that the mean motion sensitivity increased across the days of training in both the stimulation conditions with a higher enhancement in sensitivity for the anodal stimulation condition maintained in the follow-up measurements. tACS also demonstrated to be effective in modulating visual motion perception. Kar and Krekelberg (2014) hypothesized that application of tACS would induce an impairment in motion direction processing. However, contrary to their expectation, in a series of tasks stimulation delivered over the left hMT^{+} during the presentation of long stimuli (4 s) improved direction discrimination performance.

1.3 The importance of studying visual motion perception with tES

Overall, the aforementioned evidence demonstrated that to some extent visual motion perception is modulated in tES experiments. In particular, global motion perception might be an attractive topic of investigation to further our knowledge on how stimulation techniques operate when applied over the visual cortex. In fact, preliminary evidence showed that when measuring coherence thresholds using global moving stimuli it is possible to disentangle distinct polarity effects of tDCS depending on the ratio between signal and noise, but also to distinguish different proposed mechanisms of action

of the stimulation (Battaglini et al., 2017). Moreover, hf-tRNS effects on global motion have been scarcely examined and it is of particular interest to compare its effects with respect to other stimulation regimes and advance more detailed hypothesis on how this particular stimulation technique promotes behavioural and physiological changes. Furthermore, global motion perception is a complex visual process that involves several brain structures. Therefore, the ability of different tES to induce specific alterations in limited portions of the brain might be helpful to increase our understanding of the role of those cerebral areas fundamental for the operational flow in global motion processing.

1.3.1 Aims and research questions to be answered in this Thesis

tES is a promising brain stimulation technique able to modulate the activity of the visual cortex. However, most of the previous studies investigated tES effects with static stimuli, whereas its effects on motion processing have been scarcely investigated. Therefore, our goal was to further our knowledge on the effects of anodal and cathodal tDCS on global motion perception and disentangle with more precision the behavioural consequences of electrical polarity and if they are the result of modifications of the signal-to-noise ratio at the neural level. Besides, as reported in the previous paragraphs, hf-tRNS do not polarize the membrane like the tDCS, and its effects on moving stimuli and areas involved in global motion processing has been scarcely investigated. Therefore, we also aimed at investigating the effects of tRNS on global motion processing and the underlying mechanisms.

The first part of this Thesis examined the behavioural effects and underlying mechanisms of hf-tRNS and tDCS when applied over the visual cortex probed by well-established paradigms of motion perception. In Chapters 2 and 3, we address two main questions about behavioural performance:

1) *Chapter 2: Is tES effective in modulating behavioural performance in a global motion direction discrimination task? In particular we ask whether there are differences in terms of modulation between the different tES (Experiment 1.1) and if stimulation effects are specific for the stimulation site (Experiment 1.2)*

2) *Chapter 3: Global motion perception can be limited by local factors (i.e., variability of local directions estimates of motion cues) and global factors (i.e., the integration of local directions). If tES is able to improve global motion*

direction discrimination, does this improvement results from reduction in variability of local direction estimates or enhanced integration of local motion cues?

In Chapters 4 and 5, we investigate the mechanisms underlying behavioural improvements found in the previous Chapters:

3) *Chapter 4: We investigate the mechanisms underlying hf-tRNS effects on visual motion perception. In particular, we ask whether the stochastic resonance phenomenon could explain the improved performance found in previous experiments.*

4) *Chapter 5: We assess the electrophysiological aftereffects of hf-tRNS when applied over the visual cortex. In particular, by using EEG, we investigate whether offline hf-tRNS modulates the power spectral density amplitude of different oscillation bands at rest, and motion-related VEP amplitude and latency.*

1.4 Experimental chapters' overview

1.4.1 Chapter 2

Global motion direction discrimination has been shown to be sensitive to anodal and cathodal tDCS depending on the stimuli coherence. However, this was never tested with hf-tRNS and no comparison of the outcomes between these three stimulation protocols has been assessed. tRNS is a relative novel brain stimulation technique, which effects seems to increase cortical excitability and behavioural performance (Antal & Herrmann, 2016; Miniussi et al., 2013). High frequency tRNS has been demonstrated to increase behavioural performance in a series of visual task with respect to other stimulation technique such as anodal and cathodal stimulation when presenting stationary stimuli (A. Fertonani et al., 2011; Pirulli et al., 2013) and recently it has been shown that hf-tRNS and cathodal stimulation have opposite effects in reducing the directional bias produced by a radial optic flow (Pobric et al., 2018).

In Chapter 2, we tested modulation of coherence thresholds in a global motion direction discrimination task while a group of participants performed four sessions in which one among hf-tRNS, anodal tDCS, cathodal tDCS and Sham control was applied over the left hMT^{+} in random order. The task devised was a motion direction

discrimination task where a random dot kinematogram was presented on their left or right visual hemi-field. Measures of coherence threshold were estimated separately for each visual hemi-field. We also tested if hf-tRNS effects were specific for stimulation over the hMT^+ by testing its effects over the V1 and the frontal cortex. Results showed that only when hf-tRNS was delivered over the left hMT^+ it decreased coherence thresholds, but not the slope of the psychometric function. Moreover, no significant effect was found for both anodal and cathodal tDCS.

1.4.2 Chapter 3

In Chapter 1, we demonstrate that hf-tRNS decreases motion coherence threshold. However, it has been proposed that coherence threshold in a motion direction discrimination paradigm can be limited by two factors: the ability of an observer to estimate with precision local direction signals and how these signals are pulled together (Dakin, Mareschal, & Bex, 2005; Catherine Manning, Dakin, Tibber, & Pellicano, 2014; Tibber, Kelly, Jansari, Dakin, & Shepherd, 2014). In a novel paradigm called *Equivalent Noise*, Dakin et al. (2005) was able to measure separately the ability of one observer to estimate local direction of single dots (e.g. *internal noise*) and the ability to integrate these local direction together (e.g. *sampling*)

By adapting the equivalent noise paradigm proposed in Tibber et al. (2014) in Chapter 3, we investigated at which level of the visual analysis hf-tRNS affects coherence threshold. Specifically we measured hf-tRNS effects on internal noise and sampling levels. Participants performed two sessions in different days, in which hf-tRNS or Sham stimulation was delivered over the left hMT^+ in random order. In each session, participants were asked to perform a task in which they had to judge if the moving dots in the stimulus were drifting clockwise or counter-clockwise of vertical upward motion. Stimuli were presented in both the left and right visual hemi-field and levels of internal noise and sampling were estimated for each hemi-field. Results showed that hf-tRNS was able to increase *sampling* levels, thus global integration of local directions, but did not alter the *internal noise* estimates.

1.4.3 Chapter 4

In Chapter 2 and 3, we assessed if hf-tRNS could modulate motion direction discrimination performance and at what level of the visual motion integration this modulation might occur. The aim of the fourth chapter is to shed some light on the mechanism beyond such modulation. We specifically assessed the proposed mechanism based on the stochastic resonance phenomenon (Miniussi et al., 2013; van der Groen et al., 2018; van der Groen & Wenderoth, 2016), whereby the addition of an optimal amount of external interference (i.e. noise) can enhance the detection of weak stimuli. However, when too much noise is present it could lead to a worsening of the information content and of the behavioural performance (Moss et al., 2004; Ward, 2009).

It has been recently demonstrated that the intensity at which hf-tRNS is applied can be examined as a function of the level of external noise that can be injected into the system altering behavioural performance (van der Groen & Wenderoth, 2016). In the study described in Chapter 4, we tested a similar paradigm on motion perception. Different groups of participants were asked to perform a motion direction discrimination task at the 60% percent of their individual accuracy performance while bilateral hf-tRNS was delivered at different intensities (from 0.5 up to 2.25mA) or Sham stimulation. We aimed to determine at what intensity hf-tRNS would be able to increase or decrease accuracy and so provide indirect evidence of a stochastic-resonance-like mechanism to explain its effects on the visual cortex. Results supported the initial hypothesis as an increase of accuracy was registered at 1 and 1.5 mA, but the highest intensity stimulation at 2.25 mA, impaired accuracy.

1.4.4 Chapter 5

Within this thesis, we aimed to provide evidence of hf-tRNS effects on motion direction discrimination, and at which level of motion integration this effects occurs (Chapters 2 and 3). Additionally, we examined whether hf-tRNS effects are dependent from the level of current intensity (or noise) injected into the system, and if that can be explained within the stochastic resonance phenomenon (Chapter 4). Despite the promising evidence in behavioural outcomes, physiological effects, especially on the visual cortex, of the tRNS have been scarcely investigated (Antal & Herrmann, 2016). The aim of the study presented in Chapter 5 is to assess physiological effects of hf-tRNS

when delivered over the visual cortex in an offline stimulation paradigm. In this study, participants were asked to perform two experimental sessions in which bilateral hf-tRNS or Sham stimulation was delivered. Cortical activity was recorded before and after the stimulation period during each session. In detail, prior and after the stimulation period resting state activity was recorded. Additionally, after the resting state in the pre and post stimulation periods participants were also asked to perform a motion direction discrimination task while EEG activity was also recorded. Throughout this experimental procedure we aimed to measure possible hf-tRNS physiological aftereffects, which could further our knowledge on how this stimulation regime modulates cortical activity. Results showed that hf-tRNS delivered offline did not modulate either the behavioural performance or physiological measures, indicating a limitation of the stimulation protocol in altering cortical activity depending on the experimental paradigm adopted.

Chapter 2: The effects of transcranial electrical stimulations (anodal tDCS, cathodal tDCS and hf-tRNS) on global motion processing

The experiments presented in this chapter have been published in Ghin, F., Pavan, A., Contillo, A., & Mather, G. (2018). The effects of high-frequency transcranial random noise stimulation (hf-tRNS) on global motion processing: An equivalent noise approach. *Brain Stimulation*, 11(6), 1263–1275. https://doi.org/10.1016/j.brs.2018.07.048

2.1 Abstract

Global motion direction discrimination has been shown to be sensitive to anodal and cathodal tDCS depending on the stimuli coherence. However, this was never tested with high-frequency tRNS and no comparison of the outcomes between these three stimulation protocols has been made. Hf-tRNS has demonstrated to increase behavioural performance in a series of visual tasks with respect to other stimulation techniques such as anodal and cathodal stimulation when presenting stationary stimuli (Fertonani et al., 2011; Pirulli et al., 2013) and recently it has been shown that hf-tRNS and cathodal stimulation have opposite effects in reducing the directional bias produced by a radial optic flow (Pobric et al., 2018).

We tested modulation of coherence thresholds and slope in a global motion direction discrimination task while a group of participants performed four sessions in which hf-tRNS, anodal tDCS, cathodal tDCS and Sham stimulation (control) was applied over the left hMT^+ in random order. The task devised was a motion direction discrimination task where a random dot kinematogram was presented on their left or right visual hemi-field. Logistic function was used to fit the psychometric function in order to extract measures of coherence threshold and slope separately for each visual hemi-field. Results showed that hf-tRNS induced a decrement of coherence threshold in the contralateral hemi-field (right), with respect to the Sham stimulation and with respect to the ipsilateral hemi-field, but it did not have any effect on the slope. Contrary to previous finding (Antal et al., 2004c; Battaglini et al., 2017), both anodal and cathodal tDCS did not modulate coherence threshold and slope in either right and left visual hemi-field. We also tested if hf-tRNS effects were specific for stimulation over the hMT^+ by testing its effects over the primary occipital cortex and the frontal cortex. For both the control conditions results showed hf-tRNS did not make any significant modulation of the coherence threshold or slope, demonstrating that the ability of hf-tRNS in reducing coherence threshold was specific to when the stimulation was applied over the hMT^+. The decrement in coherence thresholds could be the results of hf-tRNS interacting with the neurons responding to direction signal and amplifying their activity by synchronizing their firing through a non-linear amplification of subthreshold neural oscillatory activity (Bikson et al., 2004; Fertonani et al., 2011; Miniussi et al., 2013).

2.2 Introduction

In Chapter 1, we have described the transcranial electrical stimulation (tES), a non-invasive brain stimulation technique in which low-voltage electrical current is delivered over specific cortical sites. As aforementioned it has been proposed that anodal tDCS (a-tDCS) induces a depolarization of the resting membrane potential, so increasing the neural firing rate, whereas the general effect of cathodal tDCS (c-tDCS) is to hyperpolarize the resting membrane potential and so produce a decrement in neural firing rate (Nitsche et al., 2008). Often in literature, a linear relationship has been suggested between cortical modulation and the resulting behavioural performances. Especially, the increasing and decreasing firing rate resulting from anodal and cathodal stimulation has been related to the increase and decrease in behavioural performance. However, a growing number of studies show that this is not always the case and that polarity dependent effects are influenced by several factors (Fertonani & Miniussi, 2017). For example, when used with a global motion task, the results showed that stimulus characteristics are critical factors in determining how tDCS polarity interact with the neural network state. Antal et al. (2004c) found that application of c-tDCS over the hMT^+ resulted in improved performance on a motion direction discrimination task involving coherently moving dots (i.e., signal) presented amongst randomly moving dots (i.e., noise). On the other hand, when only coherent motion was presented, motion direction discrimination performance was hindered by c-tDCS and improved by a-tDCS. Recently it has been suggested that, at low levels of signal-to-noise ratio, c-tDCS might selectively suppress the uncorrelated motion, leaving the correlated motion above the threshold, thus enhancing motion direction discrimination. On the other hand, at high levels of signal-to-noise ratio, a-tDCS might selectively improve motion coherence thresholds by increasing the probability of firing in detectors tuned to the coherent motion direction, especially those detectors that in absence of stimulation do not reach the firing threshold due to internal noise (Battaglini et al., 2017).

Differently from the tDCS, transcranial random noise stimulation (tRNS) involves delivery of random levels of current at random frequencies. In general, high-frequency tRNS (100-600/640Hz) has shown to improve behavioural performance across a wide range of visual tasks (Campana et al., 2014; Fertonani et al., 2011; Moret et al., 2018; Pirulli et al., 2013; Pobric et al., 2018; van der Groen & Wenderoth, 2016). Although its facilitatory effects have been shown in different contexts, the effects of hf-tRNS on the visual system and underlying modulatory mechanisms have been scarcely investigated,

especially if compared with the striking number of studies using tDCS (Antal & Paulus, 2008).

It has been demonstrated that hf-tRNS can improve performance in an orientation discrimination task compared to other types of electrical stimulation (including, low-frequency tRNS, a-tDCS and c-tDCS (Fertonani et al., 2011; Pirulli et al., 2013). Application of different stimulation regimes like a-tDCS, c-tDCS and low- and high-frequency tRNS within the same experimental protocol allows measuring distinct effects on performance outcomes, hypothesizing more information about each stimulation regime and in the long term the possibility to apply the more effective stimulation regimes for specific behavioural tasks. For example, it has been recently found that hf-tRNS and c-tDCS resulted in opposite effects in a motion direction detection task. Specifically, the effects of anodal, cathodal and hf-tRNS over the right hMT^+ have been investigated in a task in which a visual optic flow induced a distortion of the direction of a moving stimulus (probe), producing a biased estimate of the real direction of the probe (Pobric et al., 2018). Generally, when an observer is asked to determine the direction of a moving probe (e.g., upward) embedded into a radial flow field, the probe is seen moving toward its original direction, but also shifting toward the centre of the flow field. This shift toward the centre is known as relative tilt effect (Warren & Rushton, 2009). Pobric et al.'s (2018) findings showed that when the probe stimulus was embedded in a global optic flows (among 300 dots) the relative tilt effect increased in the cathodal tDCS condition, whereas the effect decreased in the hf-tRNS condition.

Although hypotheses to explain the effects of cathodal and anodal tDCS on visual global stimuli have been made (Antal et al., 2004c; Battaglini et al., 2017), there are still some discrepancies amongst studies (Antal et al., 2012) which might depend on the stimulation paradigm and the stimuli used. Hf-tRNS is a form of alternating current that does not polarize the neural membrane in the same way as cathodal and anodal tDCS do, and its effects on global visual motion are still unknown. Thus, the aim of this study is to compare the effects of different tES regimes in a global motion direction discrimination task and the role of the hMT^+ in global motion perception. Specifically, we estimated observers' coherence threshold while stimulating the left hMT^+ (reference electrode positioned over Cz) with c-tDCS, a-tDCS, hf-tRNS or Sham stimulation and measured their effects in terms of an increase or decrease in motion coherence threshold. Additionally to the main experiment, two additional control experiments were conducted. The first control experiment was designed to exclude that possible effects observed in the main experiment could be the result of unspecific effects of the stimulation over the

reference electrode posed over Cz adopted in the main experiment. In particular, in this condition we used a Cz - left forehead montage (e.g. areas not involved in the execution of the task) for which we did not expect any difference with respect to the Sham control condition. Furthermore, previous findings showed that modulatory effects of tES on motion direction discrimination might be limited when stimulation is applied over hMT^+ (Antal et al., 2004c). However, it has been demonstrated that the electrical current during tES protocol can spread beyond electrodes' border (Datta, Baker, Bikson, & Fridriksson, 2011) and therefore affecting the activity of nearby cortical areas (i.e. V1). Therefore, we aimed at investigating whether significant modulatory effects we might detect are the result of specific stimulation of the hMT^+ in processing global motion stimuli, or if significant effects can also be detected by stimulating lower level areas of visual analysis such as V1.

2.3 Experiment 1.1

2.3.1 Methods

2.3.1.1 Participants

The author (FG) and fifteen naïve participants (8 males, age range 18-40 yrs.) took part in Experiment 1.1. Participants were all right handed and had normal or corrected to normal visual acuity. Each participant filled in a questionnaire in order to exclude those with a history of seizure, implanted metal objects, heart problems or any neurological disease. Methods were implemented following the World Medical Association Declaration of Helsinki (2013). The present study was approved by the Ethics Committee of the University of Lincoln. Written informed consent was obtained from each participant prior to enrolment in the study and they were paid for their time.

2.3.1.2 Apparatus

Stimuli were displayed on a 20-inch HP p1230 monitor with a refresh rate of 85 Hz. Stimuli were generated with Matlab PsychToolbox (Brainard, 1997; Kleiner et al., 2007; Denis G. Pelli, 1997). The screen resolution was 1280 x 1024 pixels. Each pixel subtended 1.6 arcmin. The minimum and maximum luminance of the screen were 0.08 and 74.6 cd/m^2 respectively, and the mean luminance was 37.5 cd/m^2. A gamma-corrected lookup table (LUT) was used so that luminance was a linear function of the digital representation of the image.

2.3.1.3 Stimuli

Stimuli were random dot kinematograms (RDKs) made up by 150 white dots (diameter: 0.12 deg) presented within a circular aperture (diameter: 8 deg, density: 3 dots/deg^2). Dots drifted at a speed of 13.3 deg/s and had a limited lifetime; after 47 ms each dot vanished and was replaced by a new dot at a different random selected position within the circular window. Dots appeared asynchronously on the display and had an equal probability of being selected as a signal dot (Morgan & Ward, 1980; Newsome & Paré, 1988). This was implemented to minimize the presence of local "motion streaks" (Geisler, 1999) that could provide strong cues for direction discrimination. In addition, moving dots that moved outside the circular window were also replaced by a new dot at a different randomly location within the circular window, thus always maintaining the same density. The duration of the RDK was ~106 ms. A certain percentage of dots were signal dots, and the remaining dots were noise dots. Signal dots were constrained to move along one of the eight cardinal trajectories, whereas noise dots were positioned at new locations, randomly selected within the circular window, on each successive frame of the motion sequence (Scase, Braddick, & Raymond, 2000). We employed a brief stimulus duration and limited dot lifetime to prevent both covert attentional tracking of the stimulus motion direction and eye movements toward the stimuli (Martinez-Conde, Macknik, & Hubel, 2004).

2.3.1.4 Stimulation techniques

Stimulation was delivered by a battery driven stimulator (BrainSTIM, EMS, http://www.brainstim.it/index.php?lang=en) through a pair of saline–soaked sponge electrodes. The hf-tRNS consisted of an alternating current of 1.5 mA with zero offset, applied with random frequencies ranging from 100 to 600 Hz. The tDCS consisted of a direct current of 1.5 mA. In the Sham condition, stimulation was delivered for 30 sec before the task (Gandiga, Hummel, & Cohen, 2006). The total duration of the stimulation was ~18 min. The active electrode had an area of 16 cm² whereas the reference electrodes had an area of 60 cm². The current density was maintained well below the safety limits (Bikson et al., 2016; Fertonani, Ferrari, & Miniussi, 2015) The active electrode was placed over the left human medio-temporal complex (hMT$^+$) while the reference electrode was placed over the vertex (i.e., Cz). When the tDCS stimulation was applied, the polarity of the active electrode was anodal in the a-tDCS condition and cathodal in the c-tDCS

condition. Figure 2.1 shows a representation of the stimuli used in the experiment, the different electrode locations and the electrical waves used.

The target area was localized in all observers by using predetermined coordinates: 3 cm dorsal to inion and 5 cm leftward from there for the localization of the hMT^+. This localization technique has been used in previous studies (Campana, Cowey, & Walsh, 2002; Campana et al., 2006; Campana, Maniglia, & Pavan, 2013; Laycock, Crewther, Fitzgerald, & Crewther, 2007; Pascual-Leone et al., 1998; Pavan et al., 2011) and provides a localization that is consistent with fMRI localizers (Thompson et al., 2009).

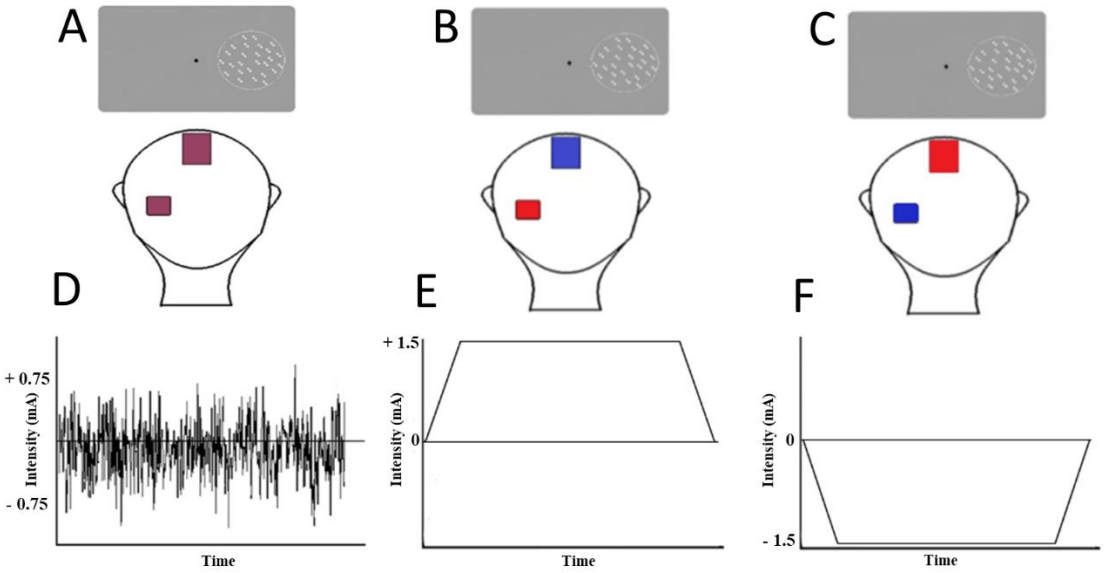

Figure 2.1. Schematic representation of stimulus, electrode location and current waves for hf-tRNS, Anodal and Cathodal tDCS. (A) hf-tRNS: polarity of electrodes (in purple) for hf-tRNS changes at random intensities and frequencies. (B) Anodal tDCS: anode electrode (in red) over left hMT^+ and cathode electrode (in blue) over Cz. (C) Cathodal tDCS: cathode electrode (in blue) over left hMT^+ and anode electrode (in red) over Cz. The white circular frame surrounding the moving dots is only for demonstrative purposes and was not presented during the experiment. (D, E, F) Representation of the electric current waves for hf-tRNS, Anodal tDCS and Cathodal tDCS, respectively.

2.3.1.5 Procedure

Observers performed an eight-alternative forced-choice task (8AFC) for motion direction discrimination. Dots were presented either in the left or in the right visual hemi-field (eccentricity: 12 deg). The observers were instructed to fixate the centre of the screen and to respond to the RDK's motion direction. A representation of the display used is shown in Figures 2.1. A-tDCS, c-tDCS, hf-tRNS and Sham stimulation were delivered in separate non-consecutive days for a total of four sessions for each participant. The stimulation was delivered during the execution of the task (online stimulation). In each block, two interleaved adaptive staircases (MLP; Grassi & Soranzo, 2009; Green, 1993)

were used, one tracking the coherence threshold for the left visual hemi-field and the other for the right visual hemi-field. Coherence threshold and slope for the left and right visual hemi-fields were each estimated from five staircases. Observers performed five blocks per stimulation session. Each staircase consisted of 32 trials.

Coherence threshold (corresponding to 70% correct in direction discrimination) and function slope were estimated for each visual hemi-field. The right visual hemi-field was contralateral to the active electrode (i.e., the electrode placed in correspondence of the left hMT^+, whereas the left visual hemi-field was ipsilateral to the stimulation site. If any of the tES regimes modulate the observers' performance on the motion coherence task, then we would expect modulation of the coherence threshold and slope for the contralateral visual hemi-field (i.e., the right visual hemi-field). Participants were unaware of the type of stimulation that was applied in each session.

Parameters' estimate of the Psychometric function

The operational flow of the staircase to estimate coherence threshold and slope of the psychometric function consisted in acquiring and storing the subject response to the *n*-th trial, selecting the psychometric function maximizing the likelihood of the first *n* trials, estimating the corresponding coherence threshold and presenting it as stimulus for the (*n*+1)-th trial. The estimate subsequent to the last trial was the output of the staircase (Grassi & Soranzo, 2009). The logistic function was used as psychometric function:

$$p(x) = \gamma + \frac{1-\gamma}{1+exp(-\beta(x-\alpha))} \qquad \text{Eq. (1.1)}$$

whose steepness parameter β was fixed to 1/2, while the midpoint α and the baseline γ were varied to maximize the likelihood. The rationale for such choice was to focus on the position of the threshold on the coherence axis, suppressing the further degree of freedom associated to the growth rate of the psychometric function. However, for the sake of completeness, we also extracted the information about the slope. The slope (*s*) of the psychometric function was computed as follows:

$$s = \frac{\beta(1-\gamma)}{4} \qquad \text{Eq. (1.2)}$$

In order to do this, we made use of a custom best-fit routine based on a Metropolis-Hastings algorithm, exploring the parameter space of the logistic function. The algorithm

randomly selected a starting point in the parameter space $\{\alpha, \beta, \gamma\}$ and computed the corresponding total likelihood:

$$l_{TOT} = \sum_n ln\,[R_n + (-1)^{R_n} p(x_n)] \qquad \text{Eq. (1.3)}$$

over the whole staircase. Here x_n is the coherence of the n-th trial, while R_n indicates the corresponding subject response (1 for correct, 0 for wrong). Thereafter, during each iteration of the Metropolis-Hastings, it performed a random step in the parameter space, computed the corresponding total likelihood and compared it to the one of the starting point. If the new likelihood was higher, the algorithm replaced the starting point with the new point, thus accepting the step. Otherwise, the step was rejected. Approximately 150k iterations were performed for each staircase, and the logistic function corresponding to the highest likelihood was returned as the best fitting curve. Using the best fit parameters, it was possible to compute an estimate for the coherence threshold T_c as the inverse logistic function

$$T_c = \alpha - \frac{1}{\beta} ln\left[\frac{1-\gamma}{p_t-\gamma} - 1\right] \qquad \text{Eq. (1.4)}$$

p_t being the 70% accuracy value acquired by the psychometric function in correspondence of the coherence threshold.

2.3.2 Results

Figure 2.2 shows the results of Experiment 1.1. A Shapiro-Wilk test showed that data for all stimulation conditions, in both visual hemi-fields, for coherence thresholds and slopes were normally distributed ($p > 0.5$), except for the coherence threshold for the left c-tDCS ($p = 0.011$). We performed a repeated measures ANOVA on the estimated coherence thresholds with stimulation type (a-tDCS, c-tDCS, hf-tRNS and Sham) and visual hemi-field (left and right) as within-subjects factors. A significant effect of the visual hemi-field ($F_{(1,15)} = 9.253$, $p = 0.008$, $\eta^2_p = 0.38$) was found, but stimulation type did not reach significance ($F_{(3,45)} = 2.689$, $p = 0.58$, $\eta^2_p = 0.152$). However, the ANOVA reported a significant interaction between stimulation type and visual hemi-field ($F_{(3,45)} = 3.036$, $p = 0.039$, $\eta^2_p = 0.168$). Table 2.1 and 2.2 shows pairwise comparisons with a False Discovery Rate (FDR) at 0.05 (Benjamini & Hochberg, 1995) and Cohen's *d* effect

size (Fritz, Morris, & Richler, 2012) [1] for the Left (Table 2.1) and Right (Table 2.2) visual hemi-field among Sham, hf-tRNS, a-tDCS and c-tDCS.

Table 2.1. Pairwise comparisons tES effects on coherence threshold left visual hemi-filed for Experiment 1.1

	hf-tRNS		**a-tDCS**		**c-tDCS**	
	p-value	***d***	***p-value***	***d***	***p-value***	***d***
Sham	0.81	0.06	0.60	0.17	0.60	0.19
hf-tRNS			0.60	0.31	0.60	0.22
a-tDCS					0.60	0.36

p-value and Cohen's *d* of pair-sample t-test (corrected using FDR at 0.05)

Table 2.2. Pairwise comparisons tES effects on coherence threshold right visual hemi-filed for Experiment 1.1

	hf-tRNS		**a-tDCS**		**c-tDCS**	
	p-value	***d***	***p-value***	***d***	***p-value***	***d***
Sham	**0.01***	**0.83**	0.86	0.04	0.60	0.2
hf-tRNS			**0.01***	**0.88**	**0.01***	**0.89**
a-tDCS					0.60	0.17

p-value and Cohen's *d* of pair-sample t-test (corrected using FDR at 0.05)

A repeated measure ANOVA was also performed on the slopes, with stimulation type and visual hemi-field as factors. It did not report any significant main effects or interaction: stimulation type ($F_{(3,45)}$ = 2.320, p = 0.09, η^2_p = 0.134), visual hemi-field ($F_{(1,15)}$ = 1.581, p = 0.23, η^2_p = 0.095), interaction stimulation type x visual hemi-field ($F_{(3,45)}$ = 0.680, p = 0.57, η^2_p= 0.043).

[1]We reported the Cohen's *d* for the t-test tests. Cohen's *d* was calculated as $d = \frac{M_A - M_B}{\sigma}$ were M_A and M_B are the two means and σ is the standard deviation for the population (Field, 2009; Fritz et al., 2012). For Cohen's *d* a large effect is 0.8, a medium effect is 0.5, and a small effect is 0.2.

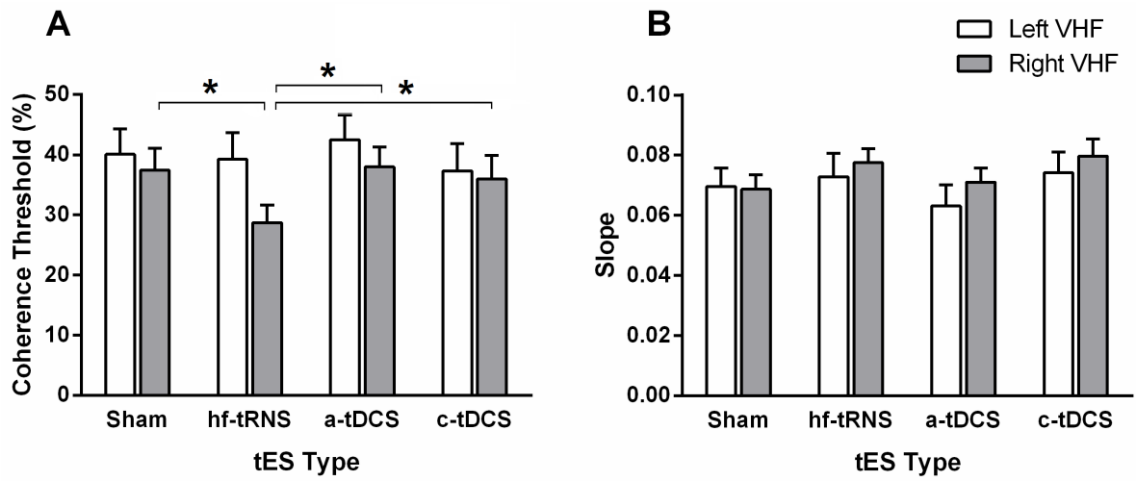

Figure 2.2. Results of Experiment 1.1. (A) Mean coherence thresholds (%) for each stimulation type and for the two visual hemi-fields. (B) Mean slopes. Error bars ±SEM. Asterisks (*) show significant differences.

2.5.2 Discussion

The results of Experiment 1.1 showed that when hf-tRNS was delivered over the left hMT^+ motion direction discrimination improved (i.e., lower coherence thresholds), but only when stimuli were presented on the contralateral visual hemi-field with respect to the stimulation site (i.e., the right visual hemi-field), indicating spatial specificity of the stimulation. In addition, hf-tRNS was the only stimulation able to modulate motion coherence thresholds, producing a coherence threshold decrement of 9% with respect to the contralateral visual hemi-field in the Sham condition, and a decrement of 11% with respect to the ipsilateral visual hemi-field when hf-tRNS was delivered. On the other hand, hf-tRNS did not modulate the slope of the psychometric function, suggesting that hf-tRNS does not modulate the discriminability of the global moving pattern.

2.4 Experiment 1.2

In Experiment 1.2 we controlled for two possible confounds that may have produced the results of Experiment 1.1 The aim of the first control experiment (Experiment 1.2A) was to exclude any unspecific effects of hf-tRNS due to the stimulation over Cz. The aim of the second control experiment (Experiment 1.2B) was to assess whether hf-tRNS selectively improves global motion direction discrimination only when it is applied over the hMT^+ (Ajina et al., 2015; Braddick et al., 2001; Händel, Lutzenberger, Thier, & Haarmeier, 2007).

2.5.3 Methods

2.4.1.1 Stimuli and procedure

Stimuli and procedure were the same as in Experiment 1.1. Twenty-four naïve participants (9 males, age range 18-40 yrs.) took part to Experiment 1.2; twelve were assigned to the first control experiment, and the other half to the second control experiment. Experiment 1.2 followed the same procedure as in Experiment 1.1 except that participants performed only two different and non-consecutive stimulation sessions in which either hf-tRNS or Sham stimulation was delivered. In Experiment 1.2A one electrode was placed over Cz and one on the left forehead. In Experiment 1.2B one electrode was placed over Cz, whereas the other electrode was placed over the left V1 (i.e., 3 cm dorsal to the inion and 1 cm leftward).

2.3.2 Results

Figure 2.4 shows the results for Experiment 1.2. A Shapiro-Wilk test showed that data for all stimulation conditions, in both visual hemi-fields, for coherence thresholds and slopes were normally distributed ($p > 0.5$), except for the coherence thresholds for the left sham ($p = 0.021$) and the right sham ($p = 0.026$) in Experiment 1.2B. A repeated measures ANOVA on the coherence thresholds with stimulation type (hf-tRNS and Sham) and visual hemi-field (left and right) as factors was performed on both control experiments. For Experiment 1.2A (i.e., left forehead stimulation), the ANOVA did not report any significant effects or interaction: stimulation type ($F_{(1,11)} = 0.159$, $p = 0.70$, $\eta^2_p = 0.014$), visual hemi-field ($F_{(1,11)} = 0.001$, $p = 0.99$, $\eta^2_p = 0.001$), interaction stimulation x visual hemi-field ($F_{(1,11)} = 0.102$, $p = 0.76$, $\eta^2_p = 0.009$). Similarly, for Experiment 1.2B (i.e., left V1 stimulation), ANOVA did not report any significant effect or interaction: stimulation type ($F_{(1,11)} = 0.398$, $p = 0.54$, $\eta^2_p = 0.035$), visual hemi-field ($F_{(1,11)} = 0.138$, $p = 0.72$, $\eta^2_p = 0.012$), interaction stimulation type x visual hemi-field ($F_{(1,11)} = 1.052$, $p = 0.33$, $\eta^2_p = 0.087$).

For Experiment 1.2A, a repeated measures ANOVA performed on the slopes reported no significant effect of the stimulation type ($F_{(1,11)} = 0.096$, $p = 0.76$, $\eta^2_p = 0.009$), no significant effect of the visual hemi field ($F_{(1,11)} = 0.024$, $p = 0.88$, $\eta^2_p = 0.002$), but a significant interaction between stimulation type and visual hemi-field ($F_{(1,11)} = 6.168$, $p = 0.03$, $\eta^2_p = 0.359$). However, since the stimulations (Sham and hf-tRNS) were applied to a region where no effect was expected, and our subsequent post-hoc comparisons with

FDR at 0.05 did not report any significant difference between left and right visual hemi-fields for hf-tRNS (p = 0.26, d = 0.32) and Sham stimulation (p= 0.26, d = 0.64). Moreover no significant difference was found between hf-tRNS and Sham stimulation for the left visual hemi-field (p = 0.29, d = 0.35) and right visual hemi-field (p > 0.09, d = 0.04). We ascribed the reported interaction to a stochastic emergence of unspecified noise. For Experiment 1.2B, a repeated measures ANOVA on the slopes did not report any significant effect or interaction: stimulation type ($F_{(1,11)}$ = 0.10, p = 0.92, η^2_p = 0.001), visual hemi-field ($F_{(1,11)}$ = 0.021, p = 0.89, η^2_p= 0.002), interaction stimulation type x visual hemi-field ($F_{(1,11)}$ = 0.274, p = 0.61, η^2_p = 0.024).

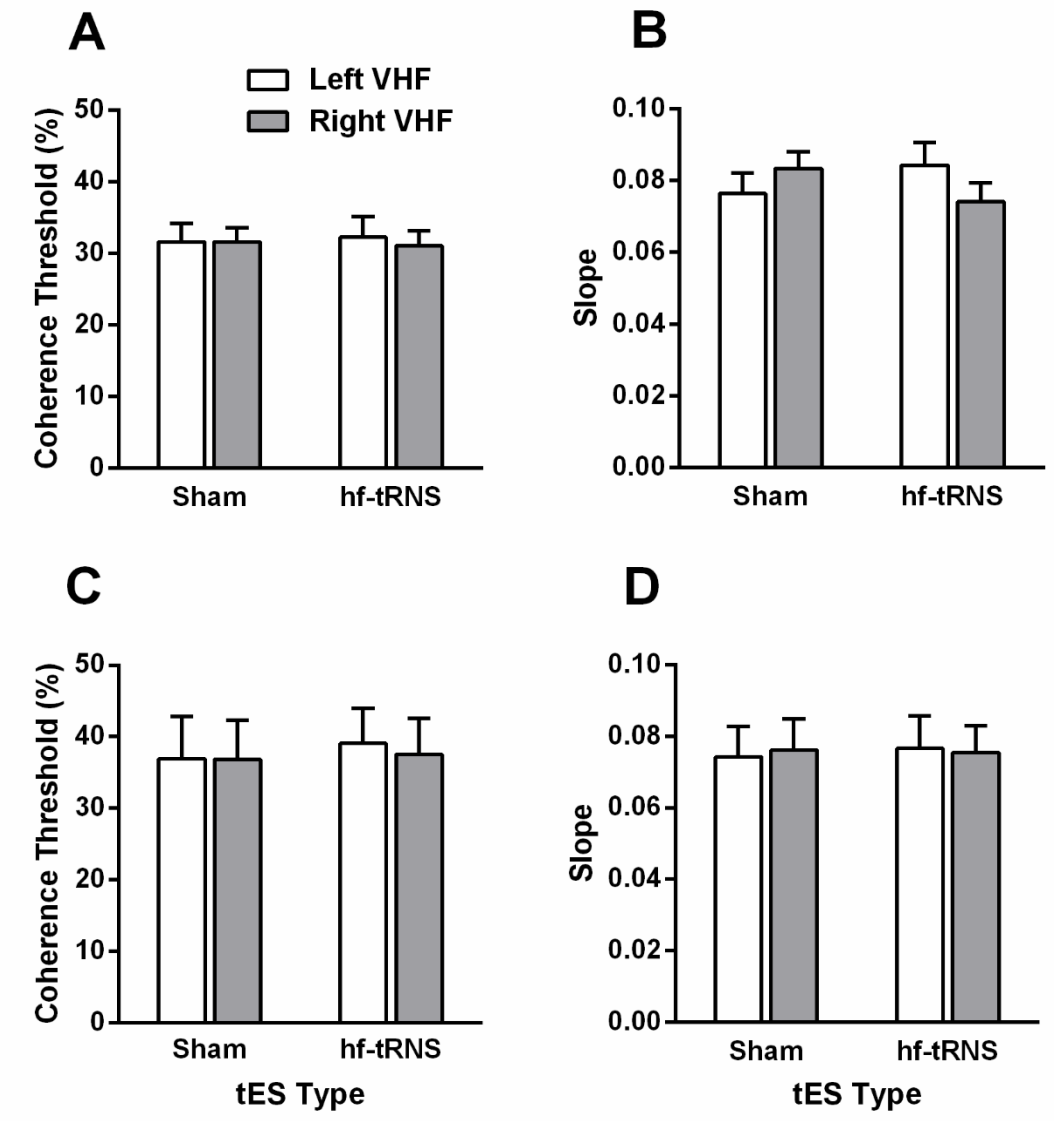

Figure 2.3. Results of Experiment 1.2. Panels A and B show mean coherence thresholds (%) and slopes for the left and right visual hemi-fields with electrodes over the left forehead and Cz (Experiment 1.2A). Panels C and D show mean coherence thresholds and slopes for the left and right visual hemi-fields with electrodes over left V1 and Cz (Experiment 1.2A). Error bars ±SEM.

2.3.3 Discussion

The results of Experiment 1.2 confirmed the spatial specificity of the effect of electrical stimulation observed in Experiment 1.1. The results of Experiment 1.2 also did not show any modulation of the function slopes, further confirming that hf-tRNS does not modulate the discriminability of global moving stimuli.

2.5 General Discussion

In a series of experiments, we assessed the effects of hf-tRNS on performance in a visual global motion task. In Experiment 1.1, we used a motion coherence task in which participants judged the global motion direction of a RDK presented either in the left or right visual hemi-field. The results showed that, compared to Sham stimulation, c-tDCS and a-tDCS, online hf-tRNS decreased the coherence thresholds for global moving stimuli, suggesting an improvement in motion direction discrimination thresholds. Importantly, this improvement was found only when stimulating the left hMT^{+} with stimuli presented in the right visual hemi-field, i.e., the contralateral visual hemi-field with respect to the stimulation site. Though we reported a modulation of motion coherence thresholds, the hf-tRNS did not modulate stimulus discriminability, as the slope of the psychometric function was not influenced by the stimulation type.

Contrary to previous results on global motion direction discrimination (Antal et al., 2004c; Battaglini et al., 2017) we did not find any modulation when a-tDCS and c-tDCS were delivered during the motion coherence task. Battaglini et al. (2017) found that depending on the motion coherence level (i.e., the signal-to-noise ratio), anodal and cathodal tDCS can lead to opposite effects. At a high level of visual noise (i.e., low coherence) MT neurons, which have a broad tuning to motion direction, could also respond to directions different from the optimal one (Albright, 1984). The authors suggested that c-tDCS might selectively suppress the uncorrelated motion signals leaving correlated signals above the threshold. This inhibitory modulation would sharpen the tuning of the local motion detectors reducing the probability of responses to non-preferred directions. On the contrary, at a low level of visual noise (i.e., high coherence), threshold reduction by a-tDCS might be the consequence of an increased probability of firing in those neurons that are tuned for the target direction, which without stimulation would remain in a subthreshold activation state.

The discrepancy resulting from our tDCS results might be attributed to the difference in the protocols used (i.e., online vs. offline stimulation). In our study the

electrical stimulation was online, whereas in Battaglini et al. (2017) it was applied prior to the task (offline stimulation). It has been suggested that in tDCS the time of application with respect to the behavioural task can lead to different outcomes (Pirulli et al., 2013, 2014). The neural effect of online tDCS is to polarize the neural membrane. Such modulation could partially be restrained by compensatory mechanisms promoted to maintain the optimal homeostasis of the system (Abraham, 2008). On the other hand, offline tDCS can induce aftereffects and promote LTP that can modulate performance on the subsequent behavioural task (Nitsche et al., 2003; Nitsche et al., 2004; Nitsche, Liebetanz, et al., 2004). A speculative explanation of the discrepancy we found is that, while in Battaglini et al.'s (2017) study observers' post stimulation performance might have benefited from LTP, in our study the same LTP could have not occurred during the execution of the task (Antal et al., 2012; Pirulli et al., 2013, 2014).

A speculative hypothesis to explain discrepancies between our data and Battaglini et al. (2017) might rely on the coherence measurement method and the task complexity. For example, in our study the coherence of the stimulus was determined via an adaptive staircase (MLP) in which the coherence was varied according to the observer's responses, whereas in Battaglini et al. (2017) observer were performing the direction discrimination task set at seven fixed levels of coherence (from 10% to 70%) with the method of constant stimuli. In particular, in their study the effects for c-tDCS were registered at low levels of coherence, while affects for a-tDCS resulted at medium and high levels of coherence. It could be possible that our task could not trigger the particular tDCS mechanisms proposed by the authors or its strength was limited by the changing of the stimulus coherence level on a trial-by-trial basis. Stimulations could have differently interacted with the neural network subjected to the neural state-dependent activity engaged by the presentation of different stimuli coherence in the two studies (Fertonani & Miniussi, 2017).

When a Cz-forehead mount was used (Experiment 1.2A) no significant difference was observed in coherence thresholds and slopes between hf-tRNS and Sham stimulation for both left and right visual hemi-fields, suggesting that the significant modulatory effect found in Experiment 1.1 was not due to unspecific effects of the stimulation. Furthermore, we hypothesized that the decrement of coherence thresholds for global motion with hf-tRNS depended on the stimulation of the left hMT^{+}, and could not be attributed to the spreading of the current flow over the cortex, also affecting earlier visual areas (Antal et al., 2004c). This prediction was confirmed by the results of a second control experiment in which we stimulated the left V1 (Experiment 1.2B). The results showed no significant

differences in coherence thresholds and slopes between hf-tRNS and Sham stimulation conditions, and no significant differences between the left and right visual hemi-fields. These results suggest specificity in the effect of hf-tRNS, for both the visual hemi-field stimulated and for cortical networks involved in the processing of global motion.

When hf-tRNS is delivered during a motion coherence task, it might interact with the ongoing neural activity responding to the directional signal, thus enhancing the activity of those neurons whose preferred direction is close to the signal direction. Specifically, hf-tRNS may engage motion detectors whose activity is below threshold and may synchronize their firing through a non-linear amplification of subthreshold neural oscillatory activity (Bikson et al., 2004; Fertonani et al., 2011; Miniussi et al., 2013; Ward, 2009). This stimulation-mediated modulation may increment the signal-to-noise ratio at the neural population level, resulting in augmented sensitivity and lower coherence levels of the stimulus.

In conclusion, the results show that hf-tRNS application decreased coherence threshold, while leaving unaffected the slope of the psychometric function. Moreover, both anodal and cathodal tDCS did not show any significant effect for both mean coherence threshold and slope. We demonstrated that hf-tRNS effects were specific for hMT^{+}, since no significant modulation resulted from stimulation of V1 and the frontal cortex.

Interestingly, it has been suggested that global motion perception can be limited by the variability in estimating local motion directions and the ability to integrate these local estimates together. Therefore, the study presented in the following Chapter aims at investigating whether hf-tRNS improvements in global motion direction discrimination are the results of the modulation of local or global processing. In order to do this, we implemented an Equivalent Noise analysis for motion direction discrimination that allowed to measure hf-tRNS effects on the precision with which each dot's direction is estimated and the number of local estimates that can be polled together.

Chapter 3: The effects of hf-tRNS on global motion processing investigated with an equivalent noise analysis

The experiment presented in this chapter has been published in Ghin, F., Pavan, A., Contillo, A., & Mather, G. (2018). The effects of high-frequency transcranial random noise stimulation (hf-tRNS) on global motion processing: An equivalent noise approach. *Brain Stimulation*, 11(6), 1263–1275. https://doi.org/10.1016/j.brs.2018.07.048

3.1 Abstract

One explanation for high coherence thresholds is that they are the consequence of a poor global integration of motion signals. However, there might be additional limiting factors in a motion coherence paradigm that could explain poor global motion processing. In fact, it has been suggested that global motion performance can be also limited by the ability of an observer to estimate the local motion directions and the precision in segregating the signal dots from the random moving dots (Dakin et al., 2005). Differently from classic coherence task the Equivalent Noise (EN) paradigm developed by Dakin et al. (2005) is based on the idea that visual integration is limited by two factors: *internal noise* and *sampling*. During the integration of globally moving dots, changes in *internal noise* would affect the precision with which each dot's direction is estimated, whereas changes in *sampling* levels would influence the number of such local estimates that can be averaged and integrated (Dakin et al., 2005). In order to determine whether hf-tRNS modulates *internal noise* or global *sampling*, we adopted an EN paradigm in which we manipulated stimulus variability (i.e., external noise) to estimate the amount of *internal noise* and *sampling* (Tibber et al., 2014). The results showed that hf-tRNS did not modulate the amount of *internal noise*. This suggests that the ability of the observers to estimate local directions was not affected by hf-tRNS. On the other hand, results indicated that hf-tRNS dramatically increased *sampling*. *Sampling* refers to the number of estimates of single dots' directions that the system can integrate. It is also possible to argue that whereas *internal noise* is linked to the selectivity bandwidth for motion direction, determining the uncertainty with which they respond to a specific direction (Manning, Dakin, Tibber, & Pellicano, 2014), *sampling* is linked to the intensity with which neurons signal a motion direction. Hf-tRNS could spare the selectivity bandwidth of the neurons, but increase the reliability of global motion direction signalling. Moreover, the hf-tRNS effects to increase *sampling* levels might be explained within the stochastic resonance framework for which hf-tRNS could increase the firing of weak signalling neurons coding for a specific motion direction (i.e., *sampling*), and therefore improve the performance.

3.2 Introduction

In Chapter 1, it has been described how the integration of local motion signals occurs in extra-striate cortex areas such as V2, V3, V3A and hMT^+ and that at this stage of elaboration extrapolation of coherent global motion can be achieved (Braddick et al., 2001; Furlan & Smith, 2016; Thompson et al., 2009).

Perception of global motion results from the integration of many local motion vectors in a given space in order to form a global percept with a specific direction (Dakin et al., 2005). Like the 8AFC motion direction discrimination task that has been used in Experiments 1.1 and 1.2 (see Chapter 2), global motion processing is often tested using specific motion coherence paradigms in which the observers are asked to judge the direction of coherently moving dots against a certain amount of randomly moving dots (Figure 3.1A; Newsome & Paré, 1988). This paradigm has been extensively used in physiological studies in both healthy and clinical observers to investigate the mechanisms underlying global motion processing. For example, motion coherence paradigms have been used to test directional and spatial frequency bandwidth of direction discrimination (Bex & Dakin, 2002; Meese & Harris, 2001). Moreover, motion coherence paradigms have been extensively used to test global motion processing in clinical populations affected by glaucoma, amblyopia, schizophrenia, Williams syndrome, autism and dyslexia (Atkinson et al., 2006; Atkinson et al., 1997; Joffe & Raymond, 1997; Li, 2002; Milne et al., 2002; Simmers, Ledgeway, & Hess, 2005; Talcott, Hansen, Assoku, & Stein, 2000), for which high coherence threshold has been found with respect to healthy controls group.

Many psychophysical studies assumed that high coherence threshold is the consequence of a poor global integration of motion signals. However, it has been suggested that there could be additional limiting factors in a motion coherence paradigm that might explain poor global motion processing. In fact, it has been proposed that global motion performance can be also limited by the ability of an observer to estimate the local motion directions (of each dots in a RDK stimulus) and the precision in separate the signal dots form the noise dots (Figure 3.1B-C; Barlow & Tripathy, 1997; Dakin, Mareschal, & Bex, 2005). Based on previous works (Barlow, 1956; Pelli, 1990) Dakin and colleagues (2005) in order to investigate factors that can influence global motion processing, developed the Equivalent Noise (EN) paradigm for motion direction discrimination. In the EN paradigm, analogous to coherent motion tasks, participants are required to discriminate the motion direction of globally moving dots against some level of noise.

EN paradigm works by assessing an observer's ability to judge global motion direction by measuring the influence of external noise (i.e., direction variability) on the performance. However, differently from the classic coherence tasks, in EN directions are drawn from a Gaussian distribution having a specific mean direction and standard deviation. In this case, noise is obtained by increasing the standard deviation of the distribution of motion directions. Therefore, in EN all dots are signal dots, but directional noise can be achieved by increasing the standard deviation with respect to the mean direction. Consequently, higher motion sensitivity depends on the ability to integrate all dot directions (Tibber et al., 2014). The EN paradigm relies on the idea that visual integration is limited by two factors: *internal noise* and *sampling*. For the direction integration of drifting dots *internal noise* would affect the precision of estimating each dot's direction, whereas *sampling* refers to the number of such estimates that can be averaged over (Dakin et al., 2005). In other words, *internal noise* would refer to the local component of motion perception, whereas *sampling* would refer to global motion processing.

Adaptation of EN analysis developed by Dakin et al. (2005) has been successfully used to study global motion processing in vulnerable populations such as in migraine (Tibber et al., 2014), schizophrenia (Tibber et al., 2015) and autism (Manning, Tibber, Charman, Dakin, & Pellicano, 2015). Moreover, motion integration factors of *sampling* and *internal noise* have been tested to study the development of motion processing abilities in childhood (Manning et al., 2014) and in their relation to fine discrimination in the periphery of the visual field (Mareschal, Bex, & Dakin, 2008). In more detail, Tibber and colleagues (2014) used an adapted version on the EN analysis to test in migraine observers, who usually show higher coherence thresholds (Chronicle & Mulleners, 1996; O'Hare & Hibbard, 2016), to study if effect is due to a limited local and global processing or the consequence of a more general integration deficit. The results showed that motion coherence thresholds for the migraine group were higher with respect to the healthy group. However, this was not attributable to a difference in level of *internal noise* and *sampling* between groups, but to a general inability for migraine observers to segregate visual noise from dot directions. Another interesting application of the EN analysis for motion direction was designed to study the development of global motion processing in children (Manning et al., 2014). In children, global motion processing can be limited by poor integration of local motion directions over space, this limitation is due to a relatively slow development of some motion processing that reaches its optimum around the mid-to-late childhood (Manning, Aagten-Murphy, & Pellicano, 2012). Specifically, Manning

et al. (2014) suggested that the relatively slower development of global motion processing could be connected to the higher variability of synaptic transmission and wider directional bandwidths range in V1 neurons in children with respect to adults. The authors argued that high neural variability, or in other words *internal noise*, might reduce the accuracy in estimating single dots directions and in turn lead to higher coherence thresholds. Thus, in order to investigate the factors that influence the developmental of global motion processing the authors applied the EN adaptation proposed in (Tibber et al., 2014) to study how internal noise and sampling develop and the impact of these factors on coherence thresholds in different age ranges. Results showed that *internal noise* levels reduced in relation to the age, whereas *sampling* levels increased. Overall, these studies demonstrated the applicability of the EN paradigm for motion direction on different contexts to study the mechanism of global motion coherence thresholds.

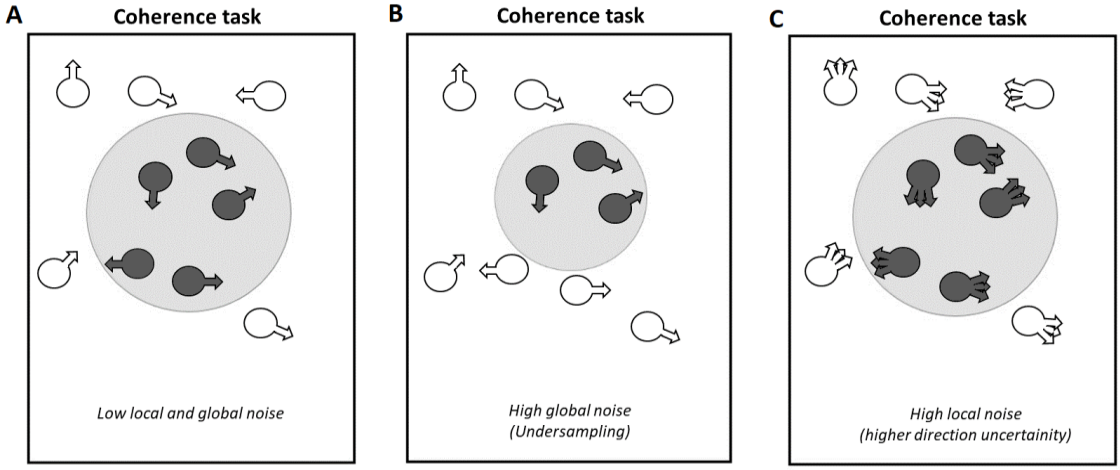

Figure 3.1. Illustration of motion coherence stimuli.
Schematic representation of a classic motion coherence stimulus with the theoretical integration (grey area) in which the performance is measured as the maximum proportion of noise dots tolerable to discriminate coherent directions (A). Observed performance results from the integration of local direction in a given region of space (grey area), and threshold can be limited by (B) the number of motion samples averaged (global factor) and (C) precision in estimate local directions. Adapted from Dakin et al. 2005.

In Chapter 2, we have demonstrated that hf-tRNS delivered over the left hMT$^+$ decreases global motion direction discrimination thresholds. EN analysis can be used to divide coherence performance into separate estimates of local and global processing. Therefore, it is of particular interest to investigate the components of global motion processing enhanced by hf-tRNS. Thus, the aim of Experiment 3 was to use the EN paradigm to investigate the neural mechanisms involved in global motion processing that

are modulated by online hf-tRNS. We implemented an EN paradigm adapted from Barlow (1956), Dakin et al. (2005), and Tibber et al. (2014). We hypothesised that the modulation of coherence thresholds by hf-tRNS that was found in Chapter 2 (Experiment 1.1) might be the result of changes in estimates of the local direction of moving dots, or alternatively on how these local motion estimates are pulled together. During the integration of globally moving dots, changes in *internal noise* would affect the precision with which each dot's direction is estimated, whereas changes in *sampling* levels would influence the number of such local estimates that can be averaged and integrated (Dakin et al., 2005). In order to distinguish between these alternatives, we adopted an Equivalent Noise (EN) paradigm, in which we manipulated stimulus variability (i.e., external noise) to estimate the amount of *internal noise* and *sampling* (Tibber et al., 2014).

Experiment 3

3.3 Methods

3.3.1 Participants

Fourteen participants took part, one who was aware of the hypothesis (AP) and thirteen naïve participants (5 males, age range 18-40 yrs.). Participants were all right handed and had normal or corrected to normal visual acuity. Each participant filled in a questionnaire in order to exclude those with a history of seizure, implanted metal objects, heart problems or any neurological disease. Methods were implemented following the World Medical Association Declaration of Helsinki (2013). The present study was approved by the Ethics Committee of the University of Lincoln. Written informed consent was obtained from each participant prior enrolment in the study and they were paid for their time.

3.3.2 Apparatus

The same apparatus as in Chapter 2 was used.

3.3.3 Stimulation technique

The same stimulator device as in Chapter 2 was used. The hf-tRNS consisted of an alternating current of 1.5 mA with zero offset, applied with random frequencies ranging from 100 to 600Hz. In the Sham condition, stimulation was delivered for 30 sec before the task (Gandiga et al., 2006). The total duration of the stimulation was ~18 min.

The active electrode had an area of 16 cm² whereas the reference electrodes had an area of 60 cm². The current density was maintained well below the safety limits (Bikson et al., 2016; Fertonani et al., 2015). The active electrode was placed over the left human medio-temporal complex (hMT^+) while the reference electrode was placed over the vertex (i.e., Cz). The target area was localized in all observers by using predetermined coordinates as in Chapter 2.

3.3.4 Stimuli and procedure

In order to assess how hf-tRNS modulates local and global processing of visual motion information (i.e., *internal noise* and *sampling*), we implemented the equivalent noise analysis (EN) similar that employed by Tibber et al. (2014). Stimuli were the same as used in Experiment 1.1 and 1.2 of Chapter 2, except for the addition of Gaussian direction noise to the signal dots. Participants performed two stimulation sessions in different days and the order of the stimulation type (either hf-tRNS or Sham) was randomized across participants. In the EN task, participants judged whether moving dots were, *on average*, drifting clockwise or counter-clockwise from vertical-upward motion. A vertical reference was provided at fixation, by means of a black vertical line (4 deg length, 0.1 deg width) crossing the fixation point. For the EN paradigm, observers performed two staircases (Levitt, 1971) separately. The first staircase controlled a "zero external noise" condition (Figure 3.2A) in which the external noise was set to zero (i.e., the standard deviation of the normal distribution of directions was set to zero). The second staircase controlled a "high external noise" condition (Figure 3.2B; i.e., the standard deviation of the normal distribution of direction was variable). In the "zero external noise" condition, a simple 1-up / 1-down staircase tracked the minimum directional offset from vertical, whereas in the "high external noise" condition a 1-up / 2-down staircase tracked the maximum level of external noise that could be tolerated by the observer. That is, the staircase tracked the standard deviation of the normal distribution of directions that produced a direction discrimination performance of 70.7%. In this latter condition, the signal level (i.e., the mean of the normal distribution of direction) was either 45° clockwise or 45° counter-clockwise (Tibber et al., 2014). Staircases terminated after 300 trials.

For each participant, for each stimulation type (hf-tRNS and Sham), and for each visual hemi-field (left and right) we estimated *internal noise* and *sampling*. All experimental blocks were preceded by eight practice trials. In addition, for the "high

external noise" condition, we inserted eight catch trials in which the standard deviation of the normal distribution of directions was set to zero, i.e., zero noise condition. This was done to ensure that participants' attention was focused and they were not guessing. In the following paragraph, we report the Equivalent Noise analysis and how *internal noise* and *global sampling* estimates were derived.

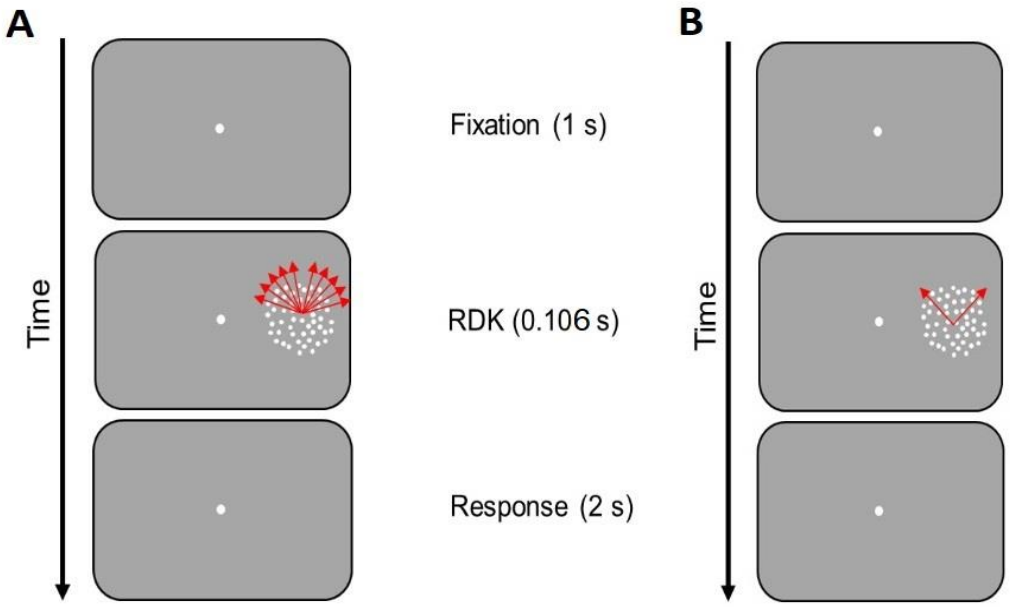

Figure 3.2. Illustration of the experimental tasks.
(A) Representation of the "zero external noise" condition in which a simple 1–up / 1-down staircase tracked the minimum directional offset from vertical. (B) The "high external noise" condition in which a 1-up / 2-down staircase tracked the maximum level of external noise that could be tolerated by the observer. The red arrows represent the direction of signal dots.

3.3.5 Equivalent Noise Analysis

The core of the Equivalent Noise (EN) parameterisation, as introduced in Dakin et al. (2005), consists in describing the total amount of uncertainty in the perception of the stimulus σ_{obs} as the quadratic sum of two independent components:

$$\sigma_{obs}^2 = \frac{\sigma_{\text{int}}^2 + \sigma_{ext}^2}{\eta_{samp}} \qquad \text{Eq. (3.1)}$$

The first component σ_{ext} is related to the noise carried by the stimulus (i.e., external noise). The second component σ_{int} encodes the uncertainty that is intrinsic to the observer (i.e.,

internal noise). The sum is rescaled by a factor η_{samp} representing the effective number of simultaneous *sampling*s that are performed on the stimulus by the observer (i.e., *sampling*). While the external noise σ_{ext} and the observed noise σ_{obs} are directly measurable, the *internal noise* σ_{int} and the number of *sampling*s η_{samp} must be computed through Eq. (3.1), thus providing an effective characterisation of the observer.

As aforementioned, and based on Tibber et al. (2014), the characterisation was performed through two independent measurements, respectively at *high external noise* and at *zero external noise*. The *high external noise* data point was the average of the last half of reversals of each 1-up / 2-down staircase: σ_{obs} was identically equal to 45° ($\pi/4$ radians), while σ_{ext} was the external noise corresponding to an observer accuracy of 70.7% in motion direction discrimination (Figure 3.3). The error associated to the measure was the standard deviation of the considered reversals. Regarding the *zero external noise* point, the staircase entries were divided into bins of 0.5° ($8.73 \cdot 10^{-3}$ radians) width. The clockwise rate of non-empty bins, defined as the ratio between the number of clockwise responses and the total number of trials pertaining to each bin, was fitted against a cumulative Gaussian function:

$$CG(\theta) = \frac{1}{2}\left[\mathrm{erf}\left(\frac{\theta-\theta_0}{\sqrt{2}s}\right) - \mathrm{erf}\left(\frac{\pi/2-\theta_0}{\sqrt{2}s}\right)\right] \qquad \text{Eq. (3.2)}$$

the angle θ_0 corresponds to the 50% clockwise rate (i.e., the subjective vertical direction), while s is the standard deviation of the original Gaussian and encodes the slope of the cumulative function. The fitted function was used to compute the angle corresponding to 70.7% clockwise rate, which was defined as σ_{obs} corresponding to vanishing σ_{ext}. The standard error associated to the observed noise was computed by propagating the fit uncertainties.

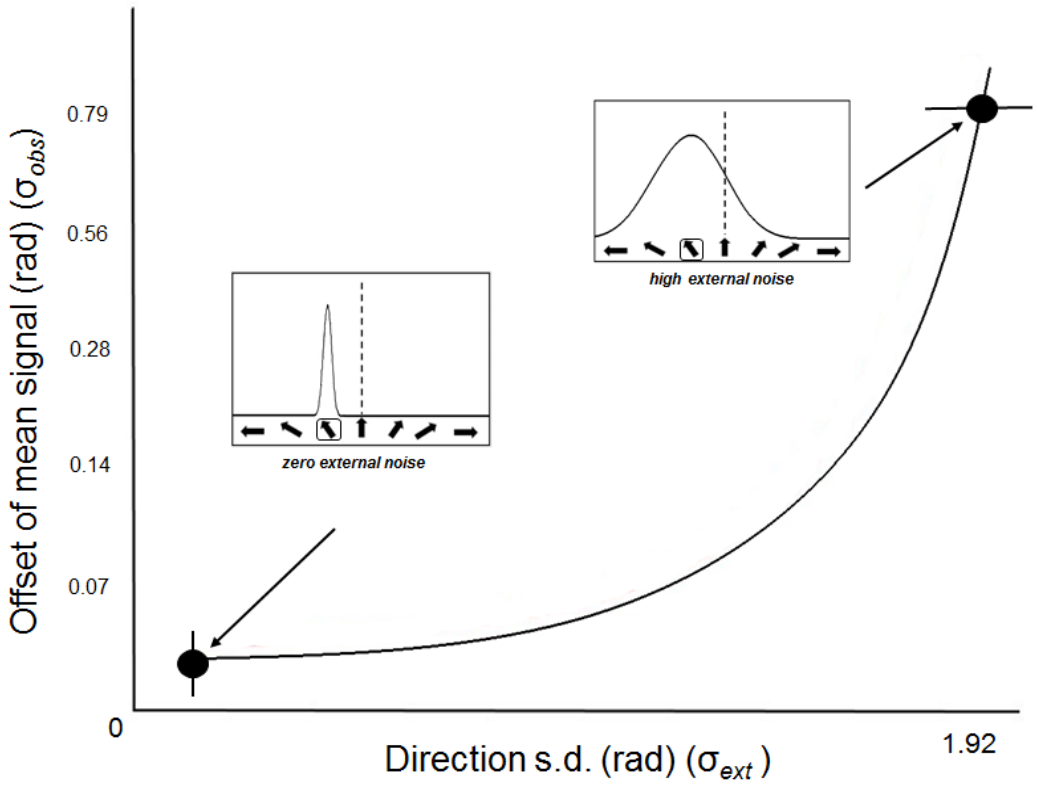

Figure 3.3. Representation of the Equivalent Noise function (solid black line).
The EN function is constrained by two threshold values: the "zero external noise" threshold, which represents the minimum directional offset from vertical that can be discriminated with no external noise, and the "high external noise" threshold, which represents the maximum level of noise (i.e., the directional standard deviation of the normal distribution of directions) that can be tolerated for a large directional offset.

Before computing the EN parameters, there is an important detail that is worthwhile to point out, related to the periodic nature of motion directions. The actual amount of external noise σ_{ext} differs from the standard deviation of the stimulus distribution (σ_{noise}), due to the wrapping generated by the periodicity of directions. The issue had already been pointed out by Dakin et al. (2005), whose solution made use of a simulated observer (based on Monte Carlo simulations) to extract the best fitting values of σ_{int} and η_{samp}. However, we used a different approach. A wrapped normal distribution of given standard deviation σ_{noise} is restricted to a 360° (2π radians) interval centred in the mean orientation. Within such interval, the distribution resembles a non-wrapped distribution as long as $\sigma_{noise} \ll 180°$ (π radians) (see Figure 3.4A). For larger values, the superposition of the Gaussian tails forces the wrapped distribution to acquire non-zero values in correspondence to the interval boundaries (see Figure 3.4B and 3.4C).

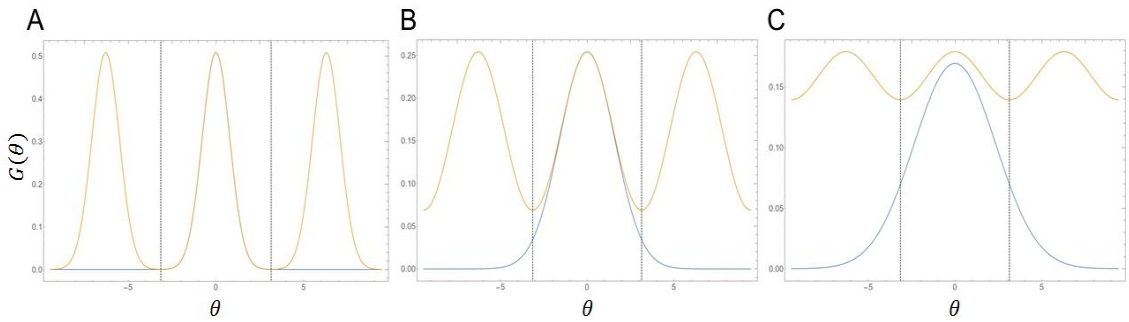

Figure 3.4. Gaussian and Wrapped Gaussian distribution at increasing σ_{noise}.
(A) Plot of Gaussian (blue) and wrapped Gaussian (yellow) distributions when σ_{noise} is 45° ($\pi/4$ radians). The extremes of the plot represent $\pm 3\pi$. (B) Plot of Gaussian (blue) and wrapped Gaussian (yellow) distributions when σ_{noise} is 90° ($\pi/2$ radians). (C) Plot of Gaussian (blue) and wrapped Gaussian (yellow) distributions when σ_{noise} is 135° ($3\pi/4$ radians). Consider the first two valleys in the interval $\pm\pi$, increasing σ_{noise} the tails of the wrapped Gaussian distribution overlap and this generates an increase of the tails (panel B) and then of the whole distribution (panel C). Besides, the wrapped Gaussian distribution widens.

Our correction consisted in generating a random set of points following a wrapped distribution of standard deviation σ_{noise} and fitting it with a non-wrapped Gaussian, whose standard deviation was then identified as the "effective width" of the distribution, i.e., the external noise σ_{ext}. By iterating the procedure for a uniform distribution of σ_{noise} in the interval $(0, \pi)$ and fitting the resulting points, we ended up with a relation between the "bare" deviation σ_{noise} and the effective σ_{ext}. As it can be seen in Figure 3.5, such relation is robustly linear for small σ_{noise} values, departing from the $\sigma_{ext} = \sigma_{noise}$ line as $\sigma_{noise} \sim 90°$ ($\pi/2$ radians). Afterwards, σ_{ext} grows quickly, exceeding 360° (2π radians) (no perceivable preferred direction) as $\sigma_{noise} \simeq 156°$ (2.72 radians). For obvious reasons, it was only necessary to apply this wrapping correction to the high noise data point.

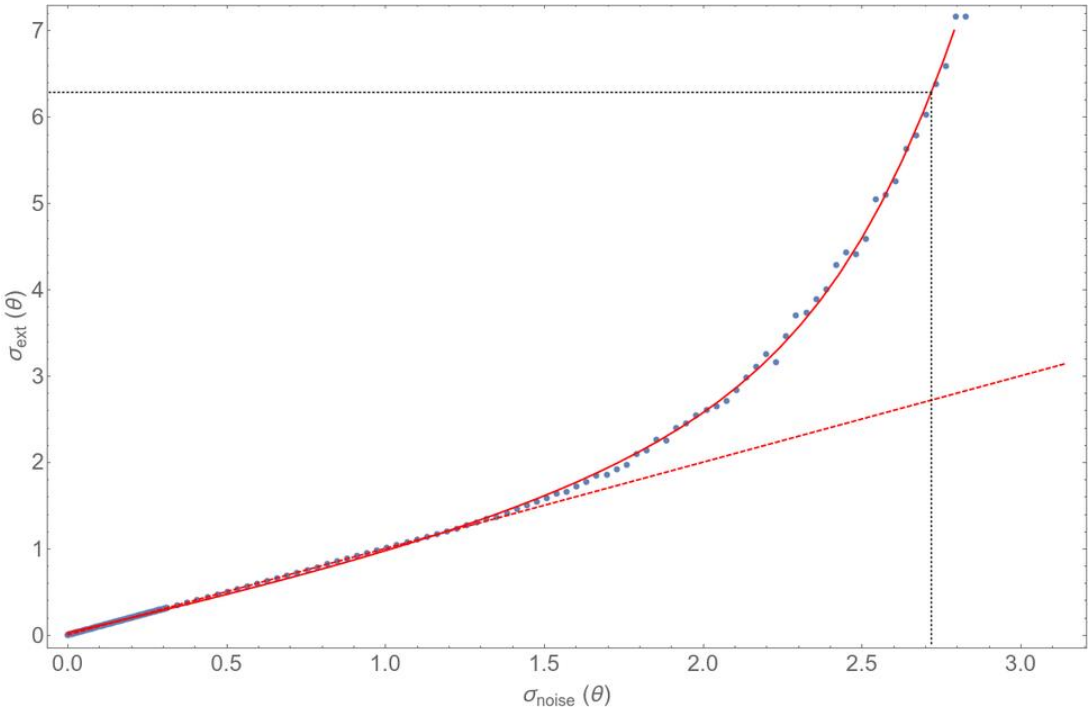

Figure 3.5. Relation between σ_{noise} and σ_{ext} (in radians).
Blue points indicate the uniform distribution of σ_{noise} fitted with a generalised hyperbolic function (solid red line). The $\sigma_{ext} = \sigma_{noise}$ line, from which the fitted curve departs at $\sigma_{noise} \sim 90°$, is depicted as well (dashed red line). Dotted black lines indicate the position of the point corresponding to $\sigma_{noise} = 156°$ (2.72 radians) and $\sigma_{ext} = 360°$ (2π radians) (no perceivable preferred direction).

Since the two data points lied in two separate regimes, it was possible to further simplify the computation of the EN parameters. First of all, assuming $\sigma_{ext} \gg \sigma_{int}$ for the high noise data point, Equation 3.1 becomes:

$$\sigma_{obs}^2 \simeq \frac{\sigma_{ext}^2}{\eta_{samp}} \qquad \text{Eq. (3.3)}$$

from which it was possible to retrieve the effective *sampling* size η_{samp} associated to each subject:

$$\eta_{samp} \simeq \frac{\sigma_{ext}^2}{\sigma_{obs}^2} \qquad \text{Eq. (3.4)}$$

The *internal noise* was then computed from the zero noise data point, for which it holds:

$$\sigma_{obs}^2 = \frac{\sigma_{\text{int}}^2}{\eta_{samp}} \quad \text{Eq. (3.5)}$$

leading to the *internal noise* estimate for each subject:

$$\sigma_{\text{int}} = \sigma_{obs}\sqrt{\eta_{samp}} \quad \text{Eq. (3.6)}$$

Obviously, each pair $\{\eta_{samp}, \sigma_{\text{int}}\}$ comes with uncertainties $\{\delta\eta_{samp}, \delta\sigma_{\text{int}}\}$ that are the simple propagations of the external noise uncertainty $\delta\sigma_{ext}$ of the high external noise point and the observed noise uncertainty $\delta\sigma_{obs}$ of the zero external noise point. The expressions defining such uncertainties are:

$$\delta\eta_{samp} = \frac{2\sigma_{ext}}{\sigma_{obs}^2}\delta\sigma_{ext} \quad \text{Eq. (3.7)}$$

$$\delta\sigma_{\text{int}} = \sqrt{\eta_{samp}(\delta\sigma_{obs})^2 + \frac{\sigma_{obs}^2}{4\eta_{samp}}\left(\delta\eta_{samp}\right)^2} \quad \text{Eq. (3.8)}$$

It is evident that observers with more precise measurements resulted in EN parameters with smaller uncertainties.

3.4 Results

Figure 3.6 shows the result of Experiment 3. Data were analysed using Generalised Estimating Equations (GEE; Liang & Zeger, 1986). GEE analysis uses a quasi-likelihood method to estimate regression coefficients (β) and standard errors (SE) with sampling distributions, and can be used to test main effects and interactions between the dependent variable and corresponding predictor variables (Ballinger, 2004). GEE can be considered an extension of generalized linear models implementing corrections for the dependency of within subjects repeated measurements, by applying a working correlation matrix.

GEE was used to analyse *internal noise* and *sampling* estimated with the EN analysis and weighted for their uncertainty values as defined in Eq. (3.7) and Eq. (3.8). Weights were entered in the GEE analysis. A Shapiro-Wilk test showed that results for *internal noise* were not normally distributed (p = 0.001) with a positive skewness 1.22 (SE: 0.32), thus a Gamma function and identity link transformation function were used

in the GEE models. In the first model, *internal noise* was the dependent variable, and stimulation type (hf-tRNS vs. Sham), visual hemi-field (right vs. left) and interaction between stimulation type and visual hemi-field were the predictors. An exchangeable correlation matrix was chosen as it showed a better fit with respect to independent and unstructured correlation matrices. Correlation matrix was selected based on the Quasi-likelihood Information Criterion (QIC criteria; Pan, 2001). Exchangeable correlation matrix is indicated when there is no logical order of the measurements and they are equally correlated within subjects and not necessarily collected over time (Horton & Lipsitz, 1999). However, it should be noted that GEE analysis is assumed to be robust even against the choice of an incorrect correlational structure (Ghisletta & Spini, 2004). No significant effect for any predictor for *internal noise* was found (Table 3.1).

Table 3.1. GEE analysis results for *internal noise* estimates

Coefficient	**Estimate (β)**	**Std.err (SE)**	**Wald**	**Pr (> |W|)**
Intercept	0.09145	0.01002	83.33	<0.001
Stimulation Type	-0.00282	0.01815	0.02	0.88
Visual hemi-field	0.004235	0.01782	0.06	0.81
Stimulation type * Visual hemi-field	-0.00932	0.022612	0.17	0.68

Estimated coefficients, standard error, Wald statistics and *p* values for stimulation type, visual hemi-field and stimulation type x visual hemi-field predictors.

The same GEE model was also applied to analyse *sampling* estimates (Table 3.2). A Shapiro-Wilk test showed that results for *sampling* were not normally distributed ($p < 0.001$) with a positive skewness 1.30 (SE: 0.32). Gamma function and identity link transformation function were used. Stimulation type (hf-tRNS vs. Sham), visual hemi-field (right vs. left) and interaction between stimulation type and visual hemi-field were included as predictors. An exchangeable working correlation matrix was also used. Comparison of parameters is illustrated in Table 3.2. The analysis reported a significant effect for stimulation type ($\beta = 1.719$, SE = 0.695, $p < 0.02$) and interaction between stimulation type and visual hemi-field ($\beta = -2.126$, SE = 0.613, $p < 0.001$), while visual hemi-field predictor did not reach statistical significance ($\beta = 0.231$, SE = 0.314, $p > 0.05$). Post-hoc comparisons with a FDR at 0.05 reported a significant difference between hf-tRNS and Sham stimulation for the right visual hemi-field ($p = 0.047$, $d = 0.36$), and a significant difference between the right visual hemi-field and the left visual hemi-field

when hf-tRNS was applied (p = 0.019, d=0.51). No significant differences were found between right and left visual hemi-field for Sham stimulation (p = 0.50, d = 0.02), between hf-tRNS and Sham when just the left visual hemi-field was considered (p = 0.24, d = 0.18), between right visual hemi-field with hf-tRNS and left visual hemi-field with Sham (p = 0.13, d = 0.30), and between right visual hemi-field with Sham stimulation and left visual hemi-field with hf-tRNS (p = 0.50, d = 0.16).

Table 3.2. GEE analysis results for *Sampling*.

Coefficient	**Estimate (β)**	**Std.err (SE)**	**Wald**	**Pr (> |W|)**
Intercept	2.609	0.181	206.74	<0.001
Stimulation Type	1.719	0.695	6.12	**0.013***
Visual hemi-field	0.231	0.314	0.54	0.48
Stimulation type * Visual hemi-field	-2.126	0.613	12.94	**<0.001***

Estimated coefficients, standard error, Wald statistics and p-value for stimulation type, visual hemi-field and stimulation type x visual hemi-field predictors.

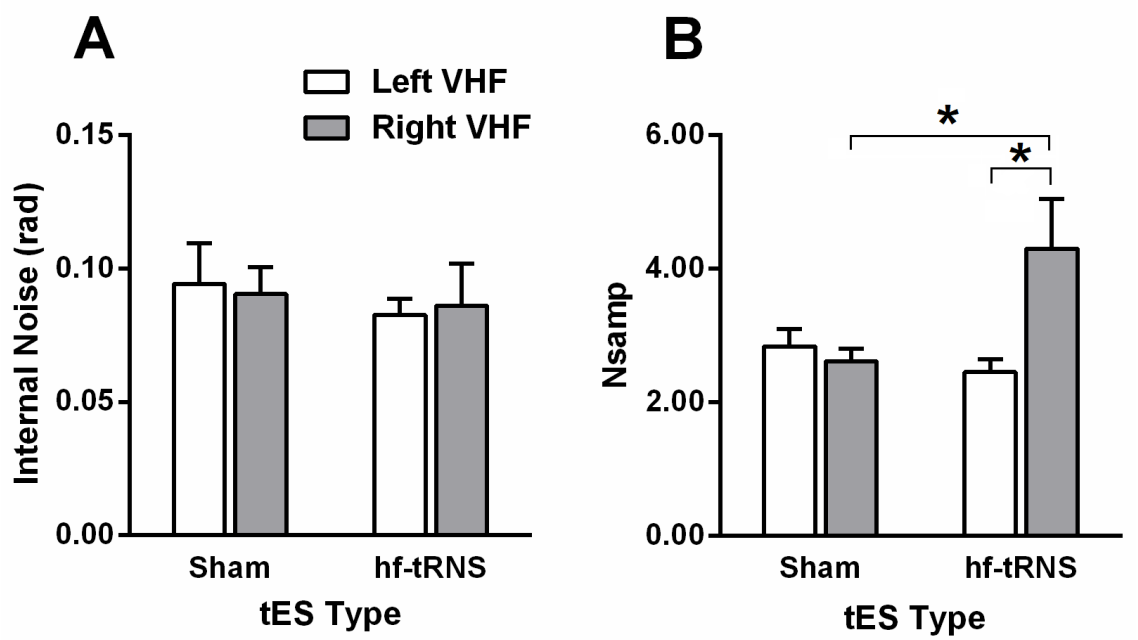

Figure 3.6. Results of Experiment 3. (A) Mean internal noise estimates (in radians) for left and right visual hemi-fields and for Sham and hf-tRNS stimulations. (B) Mean sampling estimate for left and right visual hemi-fields and for Sham and hf-tRNS stimulations. Error bars ±SEM. Asterisks (*) show significant differences.

3.5 Discussion

Classic motion coherence tasks like the one used in Chapter 2 cannot disentangle the mechanisms underlying local and global motion processing (Dakin et al., 2005; Manning et al., 2014; Tibber et al., 2014). In general, an observer's performance in a motion discrimination task is not just limited by the visual system's ability to integrate multiple motion cues across time and space (*sampling*), but also by the ability to determine individual dot trajectories and to segregate the dots composing the signal from those drifting in random directions (i.e., noise); these latter mechanisms are particularly influenced by *internal noise* (Dakin et al., 2005; Tibber et al., 2014). By using an Equivalent Noise paradigm, we aimed at estimating the amount of *internal noise* and *sampling* associated with a global motion direction discrimination task and assessing how the underlying mechanisms are modulated by hf-tRNS.

Specifically, we tested if hf-tRNS was able to modulate levels of *internal noise* and *sampling* when delivered over the left hMT^{+}. The results showed that hf-tRNS did not modulate the amount of *internal noise* with respect to Sham stimulation in both visual hemi-fields, suggesting that the ability of the observers to estimate local cue directions was not affected by the real stimulation. On the other hand, results indicated that hf-tRNS dramatically increased *sampling* for the right visual hemi-field with respect to Sham stimulation and with respect to the left visual hemi-field. *Sampling* refers to the number of estimates of single dots' directions that the system can integrate.

When motion direction discrimination performance is measured in the periphery using motion coherence paradigms or moving drifting Gabors, coherence thresholds are usually higher than those measured in the fovea (Levi, Klein, & Aitsebaomo, 1984; Raymond, 1994). Mareschal et al. (2008) by applying the EN analysis investigated if higher motion direction discrimination thresholds measured in the peripheral visual fields are the results of a high level of internal noise, lower sampling or the combination of both. The authors found that direction discrimination thresholds increased with the eccentricity of the stimulus. Most importantly, while *sampling* levels remained constant independently of the eccentricity, the threshold increment resulted from increased levels of *internal noise* (e.g., the uncertainty in estimating local directions in the stimulus). The authors suggested that the uncertainty in estimating local directions was related to the proprieties of local motion detectors present in V1, which shows a decrement of direction selectively when a stimulus is presented towards more peripheral locations in the visual field. In other words, Mareschal et al. (2008) suggested that as a function of eccentricity

within V1 there is a relationship between directional selectivity and size of receptive field, for which higher degrees of eccentricity in V1 correspond to larger receptive fields and lower directional selectivity (i.e., higher *internal noise*). Furthermore, the extent of this relationship decreases in higher level areas of visual motion processing, since the size of receptive fields shows no dependency with respect to eccentricity in VST and MT (Mikami, Newsome, & Wurtz, 1986). Manning et al. (2014) pointed out that while the EN analysis gives the estimate of *internal noise* levels, its origin is not completely defined. Therefore, it is not entirely clear the extent to which high levels of direction uncertainty in V1 neurons affects levels of *internal noise* of hMT^+ neurons. It might be possible to hypothesize that levels of *internal noise* measured during our motion direction discrimination task might be highly dependent on V1 neurons precision to signal local motion direction. On the other hand, Mareschal et al. (2008) suggest that the relative consistency of *sampling* levels across the visual field might be the result of the activity of motion selective neurons in global motion sensitive areas which might be responsible of pooling local motion direction across space. Therefore, we could speculate that delivering hf-tRNS over the hMT^+ might not be effective to modulate the direction uncertainty coded by motion sensible neurons in hMT^+ and in turn leaving *internal noise* levels unchanged. Furthermore, it is also possible to argue that whereas *internal noise* is linked to the selectivity bandwidth for motion direction, determining the uncertainty with which they respond to a specific direction (Manning et al., 2014) *sampling* is linked to the intensity with which neurons signal a motion direction. Therefore, hf-tRNS could spare the selectivity bandwidth of the neurons, but increase the reliability of global motion direction signalling.

The hf-tRNS-related *sampling* increment could depend on the stochastic resonance phenomenon. Stochastic resonance (Moss et al., 2004) is a non-linear phenomenon whereby the addition of an optimal level of a random interference (i.e., noise) can enhance the detection of weak stimuli or enhance the information content of a signal. Hf-tRNS involves a random frequency and intensity of stimulation that might induce random activity, thus neural noise, in a non-linear system like the brain that might enhance the sensitivity of neurons to a weak stimulus (Miniussi et al., 2013; Schwarzkopf et al., 2011). Recently, van der Groen and Wenderoth (2016) found that the injection of different hf-tRNS intensities modulated detection accuracy of subthreshold stimuli in a stochastic resonance manner. The effects of hf-tRNS on global motion direction discrimination might be explained within the stochastic resonance framework; that is, the neural noise induced by hf-tRNS could increase the signalling of neurons to a specific

motion direction (i.e., *sampling*), and consequently improve the performance. Therefore, to further explore this hypothesis the study presented in the next Chapter will investigate whether the underlying mechanisms of hf-tRNS can be explained within the stochastic resonance framework.

Chapter 4: Modulatory mechanisms underlying high-frequency transcranial random noise stimulation (hf-tRNS): a stochastic resonance approach

The experiments presented in this chapter have been previously published in: Pavan, A., Ghin, F., Contillo, A., Milesi, C., Campana, G., & Mather, G. (2019). Modulatory mechanisms underlying high-frequency transcranial random noise stimulation (hf-tRNS): A combined stochastic resonance and equivalent noise approach. *Brain Stimulation*. https://doi.org/10.1016/j.brs.2019.02.018

4.1 Abstract

In the last decade, hf-tRNS has demonstrated to increase both cognitive and sensory abilities. Though there is evidence that hf-tRNS induces facilitation at the behavioural level, its neural mechanisms are still debated. One proposed mechanism is that hf-tRNS effects can be explained within the stochastic resonance phenomenon. Stochastic resonance is a phenomenon whereby the addition of an optimal amount of random interference (i.e., noise) into a dynamic system can enhance the detection of threshold stimuli or enhance the information content of a signal, whereas if too much noise is added, this can hinder signal detection or information content. (McDonnell & Abbott, 2009; Moss et al., 2004; Ward, 2009). It has been suggested that due to its characteristics, hf-tRNS stimulation might induce non-focal modulation (Antal & Herrmann, 2016; Miniussi et al., 2013) and that could inject an external source of neural noise. In the present study, we assumed that the noise level injected into the system is proportional to the hf-tRNS intensity (van der Groen et al., 2018; van der Groen & Wenderoth, 2016). Specifically, in a series of experiments, we tested whether hf-tRNS delivered at different intensities modulates motion direction discrimination in a way that is compatible with the stochastic resonance phenomenon. Observers performed a motion direction discrimination task, with moving random dot kinematograms (RDKs) presented near threshold, i.e., with a motion coherence producing approximately 60% of correct direction discrimination. The results showed that, current intensities of 1.0 mA and 1.5 mA produced a significant improvement in motion direction discrimination performance, whereas performance was significantly impaired with respect to the baseline when stimulating at 2.25 mA. Taken together these results support the notion that hf-tRNS effects on the visual cortex could be explained within the stochastic resonance framework.

4.2 Introduction

The results presented in the previous chapters demonstrated that online hf-tRNS during a motion direction discrimination task decreases coherence thresholds (Chapter 2) and increases the number of directional signals that can be integrated at time (Chapter 3). However, the lack of studies at the cellular level in both human and non-humans subjects limits our understanding of the mechanism of action of this technique (Antal & Herrmann, 2016). Since its first application it has been proposed that tRNS induces a repetitive opening of the Na^+ channels (Terney et al., 2008) shortening the hyperpolarization phase. This hypothesis is supported by pharmacological evidence showing that administration of sodium channel blocker carbamazepine reduced tRNS excitability effects (Chaieb et al., 2015). Moreover, in a recent study Remedios et al. (2019) investigated the effects of short bursts (250 ms) of different random noise electrical stimulation (RNS) levels (ranging from 0 mV to 0.445 mV) on the peak amplitude of Na^+ inward current of *in-vitro* rats' pyramidal neurons from the somatosensory and auditory cerebral cortex. Their results showed that the peak amplitude changed depending on the level of random noise injected, with significant amplitude increments when intermediate "optimal RNS" levels were injected with respect to "zero RNS" and "high RNS" levels. Interestingly, peak amplitude results depicted an inverted U-like shape as a function of RNS levels with peak increments at the intermediate RNS that the authors associated to a stochastic resonance phenomenon happening at the cellular level (Bezrukov & Vodyanoy, 1995). These results seem to support the proposed hypothesis that tRNS effects observed in human studies could be explained within the stochastic resonance framework (Fertonani et al., 2011; Miniussi et al., 2013; Terney et al., 2008). Stochastic resonance phenomenon has been applied in several contexts spacing from engineering, climate models and biological systems. The general idea behind this theory is that, provided a non-linear system, if an "optimal" amount of noise is applied to the system it can lead to an enhanced output signal or information content (McDonnell & Abbott, 2009; Ward, 2009). In its simplest description, stochastic resonance results from the combination of a threshold, a subthreshold stimulus and noise (see Figure 1.2, Chapter 1). In this paradigm, a signal/stimulus can be encoded or perceived when a threshold crossing happens and if the stimulus/signal is by definition subthreshold, the chance of this to cross the threshold is limited. However, according to the stochastic resonance phenomenon, if noise is added to the stimulus/signal the probability of a threshold crossing to happen increases substantially (Moss et al., 2004).

There is psychophysical evidence that adding noise to a visual or an auditory stimulus can improve detectability and discriminability of a signal (Kitajo, Nozaki, Ward, & Yamamoto, 2003; Riani & Simonotto, 1994; Simonotto et al., 1997; Treviño, la Torre-Valdovinos, & Manjarrez, 2016; Zeng, Fu, & Morse, 2000). For example, Kitajo et al. (2003) demonstrated that the stochastic resonance phenomenon can occur in the human visual cortex by measuring responses in a sensorimotor integration task in which observers were asked to match the force of their handgrip to the luminance level of a subthreshold uniform square image. Importantly, using a mirror stereoscope, the square image was presented only in the right eye, whereas only a random visual stimulus was presented in the left eye. Results showed that the responses to the subthreshold image improved when an optimal amount of Gaussian white noise was added either to the stimuli presented in the right or left eye. Furthermore, the authors suggested that the increased detectability of the square image when noise was presented on the contralateral side (i.e. on the left eye), demonstrated that behavioural stochastic resonance can occur at a level where integration (possibly via binocular interaction) between stimulus and noise takes place. Further evidence that visual noise can increase the signal-to-noise ratio have been also recently demonstrated in a motion direction discrimination task by Treviño et al. (2016). In this study the authors investigated if additive background noise modulated the observer's ability to discriminate directions in a random dot motion task. Results showed that when an intermediate level of background noise was added to the task, it increased the number of correct responses. Furthermore, this improvement was present when motion signal and noise were presented in both eyes and when motion signal and noise were presented separately in each eye, supporting the findings of Kitajo et al. (2003) which suggested that stochastic resonance can occur at the visual cortex level.

tRNS delivers current at random intensities and frequencies within specific ranges, and it has been proposed to induce random activity and thus neural noise. Therefore, the presence of an optimal amount of neural tRNS-induced noise could enhance the sensitivity to a weak stimulus (Miniussi et al., 2013). Recently, van der Groen and colleagues (2016) found supporting evidence to explain the effects of hf-tRNS on the visual cortex within the stochastic resonance framework. In this study observers were asked to detect a Gabor patch with a vertical orientation in one among eight possible target locations around a central fixation point. Participants took part in different experimental conditions where different intensities of noise were added either visually directly on the stimulus or via hf-tRNS over the primary visual cortex. In particular, in the hf-tRNS condition the level of noise was assumed to be proportional to the intensity

of the stimulation ranging from 0 up to 1.5 mA. Results showed that contrast detection threshold improved in both experimental conditions depending on the additional intensity of noise. Specifically, contrast detection improved when the intensity of the random current was delivered at an optimal intensity level at approximately 1.0 mA. Further increasing of hf-tRNS intensity had a detrimental effect on detection performance, bringing it to the same level as when no stimulation was applied following the typical inverted U-like shape function hallmark of the stochastic resonance phenomenon (van der Groen & Wenderoth, 2016) . Importantly, the effect of the additional noise was evident only when the stimulus was presented near the individual threshold (i.e., 60% correct detection), but not when participant performed the task in a suprathreshold condition (i.e. 80% correct detection).

In the present study, we used a similar approach to that of van der Groen and Wenderoth (2016). In a series of experiments we tested whether hf-tRNS delivered at different intensities modulates motion direction discrimination in a way that is compatible with the stochastic resonance phenomenon. We also measured whether delivering hf-tRNS at an intensity above the optimal level could have a detrimental effect on motion direction discrimination. Therefore, we aimed at investigating whether the presence of facilitatory and suppressive effects of hf-tRNS at different intensities may reveal the underlying modulatory mechanism of random noise stimulation. Specifically, we devised a two-interval forced-choice motion direction discrimination task in which observers had to discriminate whether two *globally* moving random dot kinematograms (RDKs) presented in distinct temporal intervals, had the same or different motion directions. Based on van der Groen and Wenderoth (van der Groen & Wenderoth, 2016), the coherence level of the moving RDKs was adjusted to attain 60% correct direction discrimination before hf-tRNS stimulation. Hf-tRNS was then applied bilaterally over the human medial-temporal complex hMT^{+}; a visual area closely involved in dynamic information processing (Stigliani, Jeska, & Grill-Spector, 2017), with current intensities ranging from 0.5 mA to 2.25 mA. In an additional control experiment we also devised a condition to test hf-tRNS effects on suprathreshold stimuli in which observers were asked to perform the same motion direction discrimination task, but presenting moving stimuli at 100% coherence.

4.3 Experiment 4.1

The aim of Experiment 4.1A was to assess the modulatory effect of four different hf-tRNS intensities (0.5, 0.75, 1.0 and 1.5 mA) on a motion direction discrimination task. The rationale was based on the stochastic resonance phenomenon. Participants performed a motion direction discrimination task with a coherence near threshold (i.e., motion coherence producing 60% correct discrimination). We hypothesized that this weak motion signal can be boosted by adding an optimal level of external noise with hf-tRNS. In particular, we expected that increasing the stimulation intensity up to an optimal level would improve motion direction discrimination performance (Miniussi et al., 2013; Schwarzkopf et al., 2011; van der Groen et al., 2018; van der Groen & Wenderoth, 2016). Experiment 4.1B was carried out as a control condition, using Sham stimulation.

4.3.1 Methods

4.3.1.1 Participants

The author and twenty-three naïve participants (11males, age range 18-40 yrs.) took part in Experiment 4.1. Twelve participants took part in Experiment 4.1A and twelve in Experiment 4.1B. Participants were all right-handed, and with normal or corrected to normal visual acuity. Each participant filled in a questionnaire to exclude participants with implanted metal objects, heart problems, history of seizure or any neurological disease. Methods were implemented following the World Medical Association Declaration of Helsinki (2013). The present study was approved by the Ethics Committee of the University of Lincoln. Written informed consent was obtained from each participant prior the enrolment in the study and they were paid for their time.

4.3.1.2 Apparatus

The same apparatus as in Chapter 2 and 3 was used.

4.3.1.3 Stimuli

Stimuli were global motion random dot kinematograms (RDKs) made up by 400 white dots (diameter: 0.12 deg) presented at the centre of the screen within a circular aperture with a diameter of 12 deg. Dot density was 3.54 dots/deg^2. The duration of the RDK was 0.13 s. Dots drifted at a speed of 5.04 deg/s and had a limited lifetime of 47 ms (4 screen refreshes); after a dot vanished, it was replaced by a new dot at a different

randomly selected position within the circular window. Dots appeared asynchronously on the display and had an equal probability of being selected as either signal or noise dots (Morgan & Ward, 1980; Newsome & Pare, 1988). Short lifetime was implemented to minimize the presence of local "motion streaks" (Geisler, 1999) that could provide strong static cues for motion direction discrimination. In addition, dots that moved outside the circular window were replaced by a new dot at a different randomly location within the circular window, thus maintaining the same density. Signal dots were either constrained to move globally leftward or rightward. Noise dots moved in random directions.

4.3.1.4 Stimulation technique

The same stimulator device as in Chapter 2 and 3 was used. The hf-tRNS in Experiment 4.1A consisted of an alternating current delivered at four different intensities of 0.5, 0.75, 1.0 and 1.5mA with zero offset and applied with random frequencies ranging from 100 to 600 Hz. The total duration of the stimulation was approximately 20 minutes. In Experiment 4.1B Sham stimulation was delivered at 1.5 mA and for 30 s before the task (Gandiga et al., 2006). The stimulation in both Experiments 4.1A and 4.1B was delivered bilaterally; one electrode was placed over the left-hMT^+, while a second electrode was placed over the right-hMT^+. The two electrodes had an area of 16 cm^2 and the current density was maintained below the maximum safety limits (Bikson et al., 2016; Fertonani et al., 2015). The target areas were localized in all observers by using predetermined coordinates as in Chapter 2 and 3, therefore 3 cm dorsal to inion and 5 cm leftward and rightward from there for the localization of the hMT^+.

4.3.1.5 Procedure

The procedure consisted of three phases:

Phase 1: Coherence threshold estimation

In Experiment 4.1A participants took part in four experimental sessions carried out in four different and non-consecutive days, while in Experiment 4.1B participants performed one session (Sham stimulation). However, the same procedure was used in both experiments. At the beginning of each session, observers performed a two-interval forced choice (2IFC) motion direction discrimination task (Figure 4.1) to estimate the individual coherence threshold. The RDKs were presented at the centre of the screen. Participants had to report whether the RDKs presented in the two temporal intervals had

the same or different motion directions. Each trial consisted of a fixation point presented for 1 s, followed by two 0.13 s RDKs, with an interval of 0.5 s between the two presentations. An adaptive staircase (MLP; Grassi & Soranzo, 2009; Green, 1993) was used to track the coherence level producing an accuracy of 60% in motion direction discrimination. The staircase involved 32 trials.

Phase 2: Assessing the level of accuracy at coherence threshold

In order to precisely estimate the individual coherence threshold producing an accuracy of 60% in motion direction discrimination, observers performed the same direction discrimination task as in *Phase 1* at the coherence level estimated with the MLP. The coherence was kept constant across a block of 40 trials, and if the resulting accuracy was higher or lower than 60% ± 2%, the observer was asked to perform additional blocks while the coherence level of the RDK was adjusted between blocks by increasing or decreasing the number of coherently moving dots, on average, in steps of 10 dots (SD = 5 dots), until they reached the desired level of accuracy (60% ± 2%). The coherence level resulting in a performance of 60% ± 2% correct discrimination was then considered as the participant's baseline (i.e., No-tRNS condition) and was used as coherence level for the stimulation conditions.

Phase 3: The main experiment

In phase 3 of Experiment 4.1A, participants performed five blocks of the 2IFC direction discrimination task while being stimulated with hf-tRNS. The coherence level was fixed at the value established in *Phase 2* of the experiment and was kept constant across the five blocks. Each block consisted of 40 trials for a total of 200 trials. Accuracy was calculated by collating responses in each block. In each of the four experimental sessions, one stimulation intensity was applied; that is, either 0.5, 0.75, 1.0 or 1.5 mA. The different sessions (stimulation intensities) were delivered in different days. The order of stimulation intensity was randomized across participants. Observers were unaware of the type of stimulation applied in each session. The stimulation started 30 s before the first block and lasted until the end of the fifth block. The final accuracy in the No-tRNS baseline condition was the average of all the No-tRNS conditions (as found in *Phase 2*) across the four stimulation sessions. In Experiment 4.1B we used the same procedure as Experiment 4.1A, with the exception that participants performed only one stimulation session in which Sham stimulation at 1.5 mA was delivered for 30 s before the beginning

of the task. Participants always performed five blocks of the 2IFC direction discrimination task.

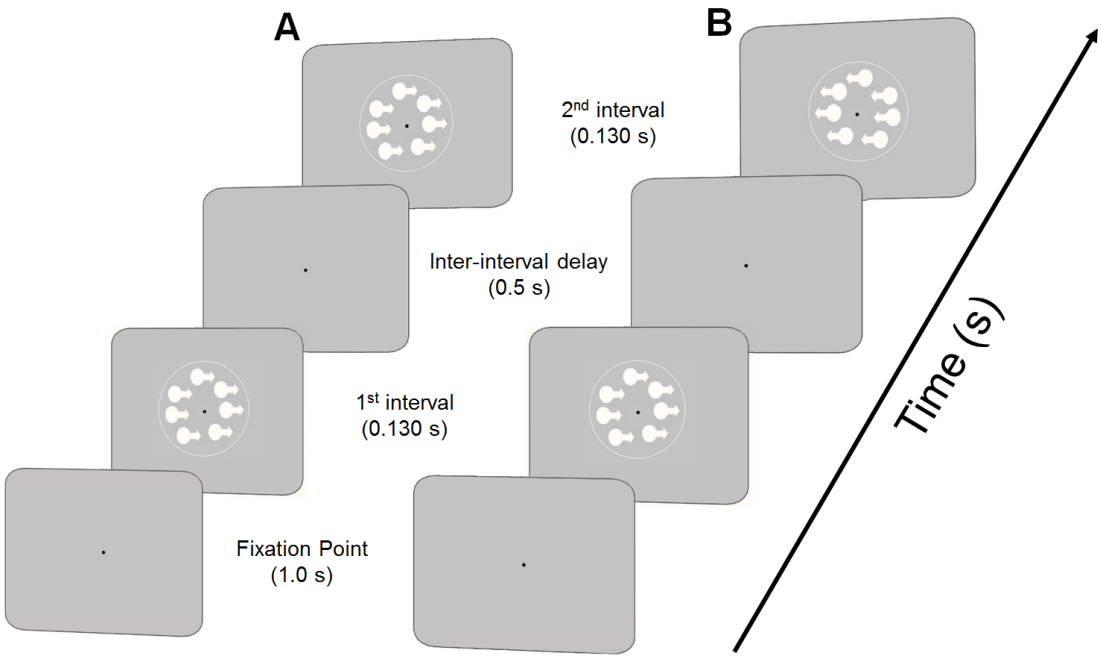

Figure 4.1. Schematic representation of the procedure used in Experiment 4.1. (A) Example of a 'same' trial, when the RDKs in the two temporal intervals have the same motion direction. (B) Example of a 'different' trial, when the RDKs have opposite motion directions. The white circular frame is reported only for demonstrative purposes and was not presented during the experiment.

4.3.2 Results

Figure 4.2 shows the results of Experiments 4.1A and 4.1B. Results showed accuracy levels above baseline values only in the 1.0 and 1.5 mA stimulation conditions. Non-parametric tests were used to establish the statistical significance of the results, because in 1A, a Shapiro-Wilk test for normality showed that residuals for the No-tRNS condition were not normally distributed ($p = 0.01$).

Firstly, a Friedman test was performed to test for possible differences between the performance values in the No-tRNS condition measured before each hf-tRNS session (i.e., hf-tRNS at 0.5, 0.75, 1.0 and 1.5 mA). The Friedman test reported no significant effect of No-tRNS measures performed before each hf-tRNS session ($\chi^2 = 0.94$, $df = 3$, $p = 0.82$).

Another Friedman test including the stimulation intensity (i.e., No-tRNS, 0.5, 0.75, 1.0 and 1.5 mA) reported a significant effect of the stimulation intensity ($\chi^2 = 22.52$,

df = 4, $p < 0.001$). In order to test for differences between the different stimulation conditions, we conducted a series of Wilcoxon Signed Rank tests corrected using False Rate Discovery (FDR) at 0.05 (Benjamini & Hochberg, 1995) and calculated the Cohen's *r* effect size of the statistic (Field, 2009; Fritz et al., 2012)[2]. The results are reported in Table 4.1. Overall, the test showed that accuracies in both 1.0 mA and 1.5 mA hf-tRNS conditions significantly differ from the No-tRNS, the 0.5 and the 0.75 mA conditions.

Table 4.1. Results for different hf-tRNS intensities on mean accuracy for Experiment 4.1A.

	Stimulation Intensity (mA)											
	0.5			**0.75**			**1.0**			**1.5**		
	Z score	***p value***	***r***	***Z score***	***p value***	***r***	***Z score***	***p value***	***r***	***Z score***	***p value***	***r***
No-tRNS	-0.628	0.78	0.13	-0.78	0.94	0.16	-2.668	**0.02***	**0.54**	-2.903	**0.01***	**0.59**
0.5				-0.267	0.88	0.05	-2.937	**0.01***	**0.60**	-2.903	**0.01***	**0.59**
0.75							- 2.578	**0.02***	**0.53**	-2.277	**0.04***	**0.46**
1.0										-0.311	0.88	0.06

Z scores and p-value of the Wilcoxon Signed Rank Tests (corrected using FDR at 0.05)

Additionally, a one-sample Wilcoxon Signed Rank test was used to compare the results of the experimental conditions to the median accuracy of 60%. The Wilcoxon Signed Rank test reported a significant difference between the median accuracy of 60% and the median of hf-tRNS at 1.0 mA ($p = 0.011$, $r = 0.74$) and the hf-tRNS at 1.5 mA ($p = 0.003$, $r = 0.86$). Comparisons between 60% and the median of No-tRNS condition ($p = 0.527$, $r = 0.18$), 0.5 mA ($p = 0.421$, $r = 0.23$) and 0.75 mA ($p = 0.929$, $r = 0.026$) were not significant.

For Experiment 4.1B (Figure 4.2B), a Shapiro-Wilk test for normality showed that the residuals for the No-tRNS and Sham 1.5 mA conditions were normally distributed ($p > 0.05$). However, as for Experiment 4.1A, we used non-parametric statistics.

[2]We reported the Cohen's *r* for both the Mann-Whitney test and the Wilcoxon Singed rank test. Cohen's r was calculated as $r = \frac{z}{\sqrt{N}}$ were *z* is the z-score obtained from the statistics and *N* is the number of total observations (Field, 2009; Fritz et al., 2012). For Cohen's *r* a large effect is 0.5, a medium effect is 0.3, and a small effect is 0.1.

It should be noted that Experiment 4.1B was conducted after Experiment 4.1A, and in Experiment 4.1B we used a stimulation intensity of 1.5 mA. This is because, though in Experiment 4.1A the accuracy for 1.0 mA and 1.5 mA were very similar (64.95% vs. 64.11%, respectively), we decided to choose the current intensity producing less dispersion around the mean (SD 5.53% and 2.27% for 1.0 and 1.5 mA, respectively). Besides, in Experiment 4.1B, the Sham condition was tested in a separate group of participants. The rationale behind this choice was that the dependent variable of Experiment 4.1A was the stimulation intensity. Therefore, to devise an appropriate control condition on the current intensity and avoid possible confounds due to the sensation of stimulation, the intensity of the Sham stimulation should have matched that of the hf-tRNS intensity producing the highest performance improvement. Since it was not possible to know the "optimal" level of stimulation intensity in advance, and thus randomize the Sham condition in the same group of participants, we decided to administer the Sham stimulation at the "optimal" current intensity level in a separate group of participants.

A Wilcoxon Signed Rank tests reported that there was no significant difference between the No-tRNS and the Sham at 1.5 mA (p = 0.78, r = 0.06). Moreover, a one-sample Wilcoxon Signed Rank test did not report any significant difference between the No-tRNS (p = 0.29, r = 0.31) or the Sham at 1.5 mA conditions (p = 0.70, r = 0.11) with respect to the median accuracy of 60%.

A Mann-Whitney U test was performed to compare the accuracy between the Sham condition at 1.5 mA and the other hf-tRNS conditions: 0.5, 0.75, 1.0, and 1.5 mA. The Mann-Whitney U test did not reveal a significant difference between Sham condition with respect to 0.5 mA (U = 71, *corrected-p* = 0.95, r = 0.01), 0.75 mA (U = 71, *corrected-p* = 0.95, r = 0.01), and 1.0 mA (U =35.5, *corrected-p* = 0.07, r = 0.43). On the other hand, we found a significant difference between hf-tRNS at 1.5 mA and the Sham at 1.5 mA (U = 28, *corrected-p* = 0.04, r = 0.52). Moreover, no significant difference was found between the No-tRNS condition in Experiment 4.1A and 4.1B (U = 51, *corrected-p* = 0.22, r = 0.25).

Figure 4.2C shows the percentage change of performance in Experiment 4.1A between the hf-tRNS conditions and the No-tRNS condition. The percentage change was calculated as follows:

$$Percentage\ Change = \frac{tRNS - NoStim}{NoStim} 100 \qquad \text{Eq. (4.1)}$$

A Friedman test reported a significant effect of the stimulation intensity ($\chi^2 = 19$, $df = 3$, $p < 0.001$). Table 4.2 illustrates Wilcoxon Signed Rank tests results (corrected using FDR at 0.05) conducted between the different stimulation intensities.

Overall results showed a significant improvement for 1.0 mA and 1.5mA with respect 0.5 mA and 0.75 mA stimulation conditions.

Table 4.2. Results for hf-tRNS intensities on percentage change for Experiment 4.1A.

	Stimulation Intensity (mA)								
	0.75			**1.0**			**1.5**		
	Z score	***p-value***	***r***	***Z score***	***p-value***	***r***	***Z score***	***p-value***	***r***
0.5	-0.267	0.79	0.05	**- 2.934**	**0.01***	**0.60**	**- 2.903**	**0.01***	**0.59**
0.75				**- 2.578**	**0.02***	**0.53**	**-2.275**	**0.03***	**0.46**
1.0							-0.356	0.79	0.15

Z scores and p-value for Wilcoxon Signed Rank test (corrected using FDR at 0.05)

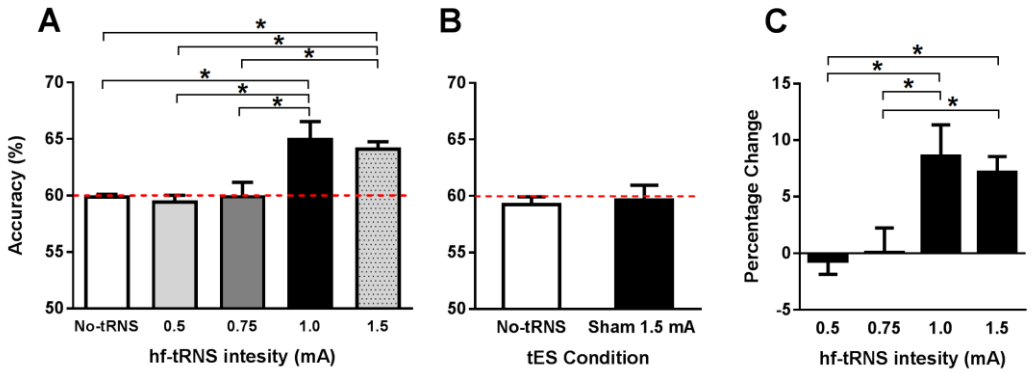

Figure 4.2. Results of Experiment 4.1. (A) Mean accuracy (%) for each stimulation condition of Experiment 4.1A: No-tRNS, 0.5, 0.75, 1.0 and 1.5 mA. (B) Mean accuracy (%) for No-tRNS and Sham at 1.5 mA of Experiment 4.1B. The red dashed line represents the 60% accuracy. (C) Percentage change between hf-tRNS conditions and No-tRNS in Experiment 4.1A. Error bars ±SEM. Asterisks (*) show significant differences.

4.3.3 Discussion

The results of Experiment 4.1 showed that hf-tRNS intensity at 1.5 mA improved performance in the motion direction discrimination task. This result is compatible with the stochastic resonance phenomenon in which the injection of an optimal level of

external noise in motion sensitive areas enhances the near-threshold motion signal, increasing the observers' discrimination performance (Schwarzkopf et al., 2011; Treviño et al., 2016; van der Groen & Wenderoth, 2016). However, the stochastic resonance framework also predicts that when an excessive amount of noise is injected into the system the behavioural performance can be disrupted (Simonotto et al., 1997; Ward, 2009). Our initial hypothesis was that, since we administered a *bilateral* stimulation, a current intensity of 1.5 mA would have injected an excessive amount of noise to induce a performance decrement. This prediction was based on the stimulation parameters of previous studies which found a peak of performance when bilateral stimulation was delivered around 0.75 mA and 1.0 mA (van der Groen & Wenderoth, 2016), and on the results of Chapter 2 and 3 alongside with studies that delivered *unilateral* stimulation and reported enhanced performance with hf-tRNS at 1.5 mA (Fertonani et al., 2011; Pirulli et al., 2013). In fact, we initially expected that the intensity range used (from 0.5 mA to 1.5 mA) would have been wide enough to detect an improvement either at 0.75 mA or at 1.0 mA and a worsening of performance at 1.5 mA. However, our results partially contradicted our prediction showing that the optimal noise level introduced by hf-tRNS was at 1.5 mA. Therefore, we designed a second experiment in which we assessed the effects of hf-tRNS at 2.25 mA, i.e., at an intensity exceeding by 0.75 mA the optimal stimulation level. If the effects of hf-tRNS can be explained within the stochastic resonance phenomenon, such high stimulation intensity should worsen participants' performance.

4.4 Experiment 4.2

4.4.1 Methods

4.4.1.1 Stimuli and procedure

Stimuli and procedure were the same as in Experiment 4.1, except for the stimulation parameters. The author and a new sample of twenty-three participants (9 males, age range 18-40 yrs.) took part in this experiment. A between-subjects designed was implemented and participants performed one experimental session. One group of twelve participants performed the experiment with hf-tRNS at 2.25 mA, whereas another group of twelve participants performed the experiment with Sham stimulation at 2.25 mA (Bikson et al., 2016; Fertonani et al., 2015). Participants were randomly assigned to the two groups.

4.4.2 Results

Figure 4.3 shows the results of Experiment 4.2. For the hf-tRNS 2.25 mA group, a Shapiro-Wilk test for normality showed that for the No-tRNS condition were not normally distributed ($p = 0.05$). For the hf-tRNS 2.25 mA group, a Wilcoxon Signed Rank tests reported that there was a significant difference between the No-tRNS condition and the hf-tRNS at 2.25 mA ($p = 0.009$, $r = 0.54$). Moreover, a one-sample Wilcoxon Signed Rank did not report any significant difference between the median accuracy of 60% and the No-tRNS condition ($p = 0.56$, $r = 0.16$), but it showed a significant difference between the 60% accuracy and the hf-tRNS at 2.25 mA ($p = 0.008$, $r = 0.77$).

For the Sham group, a Shapiro-Wilk test for normality showed that all conditions were normally distributed ($p > 0.05$). A Wilcoxon Signed Rank test reported that there was no significant difference between the No-tRNS condition and the Sham condition at 2.25 mA ($p = 0.61$, $r = 0.10$). For the Sham group one-sample Wilcoxon Signed Rank tests also showed that there was no significant difference between the median accuracy at 60% and the No-tRNS ($p = 0.305$, $r = 0.30$) and between the median accuracy at 60% and the Sham at 2.25 mA ($p = 0.97$, $r = 0.03$). Most importantly, a Mann-Whitney U test showed that there was a significant difference between hf-tRNS at 2.25 mA and the Sham at 2.25 mA ($U = 37$, $p = 0.043$, $r = 0.41$).

The hf-tRNS at 2.25 mA condition was also compared to hf-tRNS intensities of Experiment 4.1A (Figure 4.4). A Mann-Whitney U test showed that performance with hf-tRNS at 2.25 mA was significantly different from hf-tRNS at 0.5 mA ($U = 26.5$, *corrected-p* $= 0.008$, $r = 0.54$), from hf-tRNS at 0.75 mA ($U = 25.5$, *corrected-p* $= 0.008$, $r = 0.55$), from hf-tRNS at 1.0 mA ($U = 7.5$, *corrected-p* $= 0.002$, $r = 0.76$) and from hf-tRNS at 1.5 mA ($U = 3.5$, $p = 0.002$, $r = 0.81$).

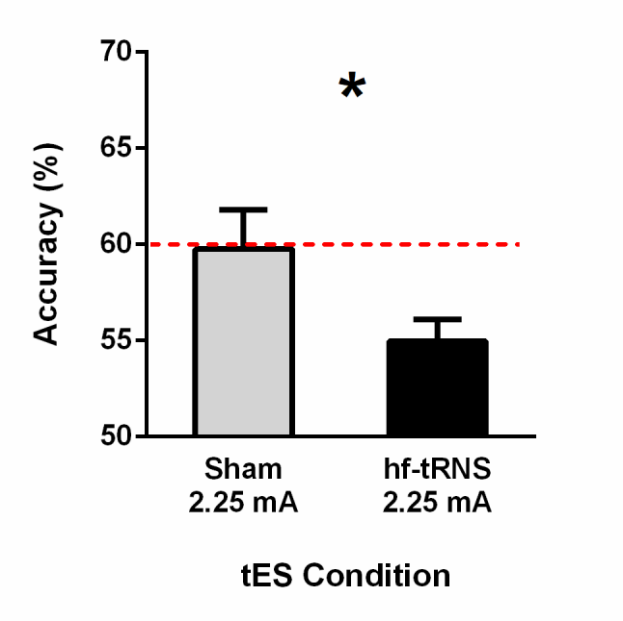

Figure 4.3. Results of Experiment 4.2. Mean accuracy (%) for Sham at 2.25 mA and hf-tRNS at 2.25 mA. The red dashed line represents the 60% accuracy. Error bars ±SEM. Asterisks (*) show significant differences.

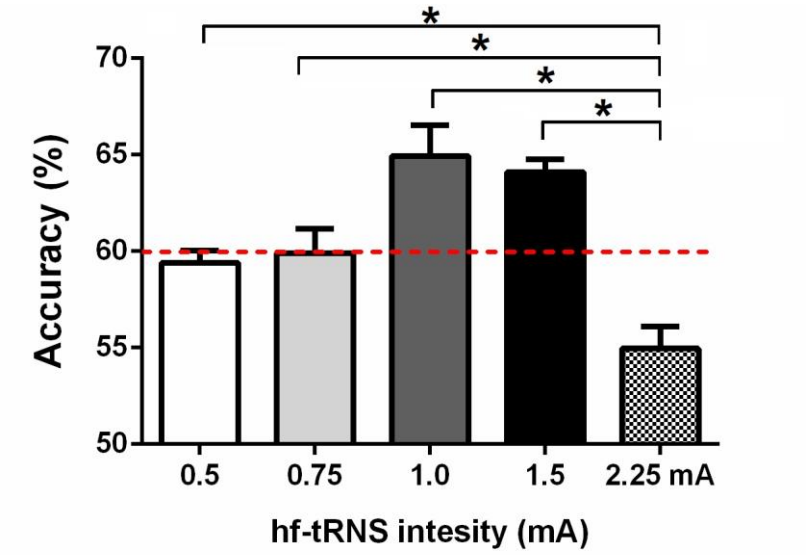

Figure 4.4. Modulation of mean accuracy (%) depending on hf-tRNS intensity. Mean accuracy for each hf-tRNS intensity in Experiment 4.1A and Experiment 4.2: 0.5, 0.75, 1.0, 1.5 and 2.25 mA. The red dashed line represents the 60% accuracy. Error bars ±SEM. Asterisks (*) show significant differences.

4.4.3 Discussion

The results of Experiment 4.2 showed that increasing the current intensity above the optimal level had a detrimental effect on direction discrimination performance, by reducing the accuracy significantly below 60%. As in Experiments 4.1A and 4.1B, under

the stimulation conditions, the task was performed with the same coherence level producing approximately 60% correct discrimination before stimulation. These results strongly suggest that a stochastic resonance phenomenon drives the modulatory effects of hf-tRNS when combined with a visual motion task.

4.5 Experiment 4.3

In Experiment 4.3, we performed an additional control condition to assess the effects of hf-tRNS when using supra-threshold stimuli. According to the stochastic resonance phenomenon additional noise has a positive role in increasing the probability of a signal to cross a given threshold only when the signal is at or sub-threshold. However, if a signal is already over the threshold the externally added noise would not affect its probability to be detected or discriminated (McDonnell & Abbott, 2009; Moss et al., 2004). In support of this concept, evidence showed that when hf-tRNS is delivered in a suprathreshold condition it does not affect behavioural performance (Rufener et al., 2017; van der Groen & Wenderoth, 2016). Therefore, we hypothesised also in our paradigm additional external noise at both hf-tRNS at 1.5 mA and 2.25 mA should have no effect on motion direction discrimination performance for suprathreshold RDKs.

4.5.1 Method

4.5.1.1 Stimuli and procedure

Stimuli and procedure were the same as used in Experiments 4.1 and 4.2. However, differently from the previous experiments we did not estimate the individual 60% threshold (as in *Phase 1* and *Phase 2* of Experiments 4.1 and 4.2), but observers performed only five blocks (*Phase 3*) of the 2IFC motion direction discrimination task at the maximum coherence level (i.e., 100% coherence). A new sample of twenty participants (10 males, age range 18-40 yrs.) took part in this experiment and were randomly assigned to one of the four groups (of five participants each) divided by stimulation condition (i.e., hf-tRNS at 1.5 mA, hf-tRNS at 2.25 mA, Sham stimulation at 1.5 mA and Sham stimulation at 2.25 mA).

4.5.2 Results

Figure 4.5 illustrates results of Experiment 4.3. A Kruskal-Wallis test showed that there was no significant effect of the stimulation on discrimination performance among

the four groups (H = 1.096, df = 3, p = 0.78). Moreover, Mann-Whitney U tests showed that there was no significant difference between the hf-tRNS at 1.5 mA group and Sham at 1.5 mA group (U = 10.5, p = 0.68), and between the hf-tRNS at 2.25 mA group and Sham at 2.25 mA group (U = 9.5, p = 0.53). Moreover, no significant difference was found between the hf-tRNS at 1.5 mA group and hf-tRNS at 2.25 mA group (U = 11.5, p = 0.83) and between the Sham at 1.5mA group and Sham at 2.25 mA group (U = 9.5, p = 0.53).

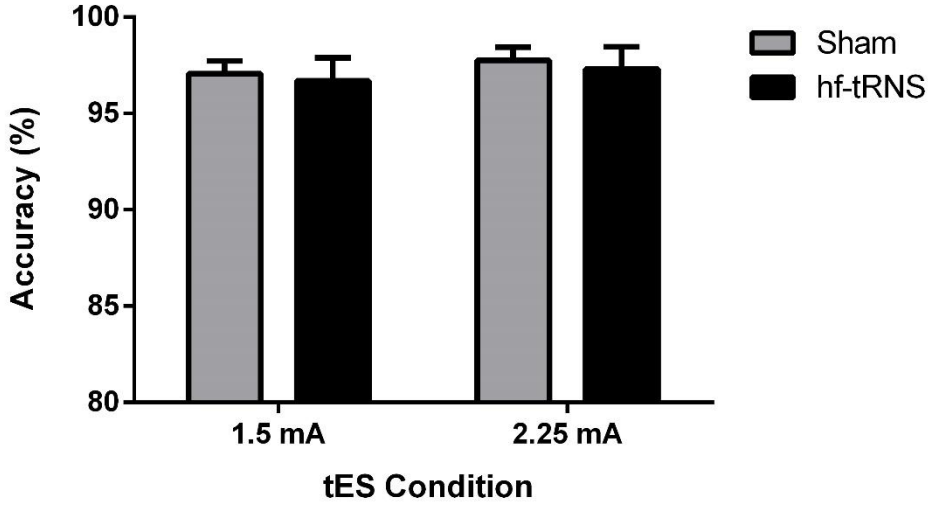

Figure 4.5. Results of Experiment 4.3. Mean accuracy (%) for stimulations at 1.5 mA and at 2.25 mA for Sham (grey) and hf-tRNS (black) respectively. Error bars ±SEM.

4.5.3 Discussion

Overall, the results confirmed our prediction that externally added noise does not modulate accuracy performance when the task is presented well above the individual threshold. This result is in accordance with the stochastic resonance phenomenon and with previous findings which showed little or no effect of the stimulation if a stimulus is presented suprathreshold (Moss et al., 2004; Rufener et al., 2017; van der Groen & Wenderoth, 2016).

4.6 General Discussion

In the present study, we compared the effects of different hf-tRNS intensities on performance in a global motion direction discrimination task and investigated if its mechanism of action could be explained within the stochastic resonance framework. Overall, the results of Experiments 4.1 and 4.2 showed that when an optimal level of hf-tRNS was applied bilaterally over the area hMT^+, motion direction discrimination performance is improved. Differently, if a higher level of current stimulation is used it has a hindering effect. It has been suggested that hf-tRNS might induce random activity at the neural level (i.e., neural noise; Fertonani & Miniussi, 2017; Fertonani et al., 2011; Terney et al., 2008). If this assumption holds, then different intensities of hf-tRNS should correspond to different levels of injected noise (van der Groen & Wenderoth, 2016). Noise is a fundamental element in the stochastic resonance phenomenon. In a non-linear system, like the brain, the addition of external noise can push a weak signal over the sensory threshold and evoke a positive response in the nervous system (Collins, Chow, & Imhoff, 1995; Kitajo et al., 2007; Kitajo et al., 2003; Schwarzkopf et al., 2011; Simonotto et al., 1999; Zeng et al., 2000). The results of Experiments 4.1A and 4.1B showed that if a stimulus was presented near threshold (i.e., at a motion coherence level producing 60% correct responses in direction discrimination), hf-tRNS applied at 0.5 mA and 0.75 mA had no effect and performance did not differ from either a No-tRNS condition or a Sham condition at 1.5 mA. However, intensities at 1.0 and 1.5 mA induced a significant increment with respect to the baseline level of 60% of correct discrimination and the No-tRNS condition. Importantly, hf-tRNS at 1.5 mA significantly improved global motion discrimination when compared to Sham stimulation at 1.5 mA. The mean percentage increase in accuracy with respect to the No-tRNS condition was 8.57% (SD = 9.66%) for the 1.0 mA and 7.18% (SD = 4.73%) for the 1.5 mA. Although hf-tRNS at 1.0 mA resulted in a higher percentage change and a slightly higher accuracy performance, it also had higher variability with a standard deviation that was almost twice the standard deviation for hf-tRNS at 1.5 mA. Therefore, we assumed the hf-tRNS at 1.5 mA to be the optimal stimulation level. The results of Experiment 4.1 partially replicated the findings in Chapters 2 and 3 in which hf-tRNS at 1.5 mA was delivered unilaterally over the left hMT^+ and decreased coherence thresholds and increased the *sampling* rate specifically for the visual hemi-field contralateral to the stimulation site. The replication of similar results in different experiments is highly valuable because it shows consistency of hf-tRNS in improving behavioural performance across different motion tasks.

Although the results from Experiment 4.1A are in line with the stochastic resonance framework, this theory also asserts that if an excessive amount of noise is added to the signal, it can hamper signal detection or discrimination (McDonnell & Abbott, 2009; Moss et al., 2004; Ward, 2009). According with this prediction, the results of Experiment 4.2 showed that when hf-tRNS at 2.25 mA was applied, it had a detrimental effect on direction discrimination performance with respect to both the 60% of correct response in the No-tRNS condition and the Sham condition at 2.25 mA. Therefore, in agreement with the stochastic resonance phenomenon, our results showed that when a visual stimulus is presented near threshold, excessive external noise affected global motion direction discrimination.

In Experiment 4.3, we predicted that when a suprathreshold stimulus (100% coherence) is presented hf-tRNS should not modulate discrimination performance. This experiment was based on the notion that stochastic resonance results from the combination of a threshold, a subthreshold stimulus and noise (Moss et al., 2004). Therefore, if a suprathreshold signal is used, the injection of additional noise should have little to no impact on the signal. In agreement with the previous findings (Rufener et al., 2017; van der Groen & Wenderoth, 2016) the results of our Experiment 4.3 confirmed this prediction; that is, when a suprathreshold stimulus was used both hf-tRNS at 1.5 mA or 2.25 mA did not improve or hinder the performance. Overall, our findings on motion direction discrimination are consistent with those of van der Groen and Wenderoth (2016) on contrast detection. The authors showed that amongst a range of hf-tRNS intensities from 0.0 to 1.5 mA, hf-tRNS at 1.0 mA was the optimal stimulation level to improve contrast detection performance with near-threshold stimuli. The modulation obtained with the hf-tRNS was also comparable to the results showed in a second condition in which visual noise was added to the stimulus.

Recently, van der Groen et al. (2018) also investigated whether decision making is sensitive to the stochastic resonance phenomenon in an two alternative forced choice motion direction discrimination task. Accuracy and reaction times data fitted with the drift diffusion model (Ratcliff, 1978; Ratcliff & Rouder, 1998; Ratcliff & Tuerlinckx, 2002) showed that adding noise with bilateral hf-tRNS while participants were asked to judge the direction of coherent motion as quickly and as accurately as possible, stimulation could increase perceptual decision. Specifically, the authors found that hf-tRNS could enhance the drift rate, related to the speed and efficiency of motion information processing. Discrepancies in the optimal hf-tRNS intensities between our study and van der Groen and colleagues (2018; 2016) might be explained in terms of

differences in the stimulation paradigm, type of task and the visual area stimulated. It has been demonstrated that differences in electrode montage lead to variability in the direction in which the current reaches the layers in the cortex and consequently how neurons are affected (Moliadze, Antal, & Paulus, 2010). Moreover, differences in the stimulation paradigm, such as the stimulation period, can lead to different outcomes. For example, while in our study stimulation was delivered at one single intensity for the entire stimulation session (approximately 20 mins), van der Groen and colleagues applied different stimulation paradigms in which either the same stimulation intensity was applied for 20 trials followed by 20 trials of no stimulation (van der Groen et al., 2018), or stimulation intensities were randomized within the stimulation session, and delivered at repeated short stimulation intervals of 2 s (van der Groen & Wenderoth, 2016).

In conclusion, these results support the notion that certain hf-tRNS effects on psychophysical performance can be explained within the stochastic resonance framework. Specifically, this study showed that when an optimal level of external noise is injected into the system, the signal-to-noise ratio is increased with a consequent improvement in direction discrimination. On the other hand, when a high (and non-optimal) level of external noise is used, performance is affected. Finally, according to the stochastic resonance phenomenon, when the visual stimulus is presented well above the threshold, injection of additional noise through hf-tRNS did not affect motion direction discrimination.

Stochastic resonance phenomenon well adapts to describe the online hf-tRNS effects on the visual cortex during the execution of a perceptual task. However, it has been demonstrated that hf-tRNS can increase neural excitability that outlast the stimulation time, but its ability in inducing aftereffects on the visual cortex have been scarcely investigated. Moreover, long-term modification could rely on different mechanisms of action such as long-term potentiation and neural plasticity. Therefore, in the next Chapter it will be investigated whether offline hf-tRNS is able to induce enduring effects on direction discrimination performance and electrophysiological activity of the visual cortex.

Chapter 5: Electrophysiological aftereffects of high frequency transcranial random noise stimulation (hf-tRNS): an EEG investigation

The experiment presented in this chapter is in preparation for publication as Ghin, F., O' Hare, L., and Pavan, A. Electrophysiological aftereffects of high frequency transcranial random noise stimulation (hf-tRNS): an EEG investigation.

5.1 Abstract

There is evidence in previous chapters that online hf-tRNS is effective in improving behavioural performance in several visual tasks (Campana et al., 2016; Fertonani et al., 2011; Pirulli et al., 2013; van der Groen & Wenderoth, 2016). However, the duration, spatial and temporal characteristics of hf-tRNS aftereffects in the visual cortex have been scarcely investigated. In the present study, we aimed at investigating the aftereffects induced by offline hf-tRNS delivered in a single session. Specifically, we investigated modulatory aftereffects of hf-tRNS on the performance on a motion direction discrimination task. EEG was used to assess the spatial and temporal dynamics of cortical activity modulated by offline hf-tRNS. In particular, we measured the amplitude and latency of EEG motion-related VEPs over the parietal-occipital cortex, and the power spectral density (PSD) amplitude at rest for delta, theta, alpha and beta bands. The results showed that the accuracy at the motion direction discrimination task was not modulated by offline hf-tRNS. Although the motion task was able to elicit distinct VEPs components (P1, N2 and P2) (Kuba, Kubová, Kremláček, & Langrová, 2007), neither their amplitudes nor their latencies showed any significant change between pre- and post-stimulation recordings. However, we found a significant increment of PSD amplitude in the alpha and beta bands between pre- and post-stimulation, but this was regardless of the stimulation type. Overall, the results show that a single session of offline hf-tRNS does not induce changes in measures of cortical activity either at rest or in a goal-oriented task. More evidence is needed to assess whether hf-tRNS can induce enduring behavioural and physiological aftereffects in the visual cortex.

5.2 Introduction

In Chapters 2 to 4 we have shown that hf-tRNS is able to improve the behavioural performance in a series of motion direction discrimination tasks. The results of Chapter 4 also showed how hf-tRNS effects on the visual cortex could be explained within the stochastic resonance framework. However, it is also of critical importance to understand the modulations that this particular stimulation regime can achieve beyond the stimulation duration. Several studies assessed the effects of hf-tRNS in inducing some medium and long-term change in corticospinal excitability over the motor cortex by measuring MEP modulation. However, they also disclosed the variability of these effects depending on duration and time of the stimulation, intensity of the stimulation and electrode montage. (Chaieb, Paulus, & Antal, 2011; Inukai et al., 2016; Moliadze, Fritzsche, & Antal, 2014; Parkin et al., 2018; Terney et al., 2008). Physiological evidence of hf-tRNS effects outside the motor system are scarcer. Some evidence of hf-tRNS ability to temporally modulate sensory-related cortical activity comes from studies measuring electrophysiological activity through EEG recordings in the auditory system (Rufener et al., 2018, 2017; Van Doren et al., 2014). Van Doren and colleagues (2014), administered 20 min of hf-tRNS stimulation bilaterally over the temporal cortex. Prior and after the stimulation, EEG consisted of 5 min of resting state recording followed by 7 minutes of auditory evoked potentials elicited via an auditory steady state response (ASSR). The results showed that offline hf-tRNS did not modulate resting state activity in all the frequency bands tested (delta, theta, alpha, beta, low and high gamma), but it did modulate ASSR power limited to 40Hz, thus within the low gamma band (33 - 45 Hz). Moreover, Rufener and colleagues (2017), recently showed that online hf-tRNS reduced latency for the N1 component in a auditory gap task. Moreover the same group of researchers also demonstrated an hf-tRNS effect in reducing peak latencies of the P3 component elicited by an auditory attentional task, but failed to find stimulation related modulation of sensory evoked potentials such as N1 and P50 (Rufener et al., 2018). Overall, these studies showed that hf-tRNS is able to induce modulation of cortical activity in different sensory systems, however more evidence is needed especially to support the results of its modulatory effects on behavioural performance on visual tasks.

An approach to investigate this issue might be to test offline hf-tRNS on the visual cortex by registering its aftereffects on spontaneous brain oscillations and VEPs measures of amplitude and latency. The possibility to measure the hf-tRNS aftereffects on brain oscillations at rest is of particular interest because it could reveal long-term nonspurious

outcomes (thus, not influenced by an altered task-dependent state) induced by the stimulation on the spontaneous oscillatory activity. Similar approaches have been previously used with both tDCS (Ardolino, Bossi, Barbieri, & Priori, 2005; Mangia et al., 2014; Puanhvuan, Nojima, Wongsawat, & Iramina, 2013; Spitoni et al., 2013; Zaehle, Sandmann, Thorne, Jäncke, & Herrmann, 2011) and tACS (Pahor & Jaušovec, 2014; Wach et al., 2013). Brain oscillations at specific frequencies reflect the general cortical activation state of distinct brain networks and have been linked to specific functional activities (Groppe et al., 2013; Mantini, Perrucci, Del Gratta, Romani, & Corbetta, 2007). For example, alpha band oscillations (8-14 Hz) have been observed predominately in the occipital cortex and with lesser magnitude in the parietal and temporal cortex (Feige et al., 2005). The inhibition-timing hypothesis suggests that, during the execution of some task an incremented synchronization in alpha activity, over brain areas that are not relevant for the task, can be associated with an active withholding of a stored information of a response. This process would reflect a proactive inhibition driven by a certain class of top-down process (Klimesch, Sauseng, & Hanslmayr, 2007). On the other hand, during a resting state period activity in alpha oscillation increases with a decrease of attention and without the presence of visual stimulation (Nunez, Wingeier, & Silberstein, 2001) and it has been related to metabolic deactivation (Moosmann et al., 2003). Beta band oscillations (15-30 Hz) are more prominent on the pre and post-central gyri and it has been suggested that synchronization of beta oscillations acts to suppress activity of the motor cortex (Miller et al., 2012) or helps to sustain tonic motor activity (Engel & Fries, 2010). Theta oscillations (4-8 Hz) have been located on the frontal midline locations (Mitchell, McNaughton, Flanagan, & Kirk, 2008) and have been associated with several cognitive functions such as working memory, visual navigation and executive attention (Debener, 2005; Onton, Delorme, & Makeig, 2005). Delta band oscillations have been recorded over wide areas of the cortex with peak activity at the frontal and central-parietal sites (Maurer & Dierks, 1991). During the resting state delta band activity has been associated with the brain's default mode network (DMN). The DMN is a concept in which the activity of a series of cortical areas is positively correlated when an observer is asked to rest quietly with the eyes closed. The DMN is suggested to reflect the default mode of ongoing intrinsic neural activity, which is constantly decreased if the subject is engaged in some goal-oriented task (Buckner, Andrews-Hanna, & Schacter, 2008; Neuner et al., 2014; Raichle et al., 2001; Raichle & Snyder, 2007).

An additional way to investigate hf-tRNS aftereffects on the visual cortex is by studying changes in VEP measures such as amplitude and latency during motion direction

discrimination. VEP responses to visual motion stimuli have been examined to study visual cortices associated with motion processing (Heinrich, 2007; Kremláček et al., 2007; Kuba et al., 2007; Miroslav Kuba et al., 2012; Kuba & Kubova, 1992; Kubova, Kuba, Hubacek, & Vit, 1990; Martin, Huxlin, & Kavcic, 2010; Niedeggen & Wist, 1998, 1999). Distinct VEPs have been often seen in response to moving stimuli. A first positive component P1 has been detected in response to motion-onset stimuli in several studies, but it seems to be more associated with low-level characteristics of the stimulus such as its luminance with respect to some motion processing. Specifically, in a motion-onset VEP study, P1 amplitude decreased in correlation with decrements of stimulus contrast (Kubová, Kuba, Spekreijse, & Blakemore, 1995). A second negative component N2, has been strictly linked to motion processing and it seems to be generated in extra-striate temporal-occipital and parietal cortical areas (Kuba et al., 2007). For instance, it has been shown that amplitude and latency of the N2 over the parietal-occipital cortex are linked with the coherence of an RDK stimulus, where an increase in coherence corresponds to an increase in the amplitude and reduction of the latency of this component (Niedeggen & Wist, 1998; Patzwahl & Zanker, 2000). A second positive peak, P2, is also found in motion VEPs, but its presence is more variable across studies and seems to be dependent to the complexity of the visual motion stimuli displayed (Kuba et al., 2007). If different VEP components reflects the activity of distinct processes of elaboration of visual motion stimuli, then the possibility to induce significant modulations in their amplitude and latency might be helpful to determine the presence of specific hf-tRNS aftereffects

Overall, the physiological effects of hf-tRNS over the visual cortex and the extent of its aftereffects on cortical activity are still unclear. Thus, the aim of this study was to explore if hf-tRNS is able to modulate cortical activity in an offline stimulation paradigm. In order to do this, we devised an experimental design that aimed to measuring changes in resting state power spectral density (PSD) across several frequency bands and VEP response amplitude and latency during a motion direction discrimination task.

Experiment 5

5.3 Method

5.3.1 Participants

The author and fifteen naïve participants took part in the study (7 males, age range 18-40 yrs.). Participants were all right handed and with normal or correct to normal vision acuity. Each participant filled in a questionnaire in order to exclude presence of metal

objects, heart problems, history of seizures or any neurological disease. Methods were implemented following the World Medical Association Declaration of Helsinki (2013). The present study was approved by the Ethics committee of the University of Lincoln. Written informed consent was obtained from each participant prior the enrolment in the study and they were paid for their time.

5.3.2 Apparatus

Stimuli were displayed on a 20-inch Iiyama HM204DTA Vision Master Pro Diamontrum U3-CRT monitor with a refresh rate of 85 Hz. Stimuli were generated with Matlab PsychToolbox (Brainard, 1997; Kleiner et al., 2007; Denis G. Pelli, 1997). The screen resolution was 1280 x 1024 pixels. Each pixel subtended 1.9 arcmin. The minimum and maximum luminance of the screen were 0.19 and 148.3 cd/m^2 respectively, and the mean luminance was 21.7 cd/m^2. A gamma-corrected lookup table (LUT) was used so that luminance was a linear function of the digital representation of the image.

5.3.3 Stimuli

Stimuli were global motion random dot kinematograms (RDKs) made up by 400 white dots (diameter: 0.12 deg) presented at the centre of the screen within a circular aperture with a diameter of 12 deg. The dots' density was 3.54 dots/deg^2. The duration of the RDK was 0.130 s. Dots drifted at a speed of 5.04 deg/s and had a limited lifetime of 47 ms. Dots appeared asynchronously on the display and had an equal probability of being selected as either signal or noise dots (Morgan & Ward, 1980; Newsome & Paré, 1988). After a dot vanished, it was replaced by a new dot at a different randomly selected position within the circular window. In addition, dots that moved outside the circular window were replaced by a new dot at a different randomly location within the circular window, thus maintaining the same density. Signal dots were either constrained to move globally leftward or rightward, whereas noise dots moved in random directions.

5.3.4 Stimulation technique

The same stimulator device as in Chapters 2 to 4 was used. The hf-tRNS consisted of an alternating current delivered at 1.5 mA with zero offset and applied with random frequencies ranging between 100 and 600 Hz. The total duration of the stimulation was 20 minutes. Sham stimulation was delivered at 1.5 mA and for 30 s (Gandiga et al., 2006).

The stimulation was delivered bilaterally. Electrodes position was determined with the 10-20 system, specifically one electrode was placed at the PO3 position while the second electrode was placed at the PO4 position. The two electrodes had an area of 16 cm^2 and the current density was maintained below the safety limits (Bikson et al., 2016; Fertonani et al., 2015).

5.3.5 EEG recording

Recordings were made using a 64-channel Biosemi Active-Two system (BIOSEMI, https://www.biosemi.com/), using Ag-AgCl electrodes. 62 electrodes were positioned using the 10-20 system, with 8 additional electrodes: 2 on the left and right mastoid, 2 infraorbital, 2 suborbital and 2 on the outer canthi of the eye. PO3 and PO4 were not used as they were replaced by the tES electrodes. Signals were firstly referenced to common-mode-sense electrode (CMS) and driven right leg electrode (DRL) (Metting van Rijn, Peper, & Grimbergen, 1990, 1991;https://www.biosemi.com/faq/cms&drl.htm) and re-referenced on the left and right mastoid. Recording were sampled at 2048 Hz and downsampled to 265 Hz offline.

5.3.6 Procedure

Participants took part in two experimental sessions carried out in two different and non-consecutive days. Both sessions had the same procedure. In one session hf-tRNS was delivered, whereas in the other session Sham stimulation was delivered. The order of the sessions was randomized across participants. Figure 5.1 shows the experimental procedure used in the study. Each session consisted of five phases:

Phase 1: Coherence threshold estimation

At the beginning of each session, observers performed a two-interval forced choice (2IFC) motion direction discrimination task to estimate the individual coherence threshold. The RDKs were presented at the centre of the screen. Participants had to report whether the RDKs presented in the two temporal intervals had the same or different motion direction (see Figure 4.1, Chapter 4). Each trial consisted of a fixation point presented for 1 s, followed by two 0.130 s RDKs, with a blank interval of 0.5 s between the two temporal presentations. The inter-trial interval was 1 s. An adaptive MLP staircase (Green, 1993; Grassi & Soranzo, 2009) was used to track the coherence level producing

an accuracy of 80% in motion direction discrimination. The staircase consisted of 32 trials and participants performed one staircase.

Phase 2: Assessing the level of accuracy at coherence threshold

In order to estimate the individual coherence threshold producing an accuracy level of 80% in direction discrimination, observers performed the same direction discrimination task at the coherence level estimated in *Phase 1*. The coherence was kept constant across a block of 40 trials, and if the resulting accuracy was higher or lower than 80% ± 5%, the observer was asked to perform additional blocks with the coherence level of the RDK manually adjusted by increasing or decreasing the coherence, on average, in steps of 10 dots (SD = 5 dots), until they reached the desired level of accuracy (80% ± 5%). The coherence level resulting in a performance of 80% ± 5% correct discrimination was used as coherence level for the pre- and post-stimulation conditions.

Phase 3: Pre-Stimulation EEG

After EEG and tES setup was completed, EEG recording of a resting state period started (i.e., pre-stimulation EEG). Specifically, participants were asked to close their eyes and maintain resting wakefulness while EEG was recorded for 5 minutes. Immediately after the resting state, participants were asked to perform five blocks of the 2IFC direction discrimination task while the EEG activity was recorded. The 2IFC task was divided in five blocks to limit fatigue and give the possibility to the participants to rest between blocks (1-2 minutes). The individual coherence level of the RDK was the one estimated in *Phase 2* and was kept constant across the five blocks. Each block consisted of 40 trials for a total of 200 trials. The final performance value was calculated by averaging the accuracy values over the five blocks.

Phase 4: Stimulation period

At the end of the fifth block of the 2IFC task, EEG recording was paused and either hf-tRNS or Sham stimulation was delivered. Observers were unaware of the type of stimulation applied in each session. hf-tRNS was applied for 20 minutes, whereas the Sham stimulation was applied only for the initial 30 s over a period of 20 minutes. During the stimulation period, participants remained in the same position, but the light in the room was turned on and participants were asked to relax.

Phase 5: Post-Stimulation EEG

In *Phase 5*, the same procedure as the *Phase 3* was implemented. EEG was recorded during 5 minutes of resting state, followed by other five more blocks of the 2IFC task.

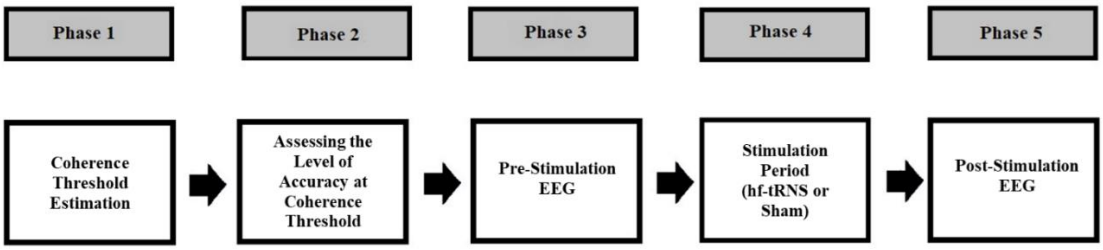

Figure 5.1. Schematic representation of the five phases employed in each experimental session for hf-tRNS and Sham.

5.3.7 EEG analysis

Data were analysed using Matlab R2018b and the EEGLAB toolbox (Delorme & Makeig, 2004). Data from 62 electrodes (PO3 and PO4 were not used, being replaced by the tRNS electrodes). Offline data were bandpass filtered between 0.1 and 40 Hz.

For the resting state period, the five-minute-long data were first divided into 2-second epochs. As there was no meaningful pre-stimulus period for these epochs, the whole epoch was used for baseline correction. Power Spectral Density (PSD) defined as mean absolute power (10*Log10(μV2/Hz)) was estimated for each epoch using the EEGLAB function "Spectopo" default settings based on a fast Fourier transform (FFT), with a default of 1 s Hamming window length and 50% overlap and then averaged over epochs for each channel. We measured PSD for delta (2-4 Hz), theta (4-8 Hz) alpha (8-14 Hz) and beta (15-30 Hz) bands (Baumgarten et al., 2016; Romei et al., 2008; Spitoni, Cimmino, Bozzacchi, Pizzamiglio, & Di Russo, 2013)

Data for the VEPs were collected during the execution of the motion direction discrimination task after the resting state period (*Phase 3* and *5* of each experimental session). Data were divided in epochs of 700 ms (-200 to 500 ms from the RDK onset). Baseline activity was removed, defined as the 200 ms before the RDK onset. VEPs were

defined as P1 (70-120 ms; Zalar, Martin, & Kavcic, 2015), N2 (135-180 ms; Kuba & Kubova, 1992), and P2 (200-300 ms; Martin, Huxlin, & Kavcic, 2010).

For both resting state period and VEPs, artefacts were removed using the EEGLAB automatic rejection procedure, thus excluding those epochs with fluctuation over ±100 μV. The Gratton and Coles correction (Gratton, Coles, & Donchin, 1983) was used to correct for eye movement artefacts (i.e., blinks and saccades). Amplitude criterion for blink detection was set at ±200 μV over a 20 ms time interval.

Data for both resting state and VEPs analysis were averaged across all participants for each stimulation condition and recording time (i.e., pre- and post-stimulation EEG). Fifteen electrodes of interest were selected, and were those surrounding the bilateral electrical stimulation sites: Pz, POz, Oz, O1, P7, P5, P3, P1, PO7, P2, P4, P6, P8, PO8, and O2.

Electrodes of interest where divided in three main parts: Left (O1, P1, P3, P5, P7, PO7), Central (OZ, POz, Pz) and Right (O2, P2, P4, P6, P8, PO8) (Figure 5.2). This organization was based on two main assumptions. Firstly, electrodes of interest were divided according to their position on each hemisphere and on the longitudinal fissure on the parieto-occipital cortex, because electrophysiological outcomes registered around stimulated areas could show discrepancies depending on their locations. For example Kubova et al. (1990) found that 60% of 80 observers showed a higher N2 amplitude in the right hemisphere. Secondly, instead of analysing data from single electrodes, we averaged data for groups of electrodes (Left, Central and Right) to measure the average modulation of cortical activity around the stimulation electrode, as the electric field generated by tES can spread beyond the borders of its stimulation electrodes (Ghin, Pavan, Contillo, & Mather, 2018). Electrodes without activity were coded as missing values, based on visual inspection of the raw data (i.e., before referencing). For the Central region, there were two electrodes coded as missing values, one in the Sham condition for one participant and one in the hf-tRNS condition for a different participant. More electrodes were missing data from the Left region with a mean of 1.8 (SD = 1.03) missing electrodes in the Sham condition, and a mean of 2.9 (SD = 1.22) missing electrodes in the hf-tRNS condition. No electrode was lost from the Right region.

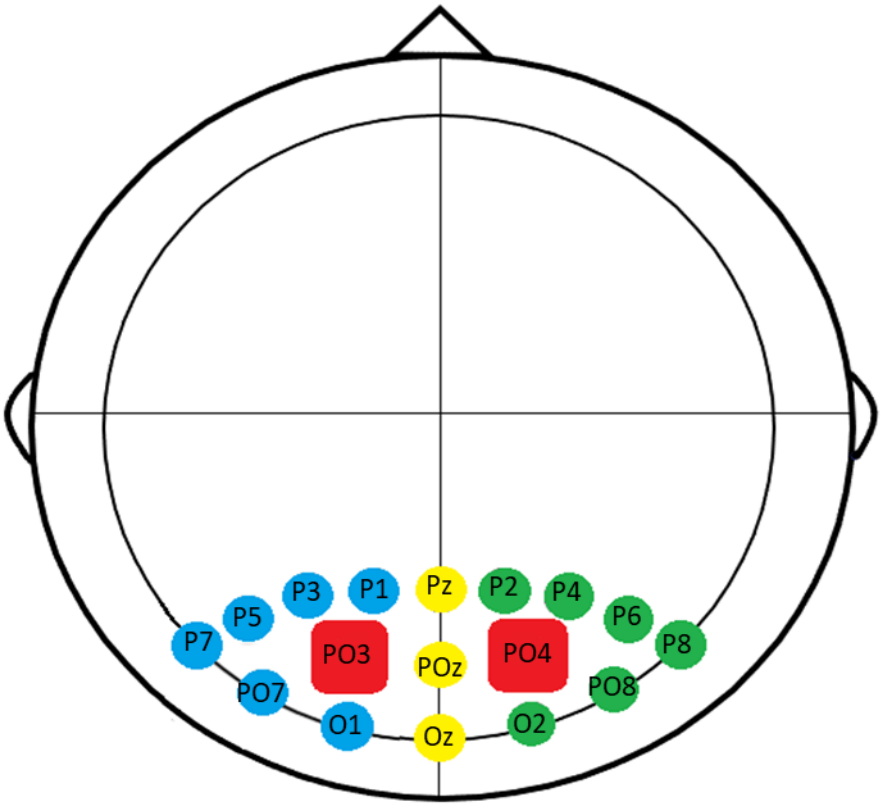

Figure 5.2. Representation and localization of the electrodes of interest. Electrode selected were Pz, POz, Oz, O1, P7, P5, P3, P1, PO7, P2, P4, P6, P8, PO8, and O2 following the 10-20 system. Electrodes were divided in three main regions: Left (blue), Central (yellow) and Right (green). The red squares illustrate the location of the tRNS electrodes that occupied the PO3 and PO4 positions.

5.4 Results

5.4.1 Behavioural results

Figure 5.3 shows the behavioural results for the motion direction discrimination task between pre- and post-stimulation for Sham and hf-tRNS conditions, respectively. A Shapiro-Wilk test reported that data were normally distributed in all the conditions ($p > 0.05$). A repeated measures ANOVA with stimulation type (hf-tRNS and Sham) and time of performance (pre- and post-stimulation) as within-subject factors was performed. The analysis did not reveal any significant effect of stimulation type ($F_{(1,15)} = 1.564$, $p = 0.230$, $\eta^2_p = 0.094$), time of performance ($F_{(1,15)} = 0.698$, $p = 0.416$, $\eta^2_p = 0.044$) or interaction between stimulation type and time of performance ($F_{(1,15)} = 1.838$, $p = 0.195$, $\eta^2_p = 0.109$). Overall, these results showed that behavioural performance was not influenced by the offline hf-tRNS stimulation.

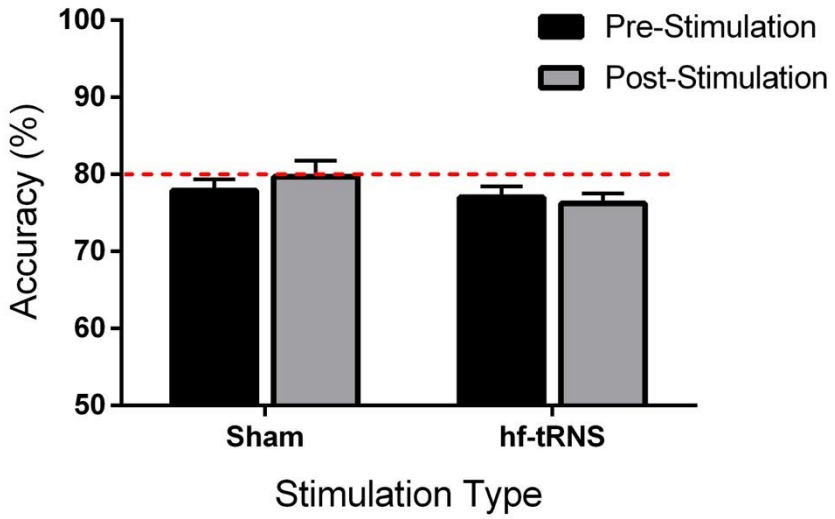

Figure 5.3. Behavioural results of Experiment 5. Mean accuracy for the motion direction discrimination task measured before and after Sham and hf-tRNS sessions. Error bars ±SEM

5.4.2 Electrophysiological results

5.4.2.1 Power Spectral Density (PSD)

For the PSD estimation, the mean absolute power for the selected electrodes and for each observer was extracted. The results from electrodes were pooled into the three regions (Left, Central, and Right), and these were averaged across all participants. Figure 5.6 shows the average PSD for each stimulation condition (hf-tRNS and Sham) and for each recording time (pre-stimulation EEG and post-stimulation EEG) for the three regions: Left, Central and Right. A Shapiro-Wilk test of normality showed that data in every condition and region were normally distributed ($p > 0.05$), except for the right electrodes in the post-stimulation EEG in the beta frequency ($p = 0.04$).

We performed a repeated measures ANOVA with stimulation type (hf-tRNS and Sham) and recording time (pre-stimulation EEG and post-stimulation EEG) as within-subjects factors separately for delta (2-4 Hz), theta (4-8 Hz), alpha (8-14 Hz) and beta (15-30 Hz) bands and for the Central, Left and Right electrodes. Results are reported Table 5.1. Overall, the repeated measures ANOVA for delta and theta bands did not reveal any significant effect for stimulation type, time of stimulation and interaction between stimulation and time in all the three regions.

However, for alpha and beta bands the repeated measures ANOVA showed a different pattern of results. In particular, for these frequency bands, the ANOVA did not

reveal a significant effect of the stimulation type for Central, Left and Right electrodes, but showed a significant effect of recording time with an increment in PSD between pre-stimulation and post-stimulation EEG in all the three electrode regions (Figure 5.4 for alpha band and Figure 5.5 for beta band). However, no significant interaction between stimulation type and time of recording was found.

Overall, the results for the resting state period showed that there was a general increment of the PSD in the alpha and beta band in the post-stimulation EEG with respect to the pre-stimulation EEG, regardless of the type of stimulation and region of the electrodes.

Table 5.1. Summary of statistic for PSD in the delta, theta, alpha and beta bands separately for Left, Central and Right electrodes.

Left Electrodes

Frequency band (Hz)		**Statistics**		
		$F_{(1,15)}$	p	η^2_p
Delta (2-4 Hz)	Stimulation	0.302	0.591	0.02
	Time	1.052	0.321	0.07
	Stimulation x Time	0.179	0.679	0.012
Theta (4-8 Hz)	Stimulation	0.034	0.855	0.002
	Time	3.316	0.089	0.181
	Stimulation x Time	0.162	0.693	0.011
Alpha (8-14Hz)	Stimulation	0.046	0.833	0.003
	Time	**17.86**	**0.001***	**0.544**
	Stimulation x Time	0.21	0.833	0.003
Beta (15-30 Hz)	Stimulation	0.532	0.477	0.034
	Time	**19.080**	**0.001***	**0.560**
	Stimulation x Time	1.351	0.263	0.083

Central Electrodes

Frequency band (Hz)		**Statistics**		
		$F_{(1,15)}$	P	η^2_p
Delta (2-4 Hz)	Stimulation	0.085	0.775	0.006
	Time	0.031	0.863	0.002
	Stimulation x Time	0.196	0.665	0.013
Theta (4-8 Hz)	Stimulation	0.042	0.840	0.003
	Time	1.193	0.292	0.074
	Stimulation x Time	0.399	0.537	0.026
Alpha (8-14Hz)	Stimulation	0.286	0.60	0.019
	Time	**17.785**	**<0.001***	**0.542**
	Stimulation x Time	0.483	0.498	0.031
Beta (15-30 Hz)	Stimulation	0.03	0.954	<0.001
	Time	**25.398**	**<0.001***	**0.629**
	Stimulation x Time	1.181	0.294	0.073

Right Electrodes

Frequency band (Hz)		**Statistics**		
		$F_{(1,15)}$	P	η^2_p
Delta (2-4 Hz)	Stimulation	1.208	0.289	0.75
	Time	0.223	0.644	0.015
	Stimulation x Time	1.484	0.242	0.090
Theta (4-8 Hz)	Stimulation	0.40	0.537	0.026
	Time	1.716	0.210	0.103
	Stimulation x Time	1.109	0.309	0.069
Alpha (8-14Hz)	Stimulation	0.669	0.426	0.43
	Time	**20.824**	**0.001***	**0.581**
	Stimulation x Time	0.669	0.420	0.044
Beta (15-30 Hz)	Stimulation	0.088	0.771	0.006
	Time	**19.635**	**<0.001***	**0.567**
	Stimulation x Time	1.968	0.181	0.116

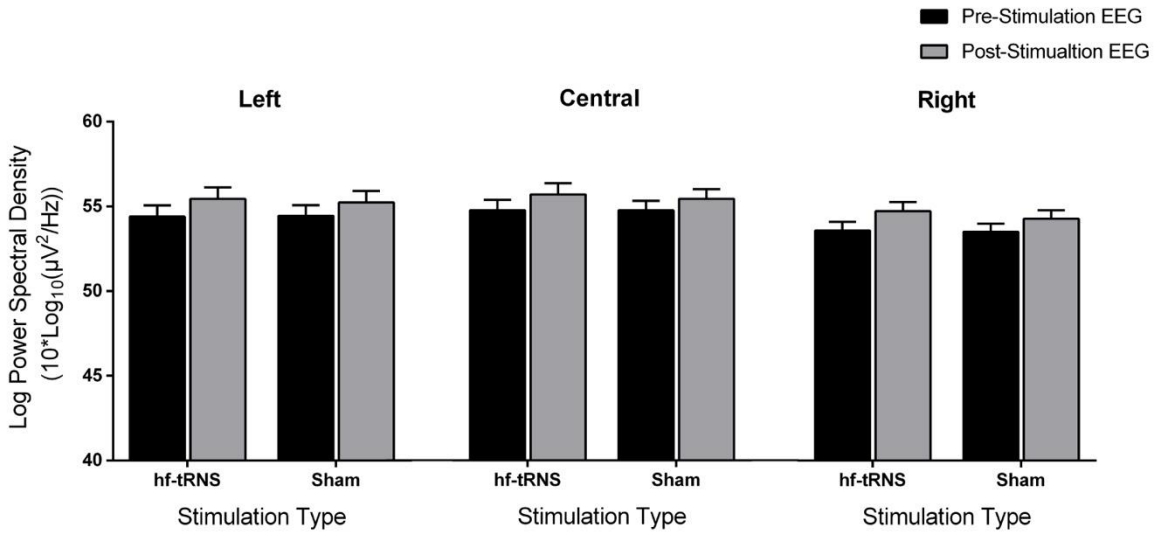

Figure 5.4. Mean alpha power spectral density ($10*\log_{10}(\mu V^2/Hz)$) for Left, Central and Right side.
Each side include mean values for hf-tRNS and Sham stimulation condition for Pre-Stimulation EEG (black) and Post-Stimulation EEG (grey). Error bars ±SEM.

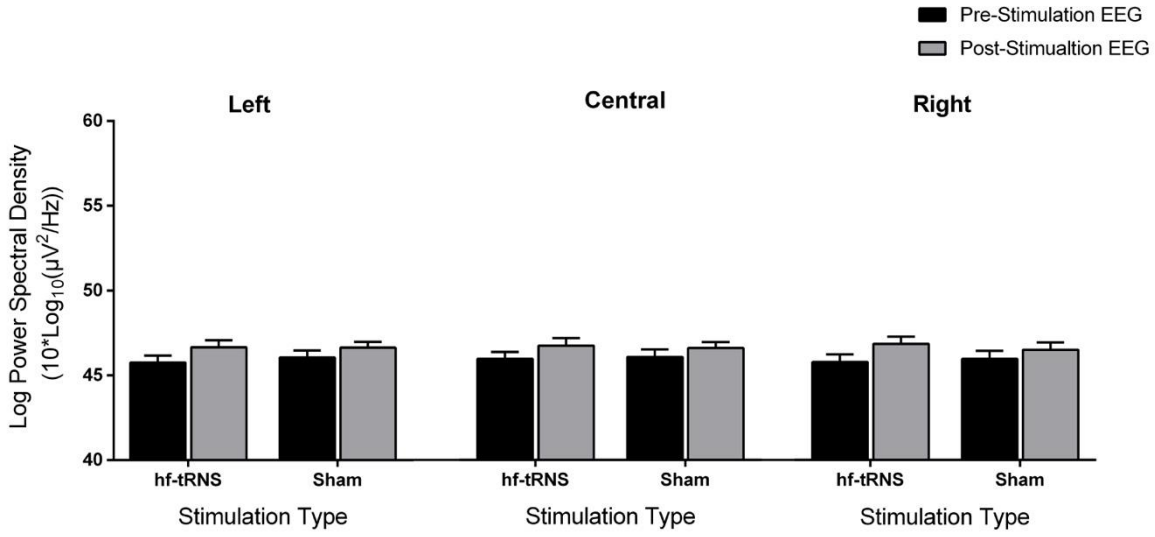

Figure 5.5. Mean Beta power spectral density ($10*\log_{10}(\mu V^2/Hz)$) for Left, Central and Right side.
Each side include mean values for hf-tRNS and Sham stimulation condition for Pre-Stimulation EEG (black) and Post-Stimulation EEG (grey). Error bars ±SEM.

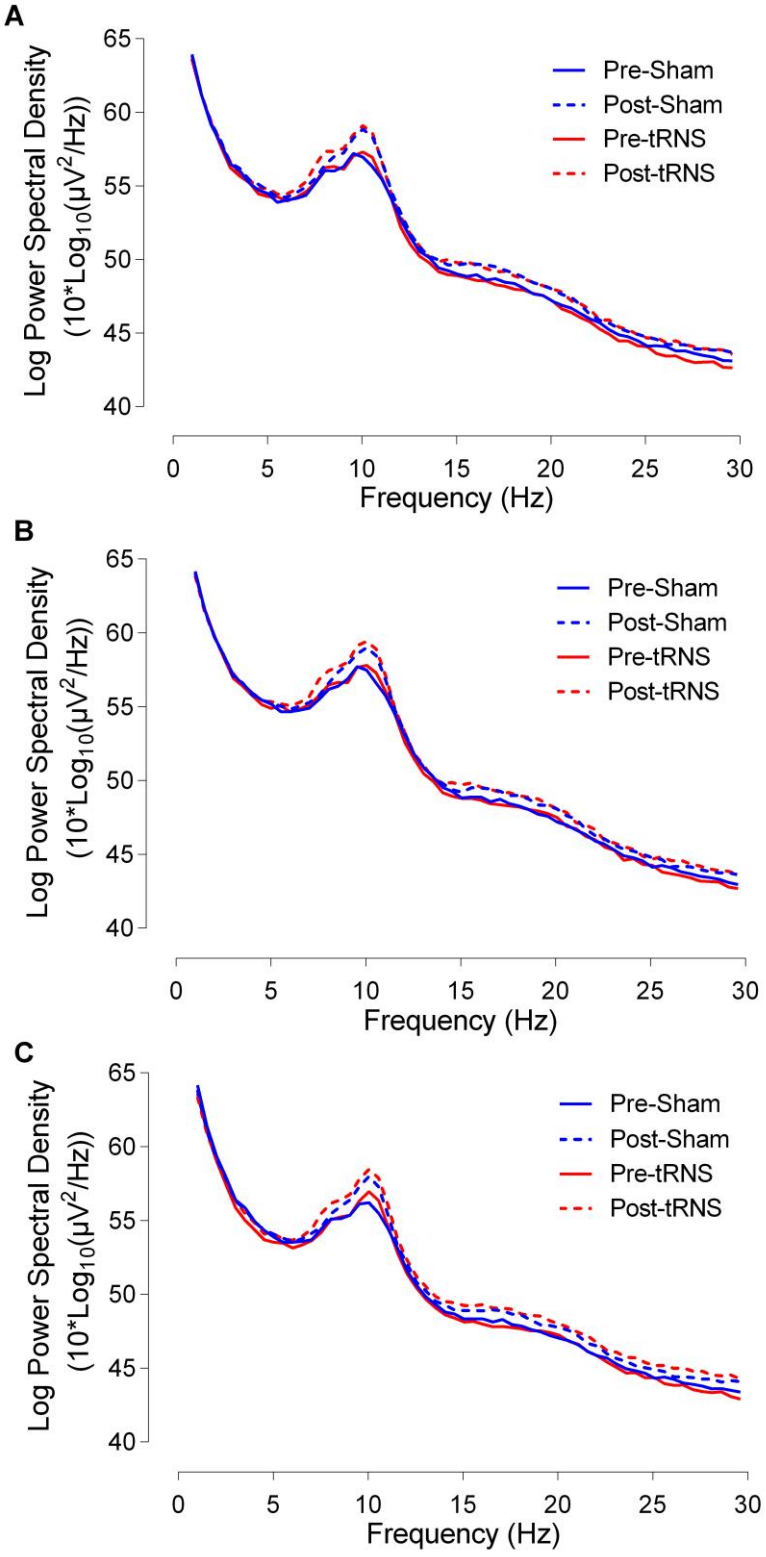

Figure 5.6. Average power spectra density during resting state. Average power spectra density ($10*\log_{10}(\mu V^2/Hz)$) for hf-tRNS (in blue) and Sham (in red) and recording time for pre-stimulation EEG (solid line) and post-stimulation EEG (dotted line). Panel A, B and C show Left, Central and Right electrodes, respectively.

5.4.2.2 Visual Evoked Potentials (VEPs)

Amplitudes

For the VEPs amplitude estimation, the mean amplitude for the selected electrodes and for each observer was extracted. Data from electrodes were pooled into the three regions (Left, Central and Right), and these were averaged across all participants.

Figure 5.7 shows VEPs for the Left electrodes. For the Left electrodes a Shapiro-Wilk test showed that data for mean amplitude for all the components of interest were normally distributed ($p > 0.05$), with except the P2 component of the post-stimulation EEG in the Sham condition ($p = 0.027$). Figure 5.8 shows VEPs for the Central electrodes. A Shapiro-Wilk test showed that data for mean amplitude for all the components of interest were normally distributed ($p > 0.05$) except the P2 component of the post-stimulation EEG hf-tRNS condition ($p = 0.035$) and the N2 component of the post-stimulation EEG hf-tRNS condition ($p = 0.044$). Figure 5.9 shows VEPs for the Right electrodes. For the Right electrodes a Shapiro-Wilk test showed that data for mean amplitude for all the components of interest were normally distributed ($p > 0.05$) with except the P1 component of the post-stimulation EEG Sham condition ($p = 0.024$).

A repeated measures ANOVA with stimulation type (hf-tRNS and Sham) and recording time (pre-stimulation EEG and post-stimulation EEG) as within-subjects factor separately for all the components (P1, N2 and P2) and for the Left, Central and Right region. Results are reported in Table 5.2. Overall, the results showed that for all the components considered, VEP mean amplitudes was not affected by offline hf-tRNS.

Table 5.2. Summary of statistic for amplitude values for P1, N2 and P2 component separately for Left, Central and Right electrodes

Left Electrodes

VEPs		Statistics		
		$F_{(1,15)}$	p	η^2_p
P1	Stimulation	0.790	0.39	0.05
	Time	0.120	0.73	0.008
	Stimulation x Time	0.001	0.99	0.001
N2	Stimulation	1.181	0.30	0.073
	Time	1.401	0.26	0.09
	Stimulation x Time	1.404	0.25	0.09
P2	Stimulation	0.316	0.60	0.021
	Time	3.206	0.09	0.176
	Stimulation x Time	0.737	0.40	0.047

Central Electrodes

VEPs		Statistics		
		$F_{(1,15)}$	p	η^2_p
P1	Stimulation	0.217	0.65	0.014
	Time	0.008	0.93	0.001
	Stimulation x Time	0.032	0.86	0.002
N2	Stimulation	0.003	0.95	<0.001
	Time	0.976	0.34	0.06
	Stimulation x Time	0.108	0.75	0.007
P2	Stimulation	0.021	0.89	0.001
	Time	0.029	0.87	0.002
	Stimulation x Time	0.446	0.51	0.029

Right Electrodes

VEPs		Statistics		
		$F_{(1,15)}$	p	η^2_p
P1	Stimulation	2.282	0.15	0.132
	Time	0.165	0.69	0.011
	Stimulation x Time	0.017	0.90	0.001
N2	Stimulation	3.928	0.07	0.208
	Time	0.018	0.89	0.001
	Stimulation x Time	0.123	0.731	0.008
P2	Stimulation	0.520	0.82	0.003
	Time	2.089	0.17	0.122
	Stimulation x Time	0.304	0.59	0.02

Latencies

For the VEP latencies estimation, the peak amplitudes and their corresponding latencies (in ms) with respect to the stimulus onset were extracted for each observer. As for the amplitude, the results from electrodes of interest were pooled into the three regions (Left, Central and Right), and these were averaged across all participants (Figure 5.7, 5.8 and 5.9). The latencies corresponding to the components peaks were highly variable across participants and a Shapiro-Wilk test showed that the data were in most cases not

normally distributed ($p < 0.05$). In order to analyse our data, we performed an Aligned Rank Transform analysis for non-parametrical data (Wobbrock, Findlater, Gergle, & Higgins, 2011). This statistical procedure allows one to perform a non-parametric analysis of variance for factorial models. The analysis implements pre-processing steps that "align" not normally distributed data before applying averaged ranks after which common ANOVA or a linear mixed model can be performed. For our data we performed this analysis by using the statistical software R (R Core Team, 2013) and the "*ARTtool*" package developed by Wobbrock et al. (2011). After the rank assignment, we performed a LMM (lme4 package for R; Bates, Mächler, Bolker, & Walker, 2015) with stimulation type (hf-tRNS and Sham) and recording time (pre-stimulation EEG and post-stimulation EEG) as within-subjects factors, and subjects as random intercepts. This analysis was performed separately for all the components (P1, N2 and P2) and for the three regions. Results are reported Table 5.3.

For the Left electrodes, the results showed a similar pattern, as there was a significant effect of the stimulation factor for the P1 component, but neither time of recording nor the interaction between stimulation type and time of recording were significant. Moreover, no significant effects were found for the P2 and the N2 components.

For the Central electrodes results showed that there was a significant effect of the stimulation factor for the P2 component, but neither time of recording nor the interaction between stimulation type and time of recording were significant. Moreover, no significant effects were found for P1 and N2 components.

For the Right electrodes, the results showed no significant effects for P1 and N2 components. However, for the Right P2 component, we found a significant interaction between stimulation type and time of recording ($p = 0.048$). To determine significant differences across stimulation conditions and time of recording on the P2 component, we performed a series of Wilcoxon Signed-Rank tests corrected with FDR at 0.05. The results showed that overall there was no significant difference between pre-stimulation EEG and post-stimulation EEG in the hf-tRNS condition (*corrected-p* = 0.41, $r = 0.31$) or between pre-stimulation EEG and post-stimulation EEG in the Sham condition (*corrected-p* = 0.44, $r = 0.21$). Moreover, no significant difference was found between pre-stimulation EEG in the Sham condition and pre-stimulation EEG in the hf-tRNS condition (*corrected-p* = 0.44, $r = 0.19$) or between post-stimulation EEG in the Sham condition and post-stimulation EEG in the hf-tRNS condition (*corrected-p* = 0.1, $r = 0.56$). Overall, these results showed that VEP latencies were not modulated by offline hf-tRNS.

Table 5.3. Summary of statistics for latencies values for P1, N2 and P2 component separately for Left, Central and Right electrodes.

Left Electrodes

VEPs		Statistics	
		$F_{(1,45)}$	p
P1	Stimulation	**5.013**	**0.03***
	Time	<0.001	0.98
	Stimulation x Time	0.858	0.36
N2	Stimulation	0.256	0.62
	Time	2.387	0.13
	Stimulation x Time	2.262	0.14
P2	Stimulation	0.086	0.77
	Time	0.812	0.37
	Stimulation x Time	0.015	0.90

Central Electrodes

VEPs		Statistics	
		$F_{(1,45)}$	p
P1	Stimulation	3.321	0.08
	Time	0.174	0.68
	Stimulation x Time	0.088	0.79
N2	Stimulation	0.663	0.42
	Time	1.882	0.18
	Stimulation x Time	0.954	0.33
P2	Stimulation	**4.245**	**0.045***
	Time	3.331	0.75
	Stimulation x Time	0.659	0.42

Right Electrodes

VEPs		Statistics	
		$F_{(1,45)}$	p
P1	Stimulation	0.097	0.76
	Time	0.47	0.50
	Stimulation x Time	0.454	0.50
N2	Stimulation	3.058	0.09
	Time	<0.001	1.0
	Stimulation x Time	0.009	0.93
P2	Stimulation	0.890	0.35
	Time	2.611	0.11
	Stimulation x Time	**4.119**	**0.048***

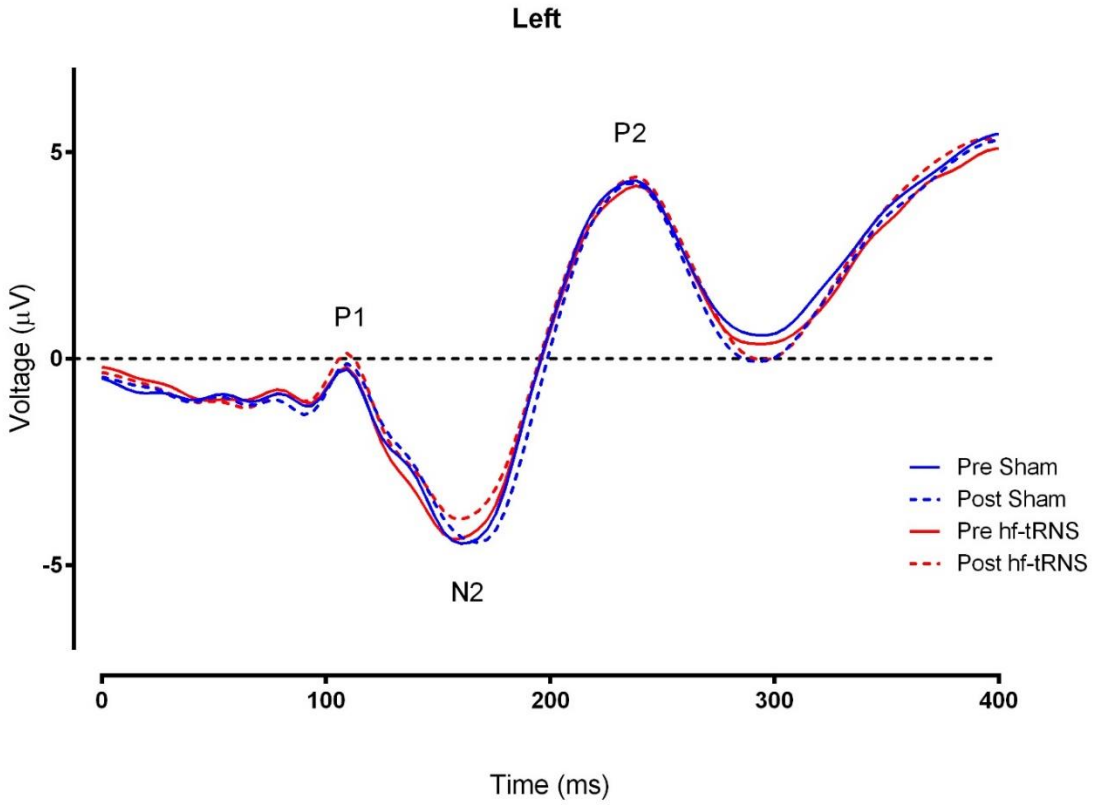

Figure 5.7. Mean Visual Evoked Potentials (VEP) for the Left electrodes (O1, P1, P3, P5, P7, PO7).
VEPs are illustrated for each stimulation condition (hf-tRNS in blue, Sham stimulation in red) and recording time: pre-stimulation EEG (solid lines) and post-stimulation EEG (dotted lines).

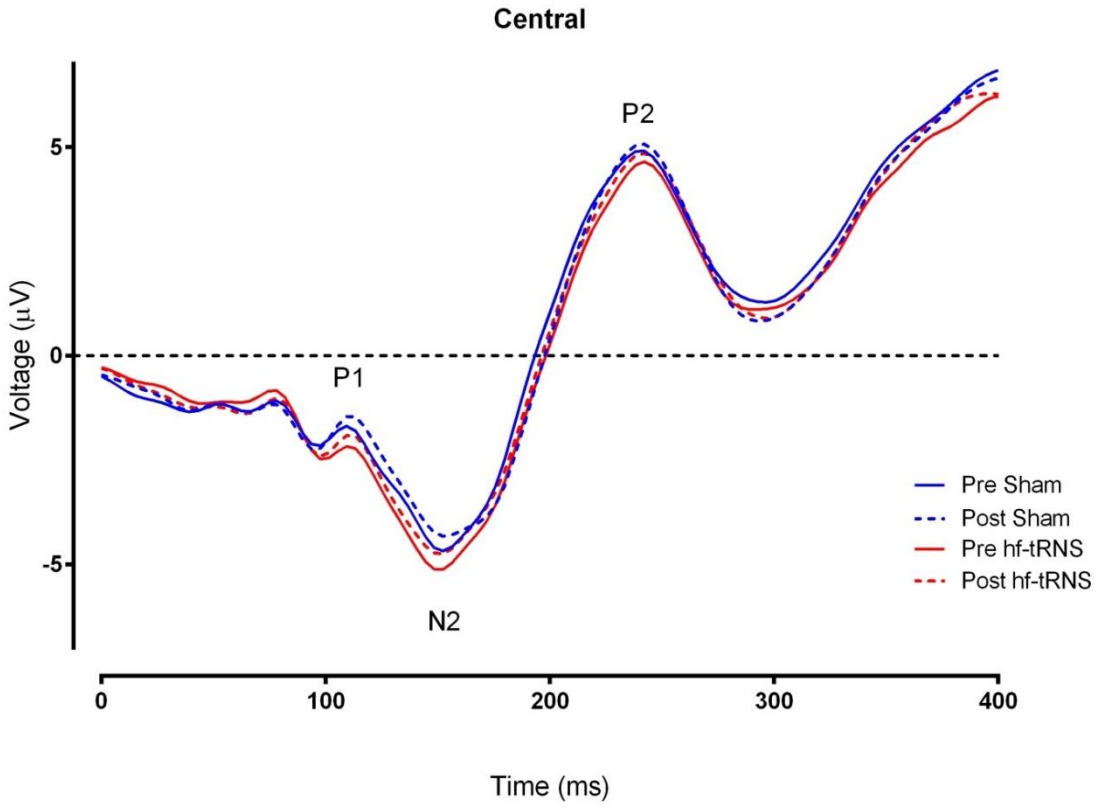

Figure 5.8. Mean Visual Evoked Potentials (VEPs) for the Central electrodes (POz, Oz, Pz).
VEPs are illustrated for each stimulation condition (hf-tRNS in blue, Sham stimulation in red) and recording time: pre-stimulation EEG (solid lines) and post-stimulation EEG (dotted lines).

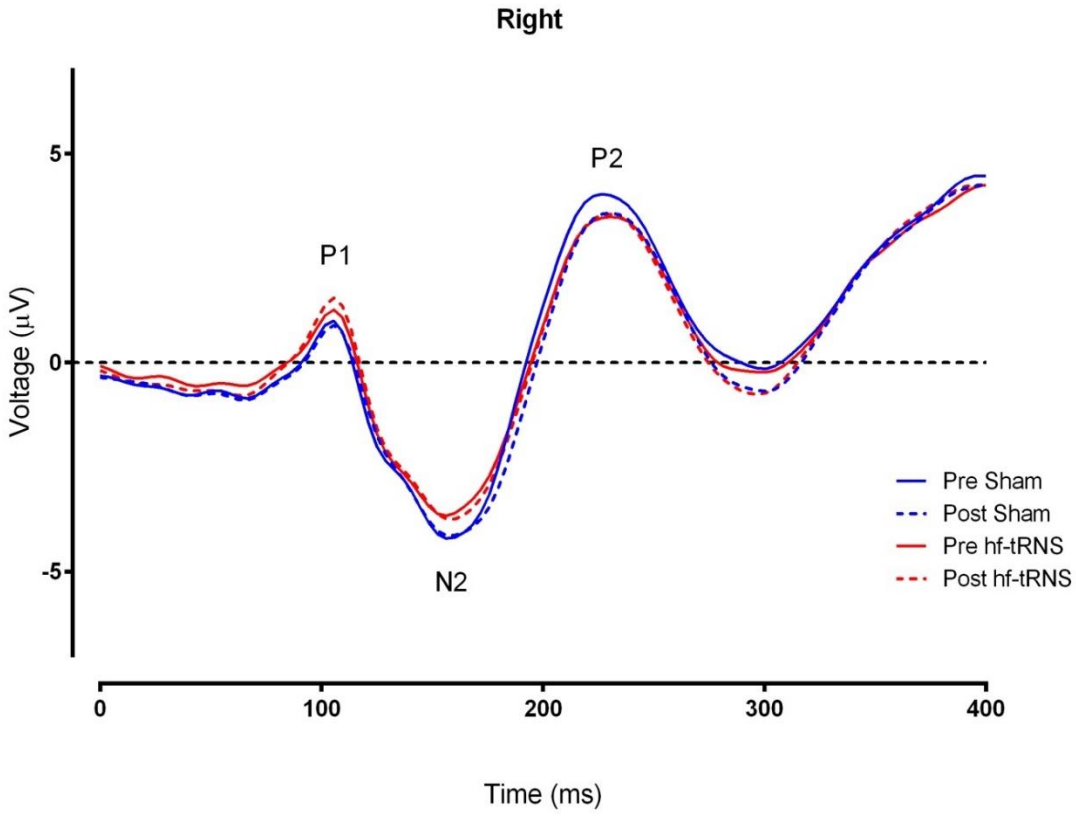

Figure 5.9. Mean Visual Evoked Potentials (VEP) for the Right electrodes (O2, P2, P4, P6, P8 and PO8).
VEPs are illustrated for each stimulation condition (hf-tRNS in blue, Sham stimulation in red) and recording time: pre-stimulation EEG (solid lines) and post-stimulation EEG (dotted lines).

5.5 Discussion

In the present study we tested if a single hf-tRNS session delivered offline was able to induce physiological modulations on brain oscillations activity at rest and measurements of amplitude and latency on motion related VEPs. Additionally, we also assessed tRNS-induced aftereffects on the motion direction discrimination performance. Overall, our results showed that 20 minutes of offline bilateral hf-tRNS was not able to induce any significant aftereffect in any of the considered measures.

Specifically, the results showed that offline hf-tRNS did not modulate performance at the motion direction discrimination task with respect to the pre-stimulation EEG and with respect to the Sham stimulation. This outcome could be the result of two main factors. Firstly, differently from the experiments presented in the previous Chapters, the stimulation was delivered offline, so before performing the task. This might show that hf-tRNS aftereffects on the visual cortex are not strong or long

lasting enough to modulate the mechanism involved in the motion visual task. These results are also in line with previous findings which showed that online hf-tRNS was able to improve the performance in orientation discrimination task, whereas when applied offline hf-tRNS did not show any significant difference with respect to a Sham stimulation (Pirulli et al., 2013). The second factor could be the high level of coherence threshold (80% ± 5%) implemented for this study. If the hf-tRNS mechanism can be explained within the stochastic resonance theory as suggested by previous studies and what we have found in Chapter 4 (Fertonani et al., 2011; Miniussi et al., 2013; Rufener et al., 2017; van der Groen & Wenderoth, 2016), then no or little effects on performance can be expected when the coherence is set well above threshold.

Electrophysiological results showed that alpha and beta band oscillations at rest significantly increased the averaged PSD on the post-stimulation EEG with respect to the pre-stimulation EEG, but this was not related to a specific stimulation condition. Furthermore, this increment was not restricted to a specific location, but was present for all Central, Left and Right electrodes. On the other hand, no significant difference was found for delta and theta bands. The level of alpha power at rest is linked to cortical excitation and metabolic activity, larger alpha power is thought to be indicative of synchronised activity and so reduced metabolic activation (Nunez & Silberstein, 2000). Recently, it has been found that alpha power can increase as the result of sustained attention and fatigue during the execution of an experimental task. For example, Benwell et al. (2019) found a significant increment of alpha power between the first half and second half of the experimental session while observers were performing either a line bisection task or a forced-choice luminance discrimination task. Similarly, we hypothesised that in our study the increased synchronization in the alpha band post-stimulation EEG with respect to the pre-stimulation EEG might be the result of an enhanced relaxation state or increased fatigue due to the sustained attention of the observers during the testing session. Results for the beta oscillations shows a similar trend. In fact, the PSD in the beta band was significantly higher in the post-stimulation EEG with respect to the pre-stimulation EEG in all electrode regions. However, similarly to the alpha band, the beta band increment in PSD was not limited to a specific stimulation condition. Beta oscillations have been associated with motor functions and evidence shows higher beta synchronizations during steady contractions or while a participant is asked to hold still after a movement (for a review, see Engel & Fries, 2010). It has been also proposed that beta band activity maintains what Engel and Fries (2010) defines as the “status quo” of the somatosensory system (Androulidakis et al., 2007; Gilbertson,

2005). However, the role of the beta band during a prolonged resting state period is less clear. Few studies showed positive correlations for alpha and beta bands at rest with metabolic activity in areas associated to the default model network (DMN) such as temporal-parietal junction, inferior parietal junction and frontal gyrus (Laufs et al., 2003; Mantini et al., 2007). Therefore, we might hypothesise that as for the alpha band, the increased beta band activity on the post-stimulation EEG might reflect a general enhanced relaxation state of the participants during the experimental sessions. Additionally, our results on oscillatory activity partially confirm previous findings, which showed that a single session of offline hf-tRNS was not able to induce any modulation of oscillatory activity during a resting state period (Van Doren et al., 2014). In general, studies that investigate the effects of tES regimes during a resting state are limited, and just few assessed an offline procedure or investigated the extent of the stimulation aftereffects. Studies applying tACS and oscillatory-tDCS showed significant stimulation aftereffects on oscillatory activity at rest, but results are somewhat mixed probably depending on difference in stimulation parameters such as intensity and duration of the stimulation or the cerebral areas of interest (for a review, see Veniero et al., 2015). Additionally, even studies that investigated the aftereffects of anodal and cathodal tDCS during rest reported contrasting results. For example Puanhvuan et al. (2013) found that cathodal tDCS increase alpha power amplitude over the parietal-occipital areas while anodal diminish it, whereas (Spitoni et al., 2013) found an increased alpha power amplitude after anodal stimulation limited to the frontal and parietal cortex. Yet, as introduced previously, it is important to mention that comparisons between these and our results should be done with caution, since different outcomes might be expected when using different experimental procedures.

The VEP analysis showed no significant aftereffect induced by offline hf-tRNS on values of amplitude and latency for the P1, the N2 and the P2 components. In regards to the amplitudes, our results seems to be in line with recent findings which showed no significant modulation of auditory ERP amplitude for N1 and P50 components (Rufener et al., 2017) in auditory gap detection task. On the other hand, contrary to our results the same study found a significant reduction on the latencies for the P50 and N1 components. However, this stimulation-mediated modulation was seen only when the auditory stimulus was presented at the individual gap detection threshold, whereas if the stimulus was presented lower or higher with respect to the threshold, no significant aftereffect was registered. Unlike from Rufener et al. (2017), in our study stimulation was delivered offline and we presented the stimuli at the 80% ± 5% of direction discrimination

threshold in order to elicit well-defined VEP components. Amplitude and latency of a motion-related component such as N2 are dependent on the coherence of the RDK stimulus, for which increments of coherence correspond an increase in the amplitude and a reduction of the latency (Niedeggen & Wist, 1998; Patzwahl & Zanker, 2000). We could speculate that the lack of significant modulation in VEP components in our study might be attributable to the high level of coherence of the stimulus employed, for which hf-tRNS aftereffects might be not strong enough to induce any reliable modulation.

Studies on hf-tRNS aftereffects on visual cortex excitability are scarce. Our results seems to suggest that a single session of offline hf-tRNS does not induce any reliable change in cortical activity when delivered bilaterally over parietal-occipital cortex. This outcome contrasts with a previous study which investigated the ability of offline hf-tRNS to modulate cortical excitability over the visual cortex (Herpich, Contò, et al., 2018). Specifically, Herpich and colleagues (2018) measured phosphene thresholds via single pulse TMS after hf-tRNS was delivered bilaterally at 1 mA for 20 min over the occipital cortex. Results showed that hf-tRNS compared to Sham stimulation was able to increase cortical excitability (lower phosphene thresholds) from immediately after the stimulation up to 60 min. Although discrepancies between studies that measure tES aftereffect on cortical excitability have been pointed out (Parkin et al., 2019), the differences between Herpich et al. (2018) and our results are substantial. A speculative explanation of this discrepancy might be attributable to the differences between the two procedures implemented to measure the cortical activity. In fact, while cortical excitability estimation via TMS is measured over a limited portion of the cortex, we recorded the electrical activity from wider regions of the scalp around the stimulation electrodes, containing a larger number of neural assembles. It might be that a single session of offline hf-tRNS might be not effective enough to induce medium/long-term modulatory effects detectable with such procedure.

Although the study presented here found inconclusive results, it does not exclude the possibility of the hf-tRNS to induce electrophysiological alteration of the normal activity when delivered in an online procedure. Future studies should investigate the difference at the behavioural and electrophysiological level between hf-tRNS delivered offline and delivered when an observer is engaged in a visual task. In fact, the effects of the stimulation could be dependent to the ongoing neural activity of the brain system. In fact, the interaction between the operating neural population and the stimulation can have a large impact on the stimulation outcomes (Romei et al., 2016). Therefore, future studies

could look at the effects of hf-tRNS on motion VEP when the stimulation is delivered concurrently with the execution of the visual task.

In conclusion, the results presented here showed that one session of offline hf-tRNS delivered bilaterally over the parietal-occipital cortex did not induce any significant aftereffect modulation of resting state power or in levels of amplitude and latency for motion-related VEPs. Considering the previous literature, these results seem to support the idea that hf-tRNS aftereffects are highly dependent on the type of stimulation paradigm employed and on the complexity of the task used. More studies are needed to understand the underlying physiological effects improving behavioural performance in single hf-tRNS session.

Chapter 6: General Discussion

6.1 Summary of results

The aim of this research was to gain further knowledge of tES effects and mechanisms of action on the human visual cortex. In order to do this, we employed well-known psychophysical paradigms to probe behavioural and electrophysiological effects of different tES techniques on global motion perception. In Chapter 2, we investigated if different tES techniques could modulate behavioural performance in a motion direction discrimination task and compared the effects of different stimulation types (see Experiment 1.1). Specifically, cathodal tDCS, anodal tDCS and hf-tRNS were applied over the left hMT^+ and changes in coherence threshold and slope of the psychometric function were measured. Our results showed that, while both cathodal and anodal tDCS did not modulate motion coherence threshold, hf-tRNS decreased the coherence threshold specifically in the visual hemi-field contralateral to the stimulation site, but did not alter the slope of the psychometric function, suggesting that hf-tRNS does not modulate the discriminability of the moving pattern. Instead, we interpreted these results in terms of hf-tRNS-related enhanced probability of the neural population responding to the signal direction to generate action potentials and therefore increasing the general signal-to-noise ratio.

In Chapter 3, we asked if decreased coherence threshold with online hf-tRNS, resulted in reduced observer's variability in precisely estimating local motion directions (i.e., reduction of *internal noise*) or an enhanced ability to pool local directions signals together (i.e., increased *sampling*). To answer this question we implemented an Equivalent Noise paradigm (Dakin et al., 2005; Tibber et al., 2014) in order to estimate measures of *internal noise* and *sampling*. We observed that hf-tRNS only increased *sampling* levels, therefore we interpreted these results as an enhanced integration process of local motion directions that operates at the hMT^+ level. On the other hand, we argued that *internal noise* might be linked to the neural direction selectivity bandwidth (Manning et al., 2015) and that stimulation might benot able to alter such neural property. Moreover, stimulation over the hMT^+ could not be as effective as modulating *internal noise* of local motion cues because the precision in processing single dots trajectory at the hMT^+ stage might be dependent ony the signal direction uncertainty originating in the primary visual cortex (Mareschal et al., 2008).

The results presented in Chapters 2 and 3 lead us to further explore the underlying mechanisms of hf-tRNS when delivered on the visual cortex. In a subsequent study

(Chapter 4) we carried out a series of experiments to investigate the proposed stochastic resonance phenomenon to explain hf-tRNS effects in the visual cortex. Stochastic resonance is a phenomenon whereby the addition of an optimal amount of random interference (i.e., noise) into a non-linear system like the brain can enhance the detection or discrimination of weak stimuli. However, if too much noise is added, this can hinder the signal or information content (McDonnell & Abbott, 2009; Moss et al., 2004; Ward, 2009). Hf-tRNS is a non-focal stimulation that delivers current at random intensity and random frequencies and it has been suggested act as an external source of neural noise (Antal & Herrmann, 2016; Miniussi et al., 2013). Experiment 4.1 found that optimal intensity of the stimulation, considered as a source of additional neural noise, enhanced direction discrimination performance, whereas Experiment 4.2 found that further increments of the intensity produced a decrement of the performance.

Our results support the hypothesis that motion direction discrimination is a visual process sensitive to the stochastic resonance phenomenon when external noise via hf-tRNS is added directly into the brain (Kitajo et al., 2003; Rufener et al., 2017; van der Groen & Wenderoth, 2016).

In Chapter 5 we sought to investigate whether offline hf-tRNS was able to induce long-term behavioural and electrophysiological aftereffects on the visual cortex. Therefore EEG activity was recorded prior to (pre-stimulation EEG) and after (post-stimulation EEG) 20 minutes of bilateral hf-tRNS over the hMT^{+}. Both pre and post-stimulation EEG periods consisted of five minutes of resting state followed by the execution of a motion direction discrimination task. Mean values of the power spectral density (PSD) for delta, theta, alpha and beta oscillation bands from the resting state periods, and visual evoked potentials (VEPs), mean amplitude and latency for the P1, N2 and P2 components elicited by the visual moving stimulus were measured. Direction discrimination performance was also analysed. The results showed that hf-tRNS delivered offline did not affect behavioural performance, which might be due to the high individual coherence threshold (80±5%) used for this experiment. Another possibility is that, to obtain a performance improvement, hf-tRNS needs to be delivered when the neural population coding for the direction signal is actively engaged in a task. Moreover, results also showed that offline hf-tRNS did not modulate the recorded EEG activity. Specifically, VEPs mean amplitude and latency for all the components were not affected by the stimulation. Although we found a significant statistical interaction between stimulation type and time of recording for the P2 latency, corrected post-hoc comparisons did not reveal any significant difference between pre and post-stimulation EEG in the hf-

tRNS condition. Moreover, we found an increased power spectral density between pre and post-stimulation resting state period for alpha and beta bands. However, this increment was not specific for the hf-tRNS stimulation and we argued that it might be the result of an increased relaxation state of the participants. We concluded by suggesting that a single session of offline hf-tRNS might not be effective in inducing enduring aftereffects on the visual cortex.

6.2 Possible tRNS mechanisms of action

The consistent employment of tDCS and tACS studies with respect to tRNS in human participants and the near absence of animal studies investigating the effects of this stimulation protocol leaves many open questions about its effects on the neural activity. The hypotheses proposed to explain tRNS modulatory activity rely mostly on observations of changes in behavioural performance or on indirect measures of cortical activity via neuroimaging techniques that involve large neuronal networks. Since human recordings of single neural activity are very rare and involve surgical procedures on patients, the investigation of tRNS effects at the neural level remain very complicated to explore. Therefore, for the time being it remains somewhat challenging to explain the physiological mechanisms of action at the origin of its effects on the human brain. The findings of Chaieb et al. (2015) showed a decreased excitability induce by full spectrum tRNS (0.1- 640 Hz) after administration of a sodium channel blocker. This was the first evidence in support of Terney et al.'s (2008) previous suggestion that tRNS effects might depend on an alteration of the normal activity of Na^+ channels. This would result in an increased probability to generate an action potential and a reduced membrane repolarization time-window.

The hypothesis suggesting an alteration of the normal Na^+ voltage-gated channel activity, seems to be in agreement with recent *in vitro* studies investigating the effects of electrical random noise stimulation (RNS) on rat's neurons of the sensorimotor and auditory cortex (Remedios et al., 2019) and dorsal root ganglia (Onorato et al., 2016). Specifically, results showed that electric random noise stimulation enhanced action potential firing due to an increased recruitment of Na^+ channels (Onorato et al., 2016) and an increased amplitude of Na^+ inward currents resulting from the increased activation of the voltage-gated channels (Remedios et al., 2019). More interestingly, in both of these studies the modulatory effects of the stimulation showed features compatible with the stochastic resonance phenomenon depending on the RNS levels in terms of amplitude

(Onorato et al., 2016) and voltage (Remedios et al., 2019). In particular Onorato et al. (2016) suggested that their results provide a proof of principle that external noise can enhance via stochastic resonance the recruitment of Na^+ channels responsible for generating action potentials in sensory neurons. Although a translation of the same mechanism applying from single neurons activity to larger neural networks usually manipulated in human tES protocols must be cautious, this evidence could give theoretical support to the tRNS behavioural effects (Remedios et al., 2019). Therefore, the improvements showed in Chapters 2 to 4 could be a result of the online hf-tRNS enhancing the probability of neural firing and consequently increasing the overall activity of interconnected neurons coding for the directional signal. However, this modulatory effect would not be an all-or-nothing phenomenon, but subject to the level of perturbation (i.e., noise) caused by a given hf-tRNS intensity. As a result, our studies showed an enhanced behavioural performance following an inverted U-like shape function characteristic of the stochastic resonance phenomenon as we found in Chapter 4.

6.3 Study issues and general tES limitations

In Chapter 2, we found that both anodal and cathodal tDCS did not affect motion direction discrimination. These results contrast with some previous findings (Antal et al., 2004c; Battaglini et al., 2017). We argued that these discrepancies could be the result of the stimulation paradigm implemented (online versus offline) and the type of psychophysical procedure used to estimate coherence threshold and slope of the psychometric function (see also paragraph 2.5, Chapter 2). Noteworthy, recent reviews and meta-analyses illustrated that many factors can influence stimulation behavioural results (Fertonani & Miniussi, 2017; Jacobson, Koslowsky, & Lavidor, 2012). For example, the fact that our results for anodal and cathodal tDCS in Experiment 1.1 did not support previous findings (Antal et al., 2004c; Battaglini et al., 2017), gives a cautionary demonstration that tES is a complex technique and unexpected results can arise from the high number of variables and stimulation parameters at play that can influence the final outcome. The high variability of tES results has also led to active debates about its actual effectiveness. Recently, a few authors have expressed important criticisms about this neuromodulatory technique (Horvath, Carter, & Forte, 2014; Horvath, 2015; Horvath, Forte, & Carter, 2015a; Horvath, Forte, & Carter, 2015b) which also triggered some interesting responses (Antal, Keeser, Priori, Padberg, & Nitsche, 2015; Nitsche, Bikson, & Bestmann, 2015; Price & Hamilton, 2015). The central idea that probably comes out

from these discussions is that more care should be taken in generalizing findings from single studies if the basic mechanisms of action are still uncertain. In relation to the results presented in this project there is still little evidence about hf-tRNS mechanisms of action, and how stimulation effects can be influenced by the stimulation parameters, characteristic of the task and individual differences. For example, in Chapter 4 we focused on stimulation intensity, and hf-tRNS at 1.5 mA was found to be the "optimal" current intensity boosting motion direction discrimination performance. However, improvements were not limited to this condition. In fact, we found some improvement with respect to the baseline (No-tRNS) when hf-tRNS was also delivered at 1.0 mA. Although we did not estimate the "optimal" intensity at the individual level and the analysis was conducted at group level, these results demonstrated that there is a certain variability for optimal stimulation intensity across the sample. Interestingly, this notion has already been pointed out by van der Groen and Wenderoth (2016) who also showed some degree of variability for what was the "optimal" hf-tRNS intensity to decrease contrast detection threshold, demonstrating that there is hardly a good-for-all intensity.

Furthermore, it is important to highlight the fact that generally tES has a lower spatial resolution with respect to other stimulation techniques such as TMS, and several computational models show how the current can spread over the borders of the stimulation electrodes and that the current flow can be highly dependent on the type of montage used and the position of the reference electrode (Bikson, Datta, Rahman, & Scaturro, 2010; Datta, Baker, Bikson, & Fridriksson, 2011; Opitz et al., 2016). For these reasons in the study described in Chapter 2 we devised two additional control conditions in order to assess if the stimulation effects we reported were specific for the stimulation site in the visual cortex (Experiment 1.2B) and to control for nonspecific effects of the reference electrode over Cz (Experiment 1.2A). The results showed that in both control experiments (Experiment 1.2A and 1.2B) hf-tRNS did not induce any significant effect, therefore we concluded that the stimulation-mediated modulation that promoted a decrease of coherence threshold was limited to an alteration of the normal activity in temporal-occipital cortex. Although we implemented these additional controls, a limiting factor of our study is that is possible to speculate that the current injected on the targeted area still spread beyond the electrode borders. Moreover, even if we measured the position of the hMT^{+} using predetermined coordinates based on previous studies (Campana et al., 2002, 2006, 2013; Laycock et al., 2007; Pascual-Leone et al., 1998; Pavan et al., 2011) and despite the fact that these coordinates are consistent with fMRI localizer (Thompson et al., 2009) this procedure cannot account for individual morphological differences of

the scalp and of the convolutions of the cortex. Therefore, it is not possible to exclude that other areas such as the lateral occipital cortex could have been partially affected by the stimulation.

The results of Chapter 5 seem to indicate that a single session of offline hf-tRNS does not induce any long-term modulation on cortical activity and to our knowledge this was the first experiment combining EEG and offline hf-tRNS over the visual cortex. Although it is always critical to outline all the possible issues in a study that overall did not show any significant results, there are few points that certainly need to be considered. Firstly, the number of missing electrodes for the Left region was quite considerable. It is still not clear the reason for this discrepancy with respect to the Right region for which there were no missing electrodes. It was probably due to technical issues with the recording equipment that was customized for this experiment. Despite not finding any significant effect of the stimulation from all Left, Central and Right regions, we cannot exclude the possibility that the data of the activity of these missing electrodes could have affected the results for the Left Region. Furthermore, even if we have shown that offline hf-tRNS did not influence oscillatory activity at rest and VEPs amplitude and latency, in this thesis we did not analyse the aftereffects of hf-tRNS on oscillatory activity during the motion task. Thus, we cannot exclude the presence of aftereffects on band oscillatory activity during the execution of the motion task. It has been demonstrated that the level of alpha power before the stimulus onset can predict visual perception performance, for which low alpha power is associated with an improved perception discrimination performance (Hanslmayr et al., 2007, 2005). Therefore, future studies should investigate if offline hf-tRNS could modulate pre-stimulus oscillatory activity and consequently behavioural performance. Moreover, even if we consider the assumption that a single session of hf-tRNS might not be expected to have a large aftereffect on cortical activity at rest and on motion-related VEPs, it still would be interesting to see whether this would still be the case after repeated stimulation sessions. For example, five sessions of bilateral hf-tRNS of the dorsolateral prefrontal cortex (DLPFC), when embedded in a cognitive training paradigm, has proved to increase calculation learning and memory recall based on arithmetic ability (Snowball et al., 2013). Noteworthy, these behavioural improvements were associated with an alteration of the cerebral blood flow and metabolic activity.

6.4 Conclusion and future directions

To conclude, we demonstrated that online hf-tRNS can improve motion direction discrimination and found this improvement to be specific to stimulation delivered over extra-striate visual areas such as hMT^{+}. Whilst the stochastic resonance phenomenon seems to explain online stimulation effects, probably increasing the activity of those neurons signalling the motion direction, we did not find any enduring effects when the stimulation was applied in an offline protocol. However, more research should be conducted to investigate if this particular type of stimulation does not induce long-term modulations of neural activity if delivered offline on the visual cortex.

To further the knowledge of this technique future studies should investigate the effects of online hf-tRNS in combination with neuroimaging techniques. So far, only a few studies have investigated the effects of online random noise stimulation in combination with fMRI (Saiote et al., 2013) or EEG (Rufener et al., 2018, 2017; Zama & Kitajo, 2019). In particular, a combination of online tRNS and EEG could be helpful in identifying the electrophysiological hallmarks of the stochastic resonance phenomenon in the brain activity.

In fact, it has been found that an optimal amount of tactile or auditory noise can increase electrophysiological activity such as power spectrum (Manjarrez, Diez-Martínez, Méndez, & Flores, 2002), VEP amplitude (Méndez-Balbuena et al., 2015) and event-related spectral perturbation (ERSP) in a stochastic resonance manner. Moreover, Méndez-Balbuena et al. (2015) demonstrated that their participants exhibited individual differences in the optimal noise level resulting in the highest VEP amplitude, in agreement with the individual differences in optimal hf-tRNS intensity levels that increased contrasts detection threshold (van der Groen & Wenderoth, 2016). Therefore, the benefits of probing stimulation paradigms coupled with EEG techniques could be multiple. Firstly, it could increase the amount of supporting evidence that tRNS effects at the perceptual level can be explained within the stochastic resonance framework, increasing our knowledge on its mechanisms of action. Secondly, it would be helpful to optimize individual stimulation parameters to advance its application in clinical settings.

Additionally, our findings encourage the possibility that hf-tRNS could be integrated into a perceptual learning paradigm aimed at improving motion perception processing in observers with impaired or underperforming global motion integration. Several studies showed that when hf-tRNS is embedded in a visual perceptual learning paradigm it increases behavioural performance in healthy observers (Contemori, Trotter,

Cottereau, & Maniglia, 2019; Fertonani et al., 2011; Pirulli et al., 2013), and in participants with visual deficits such as amblyopia and cortical blindness (Campana et al., 2014; Herpich, Melnick, et al., 2018; Moret et al., 2018). Interestingly it has also been demonstrated that, hf-tRNS can produce the same improvements as behavioural perceptual training alone, but in a much shorter time (Camilleri et al., 2016, 2014). hf-tRNS effects on global motion processing could be helpful to dyslexic readers showing impaired motion and speed discrimination associated with dysfunctions and alterations of the magnocellular pathway and sensitivity toward motion (Chase & Stein, 2003; Stein, 2001). Moreover, readers with dyslexia have higher global motion coherence thresholds with respect to normal readers, especially if the moving stimulus is presented at low signal-to-noise ratio (Conlon, Lilleskaret, Wright, & Stuksrud, 2013) and perceptual learning based on discrimination of coherent motion has been shown to be effective in improve reading skills (Gori, Seitz, Ronconi, Franceschini, & Facoetti, 2016). It would be interesting to investigate whether a visual motion perceptual learning paradigm coupled with hf-tRNS would be effective in increasing global motion performance and if these improvements could be transferable to reading skills such as reading speed and fluency.

It is also worth mentioning that in this project we decided to focus our interest on the high-frequency range of tRNS instead of the low-frequency range or the whole spectrum. This decision was based on previous findings which showed that, with respect to the high-frequency range, low-frequency tRNS did not increase cortical excitability of the motor cortex and visual orientation discrimination performance (Fertonani et al., 2011; Terney et al., 2008). Little is known about what is the real impact of the frequency range in tRNS studies. For example, the discrepancy between high and low frequency tRNS outcomes has been suggested to be related to the time constant (i.e., the time needed for the neural membrane to return to its resting status after receiving an input signal) of cell bodies and dendrites that is between 1 and 10 ms (Kandel, Schwartz, & Jessell, 2000). Therefore it has been speculated that stimulation frequencies between 100 and 1000 Hz would be optimal to increase neural communication (Fertonani et al., 2011). However, this hypothesis has not been directly examined. Future research should examine in detail whether different frequency ranges of tRNS have specific consequences on behavioural performance and brain activity.

References

Aaen-Stockdale, C., & Thompson, B. (2012). Visual motion: from cortex to percept. In *Visual Cortex - Current Status and Perspectives* (Vol. 2, p. 64). InTech. https://doi.org/10.5772/50402

Abraham, W. C. (2008). Metaplasticity: tuning synapses and networks for plasticity. *Nature Reviews Neuroscience*, *9*(5), 387. https://doi.org/doi: 10.1038/nrn2356.

Accornero, N., Li, P., Maurizio, V., & Riccia, L. (2007). Visual evoked potentials modulation during direct current cortical polarization. *Experimental Brain Research*, *178*, 261–266. https://doi.org/10.1007/s00221-006-0733-y

Ajina, S., Kennard, C., Rees, G., & Bridge, H. (2015). Motion area V5/MT+ response to global motion in the absence of V1 resembles early visual cortex. *Brain*, *138*(1), 164–178. https://doi.org/10.1093/brain/awu328

Albright, T. D. (1984). Direction and orientation selectivity of neurons in visual area MT of the macaque. *Journal of Neurophysiology*, *52*(6), 1106–1130. Retrieved from http://jn.physiology.org/content/52/6/1106.abstract

Albright, T. D., & Stoner, G. R. (1995). Visual motion perception. *Scientific American*, *92*, 2433–2440. https://doi.org/10.1038/scientificamerican0675-76

Androulidakis, A. G., Doyle, L. M. F., Yarrow, K., Litvak, V., Gilbertson, T. P., & Brown, P. (2007). Anticipatory changes in beta synchrony in the human corticospinal system and associated improvements in task performance. *European Journal of Neuroscience*, *25*(12), 3758–3765. https://doi.org/10.1111/j.1460-9568.2007.05620.x

Antal, A., Keeser, D., Priori, A., Padberg, F., & Nitsche, M. A. (2015). Conceptual and procedural shortcomings of the systematic review "Evidence that transcranial direct current stimulation (tDCS) generates little-to-no reliable neurophysiologic effect beyond MEP amplitude modulation in healthy human subjects: a systematic r. *Brain Stimulation*, *8*(4), 846–849. https://doi.org/10.1016/j.brs.2015.05.010

Antal, A., Nitsche, M. A., Kruse, W., Kincses, T. Z., Hoffmann, K. P., & Paulus, W. (2004). Direct current stimulation over V5 enhances visuomotor coordination by improving motion perception in humans. *Journal of Cognitive Neuroscience*, *16*(4), 521–527. https://doi.org/10.1162/089892904323057263

Antal, A., Kincses, T. Z., Nitsche, M. A., & Paulus, W. (2003). Modulation of moving phosphene thresholds by transcranial direct current stimulation of V1 in human. *Neuropshycologia*, *41*, 1802–1807. https://doi.org/10.1016/S0028-3932(03)00181-7

Antal, A., Nitsche, M. A., & Paulus, W. (2001). External modulation of visual perception in humans. *Neuroreport*, *12*(16), 3553–3555. https://doi.org/10.1097/00001756-200111160-00036

Antal, A., Chaieb, L., Cziraki, C., Paulus, W., & Greenlee, M. W. (2012). Cathodal stimulation of human MT+ leads to elevated fMRI signal: a tDCS-fMRI study. *Restorative Neurology and Neuroscience*, *30*(3), 255–263. https://doi.org/10.3233/RNN-2012-110208

Antal, A., Edina, V. T., Kincses, T. Z., Nitsche, M. A., & Paulus, W. (2004). Oscillatory

brain activity and transcranial direct current stimulation in humans. *NuroReport*, *15*(8), 13–16. https://doi.org/10.1097/01.wnr.0000127460.08361.84

Antal, A., & Herrmann, C. S. (2016). Transcranial alternating current and random noise stimulation: possible mechanisms. *Neural Plasticity*, *2016*(January). https://doi.org/10.1155/2016/3616807

Antal, A., Kincses, T. Z., Nitsche, M. A., Bartfai, O., & Paulus, W. (2004). Excitability changes induced in the human primary visual cortex by transcranial direct current stimulation: direct electrophysiological evidence. *Investigative Ophthalmology & Visual Science*, *45*(2), 702–707. https://doi.org/10.1167/iovs.03-0688

Antal, A., Nitsche, M. A., & Paulus, W. (2006). Transcranial direct current stimulation and the visual cortex. *Brain Research Bulletin*, *68*(6), 459–463. https://doi.org/10.1016/j.brainresbull.2005.10.006

Antal, A., & Paulus, W. (2008). Transcranial direct current stimulation and visual perception. *Perception*, *37*(3), 367–374. https://doi.org/10.1068/p5872

Ardolino, G., Bossi, B., Barbieri, S., & Priori, A. (2005). Non-synaptic mechanisms underlie the after-effects of cathodal transcutaneous direct current stimulation of the human brain. *Journal of Physiology*, *568*(2), 653–663. https://doi.org/10.1113/jphysiol.2005.088310

Association, W. M. (2013). World medical association declaration of helsinki: Ethical principles for medical research involving human subjects. *JAMA*, *310*(20), 2191–2194. https://doi.org/10.1001/jama.2013.281053

Atkinson, J., Braddick, O., Rose, F. E., Searcy, Y. M., Wattam-Bell, J., & Bellugi, U. (2006). Dorsal-stream motion processing deficits persist into adulthood in Williams syndrome. *Neuropsychologia*, *44*(5), 828–833. https://doi.org/10.1016/j.neuropsychologia.2005.08.002

Atkinson, J., King, J., Braddick, O., Nokes, L., Anker, S., & Braddick, F. (1997). A specific deficit of dorsal stream function in Williams' syndrome. *Neuroreport*, *8*(8), 1919–1922.

Ballinger, G. A. (2004). Using generalized estimating equations for longitudinal data analysis. *Organizational Research Methods*, *7*(2), 127–150. https://doi.org/10.1177/1094428104263672

Barlow, H. B. (1956). Retinal noise and absolute threshold. *Journal of the Optical Society of America*, *46*(8), 634. https://doi.org/10.1364/JOSA.46.000634

Barlow, H., & Tripathy, S. P. (1997). Correspondence Noise and Signal Pooling in the Detection of Coherent Visual Motion. *The Journal of Neuroscience*, *17*(20), 7954–7966. https://doi.org/10.1523/JNEUROSCI.17-20-07954.1997

Bates, D., Mächler, M., Bolker, B., & Walker, S. (2015). Fitting linear mixed-effects models using lme4. *Journal of Statistical Software*, *67*(1). https://doi.org/10.18637/jss.v067.i01

Batsikadze, G., Moliadze, V., Paulus, W., Kuo, M.-F., & Nitsche, M. A. (2013). Partially non-linear stimulation intensity-dependent effects of direct current stimulation on motor cortex excitability in humans. *The Journal of Physiology*, *591*(7), 1987–2000. https://doi.org/10.1113/jphysiol.2012.249730

Battaglini, L., Noventa, S., & Casco, C. (2017). Anodal and cathodal electrical

stimulation over V5 improves motion perception by signal enhancement and noise reduction. *Brain Stimulation*, *10*(4), 773–779. https://doi.org/10.1016/j.brs.2017.04.128

Beckers, G., & Zeki, S. (1995). The consequences of inactivating areas V1 and V5 on visual motion perception. *Brain*, *118*(1), 49–60. https://doi.org/10.1093/brain/118.1.49

Benjamini, Y., & Hochberg, Y. (1995). Controlling the false discovery rate: a practical and powerful approach to multiple testing. *Journal of the Royal Staiticatal Society*, *57*(1), 289–300. https://doi.org/http://www.jstor.org/stable/2346101

Benwell, C. S. Y., London, R. E., Tagliabue, C. F., Veniero, D., Gross, J., Keitel, C., & Thut, G. (2019). Frequency and power of human alpha oscillations drift systematically with time-on-task. *NeuroImage*, *192*(September 2018), 101–114. https://doi.org/10.1016/j.neuroimage.2019.02.067

Bex, P. J., & Dakin, S. C. (2002). Comparison of the spatial-frequency selectivity of local and global motion detectors. *Journal of the Optical Society of America A*, *19*(4), 670. https://doi.org/10.1364/JOSAA.19.000670

Bezrukov, S. M., & Vodyanoy, I. (1995). Noise-induced enhancement of signal transduction across voltage-dependent ion channels. *Nature*, *378*(6555), 362–364. https://doi.org/10.1038/378362a0

Bienenstock, E. L., Cooper, L. N., & Munro, P. W. (1982). Theory for the development of neuron selectivity: orientation specificity and binocular interaction in visual cortex. *The Journal of Neuroscience : The Official Journal of the Society for Neuroscience*, *2*(1), 32–48. https://doi.org/10.1371/journal.ppat.0020109

Bikson, M., Datta, A., Rahman, A., & Scaturro, J. (2010). Electrode montages for tDCS and weak transcranial electrical stimulation: Role of "return" electrode's position and size. *Clinical Neurophysiology*, *121*(12), 1976–1978. https://doi.org/10.1016/j.clinph.2010.05.020

Bikson, M., Grossman, P., Thomas, C., Zannou, A. L., Jiang, J., Adnan, T., … Woods, A. J. (2016). Safety of transcranial direct current stimulation: evidence based update 2016. *Brain Stimulation*, *9*(5), 641–661. https://doi.org/10.1016/j.brs.2016.06.004

Bikson, M., Inoue, M., Akiyama, H., Deans, J. K., Fox, J. E., Miyakawa, H., & Jefferys, J. G. R. (2004). Effects of uniform extracellular DC electric fields on excitability in rat hippocampal slices *in vitro*. *The Journal of Physiology*, *557*(1), 175–190. https://doi.org/10.1113/jphysiol.2003.055772

Billino, J., Bremmer, F., & Gegenfurtner, K. R. (2008). Motion processing at low light levels: Differential effects on the perception of specific motion types. *Journal of Vision*, *8*(3), 14.1-10. https://doi.org/10.1167/8.3.14.Introduction

Bindman, L. J., Lippold, O. C. J., & Redfearn, J. W. T. (1964). The action of brief polarizing currents on the cerebral cortex of the rat (1) during current flow and (2) in the production of long-lasting after-effects. *The Journal of Physiology*, *172*(3), 369–382. https://doi.org/10.1113/jphysiol.1964.sp007425

Braddick, O. J., O'Brien, J. M. D., Wattam-Bell, J., Atkinson, J., Hartley, T., & Turner, R. (2001). Brain areas sensitive to coherent visual motion. *Perception*, *30*(1), 61–72. https://doi.org/10.1068/p3048

Brainard, D. H. (1997). The psychophysics toolbox. *Spatial Vision*, *10*(4), 433–436. https://doi.org/10.1163/156856897X00357

Bromm, B. (1968). Die natrium-gleichrichtung der unterschwellig erregten membran in der quantitativen formulierung der ionentheorie. *Pflügers Archiv Journal of Physiology*, *302*(3), 233–244. https://doi.org/10.1007/BF00586728

Buckner, R. L., Andrews-Hanna, J. R., & Schacter, D. L. (2008). The brain's default network: anatomy, function, and relevance to disease. *Annals of the New York Academy of Sciences*, *1124*, 1–38. https://doi.org/10.1196/annals.1440.011

Burr, D., & Thompson, P. (2011). Motion psychophysics: 1985-2010. *Vision Research*, *51*(13), 1431–1456. https://doi.org/10.1016/j.visres.2011.02.008

Camilleri, R., Pavan, A., & Campana, G. (2016). The application of online transcranial random noise stimulation and perceptual learning in the improvement of visual functions in mild myopia. *Neuropsychologia*, *89*, 225–231. https://doi.org/10.1016/j.neuropsychologia.2016.06.024

Camilleri, R., Pavan, A., Ghin, F., Battaglini, L., & Campana, G. (2014). Improvement of uncorrected visual acuity (UCVA) and contrast sensitivity (UCCS) with perceptual learning and transcranial random noise stimulation (tRNS) in individuals with mild myopia. *Frontiers in Psychology*, *5*(OCT), 1–6. https://doi.org/10.3389/fpsyg.2014.01234

Campana, G., Camilleri, R., Moret, B., Ghin, F., & Pavan, A. (2016). Opposite effects of high- and low-frequency transcranial random noise stimulation probed with visual motion adaptation. *Scientific Reports*, *6*(1), 38919. https://doi.org/10.1038/srep38919

Campana, G., Camilleri, R., Pavan, A., Veronese, A., & Giudice, G. Lo. (2014). Improving visual functions in adult amblyopia with combined perceptual training and transcranial random noise stimulation (tRNS): A pilot study. *Frontiers in Psychology*, *5*(DEC), 1–6. https://doi.org/10.3389/fpsyg.2014.01402

Campana, G., Cowey, A., & Walsh, V. (2002). Priming of motion direction and area V5/MT: a test of perceptual memory. *Cerebral Cortex (New York, N.Y. : 1991)*, *12*(6), 663–669. https://doi.org/10.1093/cercor/12.6.663

Campana, G., Cowey, A., & Walsh, V. (2006). Visual area V5/MT remembers "what" but not "where." *Cerebral Cortex*, *16*(12), 1766–1770. https://doi.org/10.1093/cercor/bhj111

Campana, G., Maniglia, M., & Pavan, A. (2013). Common (and multiple) neural substrates for static and dynamic motion after-effects: A rTMS investigation. *Cortex*, *49*(9), 2590–2594. https://doi.org/10.1016/j.cortex.2013.07.001

Cecere, R., Rees, G., & Romei, V. (2015). Individual differences in alpha frequency drive crossmodal illusory perception. *Current Biology*, *25*(2), 231–235. https://doi.org/10.1016/j.cub.2014.11.034

Chaieb, L., Antal, A., & Paulus, W. (2015). Transcranial random noise stimulation-induced plasticity is NMDA-receptor independent but sodium-channel blocker and benzodiazepines sensitive. *Frontiers in Neuroscience*, *9*(APR), 1–9. https://doi.org/10.3389/fnins.2015.00125

Chaieb, L., Kovacs, G., Cziraki, C., Greenlee, M., Paulus, W., & Antal, A. (2009). Short-

duration transcranial random noise stimulation induces blood oxygenation level dependent response attenuation in the human motor cortex. *Experimental Brain Research*, *198*(4), 439–444. https://doi.org/10.1007/s00221-009-1938-7

Chaieb, L., Paulus, W., & Antal, A. (2011). Evaluating aftereffects of short-duration transcranial random noise stimulation on cortical excitability. *Neural Plasticity*, *2011*. https://doi.org/10.1155/2011/105927

Chase, C., & Stein, J. (2003). Visual magnocellular deficits in dyslexia. *Brain*, *126*(9), 2E – 2. https://doi.org/10.1093/brain/awg217

Cho, K., Aggleton, J. P., Brown, M. W., & Bashir, Z. I. (2001). An experimental test of the role of postsynaptic calcium levels in determining synaptic strength using perirhinal cortex of rat. *The Journal of Physiology*, *532*(2), 459–466. https://doi.org/10.1111/j.1469-7793.2001.0459f.x

Chronicle, E. P., & Mulleners, W. M. (1996). Visual system dysfunction in migraine: a review of clinical and psychophysical findings. *CephalalgiaWkhvh, R I Pd, Skhqrphqd*, *16*(8), 525–535. https://doi.org/10.1046/j.1468-2982.1996.1608525.x

Collins, J J, Chow, C. C., & Imhoff, T. T. (1995). Stochastic resonance without tuning. *Nature*, *376*(6537), 236–238. https://doi.org/10.1038/376236a0

Collins, J., Imhoff, T. T., & Grigg, P. (1996). Noise-enhanced tactile sensation. *Nature*, *383*(6603), 770–770. https://doi.org/10.1038/383770a0

Conlon, E. G., Lilleskaret, G., Wright, C. M., & Stuksrud, A. (2013). Why do adults with dyslexia have poor global motion sensitivity? *Frontiers in Human Neuroscience*, *7*(December), 1–12. https://doi.org/10.3389/fnhum.2013.00859

Contemori, G., Trotter, Y., Cottereau, B. R., & Maniglia, M. (2019). tRNS boosts perceptual learning in peripheral vision. *Neuropsychologia*, *125*(June 2018), 129–136. https://doi.org/10.1016/j.neuropsychologia.2019.02.001

Cordo, P., Inglis, J. T., Verschueren, S., Collins, J. J., Merfeld, D. M., Rosenblum, S., … Moss, F. (1996). Noise in human muscle spindles. *Nature*, *383*(6603), 769–770. https://doi.org/10.1038/383769a0

Cowey, A., Campana, G., Walsh, V., & Vaina, L. M. (2006). The role of human extra-striate visual areas V5/MT and V2/V3 in the perception of the direction of global motion: a transcranial magnetic stimulation study. *Experimental Brain Research*, *171*(4), 558. https://doi.org/10.1007/s00221-006-0479-6

Dakin, S. C., Mareschal, I., & Bex, P. J. (2005). Local and global limitations on direction integration assessed using equivalent noise analysis. *Vision Research*, *45*(24), 3027–3049. https://doi.org/10.1016/j.visres.2005.07.037

Das, S., Holland, P., Frens, M. A., & Donchin, O. (2016). Impact of transcranial direct current stimulation (tDCS) on neuronal functions. *Frontiers in Neuroscience*, *10*(November), 1–7. https://doi.org/10.3389/fnins.2016.00550

Datta, A., Baker, J. M., Bikson, M., & Fridriksson, J. (2011). Individualized model predicts brain current flow during transcranial direct-current stimulation treatment in responsive stroke patient. *Brain Stimulation*, *4*(3), 169–174. https://doi.org/10.1016/j.brs.2010.11.001

Debener, S. (2005). Trial-by-trial coupling of concurrent electroencephalogram and functional magnetic resonance imaging identifies the dynamics of performance

monitoring. *Journal of Neuroscience*, *25*(50), 11730–11737. https://doi.org/10.1523/JNEUROSCI.3286-05.2005

Delorme, A., & Makeig, S. (2004). EEGLAB: an open source toolbox for analysis of single-trial EEG dynamics including independent component analysis. *Journal of Neuroscience Methods*, *134*(1), 9–21. https://doi.org/10.1016/j.jneumeth.2003.10.009

Dormal, V., Javadi, A. H., Pesenti, M., Walsh, V., & Cappelletti, M. (2016). Enhancing duration processing with parietal brain stimulation. *Neuropsychologia*, *85*, 272–277. https://doi.org/10.1016/j.neuropsychologia.2016.03.033

Douglass, J. K., Wilkens, L., Pantazelou, E., & Moss, F. (1993). Noise enhancement of information transfer in crayfish mechanoreceptors by stochastic resonance. *Nature*, *365*, 337. Retrieved from https://doi.org/10.1038/365337a0

Engel, A. K., & Fries, P. (2010). Beta-band oscillations-signalling the status quo? *Current Opinion in Neurobiology*, *20*(2), 156–165. https://doi.org/10.1016/j.conb.2010.02.015

Feige, B., Scheffler, K., Esposito, F., Di Salle, F., Hennig, J., & Seifritz, E. (2005). Cortical and subcortical correlates of electroencephalographic alpha rhythm modulation. *Journal of Neurophysiology*, *93*(5), 2864–2872. https://doi.org/10.1152/jn.00721.2004

Fertonani, A., Pirulli, C., & Miniussi, C. (2011). Random Noise Stimulation Improves Neuroplasticity in Perceptual Learning. *Journal of Neuroscience*, *31*(43), 15416–15423. https://doi.org/10.1523/JNEUROSCI.2002-11.2011

Fertonani, A., Ferrari, C., & Miniussi, C. (2015). What do you feel if I apply transcranial electric stimulation? Safety, sensations and secondary induced effects. *Clinical Neurophysiology*, *126*(11), 2181–2188. https://doi.org/10.1016/j.clinph.2015.03.015

Fertonani, A., & Miniussi, C. (2017). Transcranial Electrical Stimulation: What we know and do not know about mechanisms. *The Neuroscientist*, *23*(2), 109–123. https://doi.org/10.1177/1073858416631966

Field, A. (2009). *Discovering Statistics Using SPSS (third edition)* (3rd ed.). London: Sage Publications Ltd.

Flöel, A. (2014). tDCS-enhanced motor and cognitive function in neurological diseases. *NeuroImage*, *85*, 934–947. https://doi.org/10.1016/j.neuroimage.2013.05.098

Freeman, D. K., Eddington, D. K., Rizzo, J. F., & Fried, S. I. (2010). Selective activation of neuronal targets with sinusoidal electric stimulation. *Journal of Neurophysiology*, *104*(5), 2778–2791. https://doi.org/10.1152/jn.00551.2010

Fritz, C. O., Morris, P. E., & Richler, J. J. (2012). Effect size estimates: Current use, calculations, and interpretation. *Journal of Experimental Psychology: General*, *141*(1), 2–18. https://doi.org/10.1037/a0024338

Furlan, M., & Smith, A. T. (2016). Global motion processing in human visual cortical areas V2 and V3. *Journal of Neuroscience*, *36*(27), 7314–7324. https://doi.org/10.1523/JNEUROSCI.0025-16.2016

Gandiga, P. C., Hummel, F. C., & Cohen, L. G. (2006). Transcranial DC stimulation (tDCS): a tool for double-blind sham-controlled clinical studies in brain stimulation.

Clinical Neurophysiology, *117*(4), 845–850. https://doi.org/10.1016/j.clinph.2005.12.003

Gegenfurtner, K. R., Mayser, H. M., & Sharpe, L. T. (2000). Motion perception at scotopic light levels. *Journal of the Optical Society of America A*, *17*(9), 1505. https://doi.org/10.1109/CTS.2016.23

Geisler, W. S. (1999). Motion streaks provide a spatial code for motion direction. *Nature*, *400*(6739), 65–69. https://doi.org/10.1038/21886

Ghin, F., Pavan, A., Contillo, A., & Mather, G. (2018). The effects of high-frequency transcranial random noise stimulation (hf-tRNS) on global motion processing: An equivalent noise approach. *Brain Stimulation*, *11*(6), 1263–1275. https://doi.org/10.1016/j.brs.2018.07.048

Ghisletta, P., & Spini, D. (2004). An introduction to generalized estimating equations and an application to assess selectivity effects in a longitudinal study on very old individuals. *Journal of Educational and Behavioral Statistics*, *29*(4), 421–437. https://doi.org/10.3102/10769986029004421

Gilbertson, T. (2005). Existing motor state is favored at the expense of new movement during 13-35 Hz oscillatory synchrony in the human corticospinal system. *Journal of Neuroscience*, *25*(34), 7771–7779. https://doi.org/10.1523/JNEUROSCI.1762-05.2005

Gori, S., Seitz, A. R., Ronconi, L., Franceschini, S., & Facoetti, A. (2016). Multiple causal links between magnocellular–dorsal pathway deficit and developmental dyslexia. *Cerebral Cortex*, *26*(11), 4356–4369. https://doi.org/10.1093/cercor/bhv206

Grassi, M., & Soranzo, A. (2009). MLP: a MATLAB toolbox for rapid and reliable auditory threshold estimation. *Behavior Research Methods*, *41*(1), 20–28. https://doi.org/10.3758/BRM.41.1.20

Gratton, G., Coles, M. G. H., & Donchin, E. (1983). A new method for off-line removal of ocular artifact. *Electroencephalography and Clinical Neurophysiology*, *55*(4), 468–484. https://doi.org/https://doi.org/10.1016/0013-4694(83)90135-9

Green, D. M. (1993). A maximum-likelihood method for estimating thresholds in a yes–no task. *The Journal of the Acoustical Society of America*, *93*(4), 2096–2105. https://doi.org/10.1121/1.406696

Greer, P. L., & Greenberg, M. E. (2008). From synapse to nucleus: calcium-dependent gene transcription in the control of synapse development and function. *Neuron*, *59*(6), 846–860. https://doi.org/10.1016/j.neuron.2008.09.002

Groppe, D. M., Bickel, S., Keller, C. J., Jain, S. K., Hwang, S. T., Harden, C., & Mehta, A. D. (2013). Dominant frequencies of resting human brain activity as measured by the electrocorticogram David. *Neuroimage*, *79*(1), 223–233. https://doi.org/10.1016/j.neuroimage.2013.04.044.

Händel, B., Lutzenberger, W., Thier, P., & Haarmeier, T. (2007). Opposite dependencies on visual motion coherence in human area MT+ and early visual cortex. *Cerebral Cortex*, *17*(7), 1542–1549. https://doi.org/10.1093/cercor/bhl063

Hanslmayr, S., Aslan, A., Staudigl, T., Klimesch, W., Herrmann, C. S., & Bäuml, K. H. (2007). Prestimulus oscillations predict visual perception performance between and within subjects. *NeuroImage*, *37*(4), 1465–1473.

https://doi.org/10.1016/j.neuroimage.2007.07.011

Hanslmayr, S., Klimesch, W., Sauseng, P., Gruber, W., Doppelmayr, M., Freunberger, R., & Pecherstorfer, T. (2005). Visual discrimination performance is related to decreased alpha amplitude but increased phase locking. *Neuroscience Letters*, *375*(1), 64–68. https://doi.org/10.1016/j.neulet.2004.10.092

Heinrich, S. P. (2007). A primer on motion visual evoked potentials. *Documenta Ophthalmologica*, *114*(2), 83–105. https://doi.org/10.1007/s10633-006-9043-8

Helfrich, R. F., Schneider, T. R., Rach, S., Trautmann-Lengsfeld, S. A., Engel, A. K., & Herrmann, C. S. (2014). Entrainment of brain oscillations by transcranial alternating current stimulation. *Current Biology*, *24*(3), 333–339. https://doi.org/10.1016/j.cub.2013.12.041

Herpich, F., Contò, F., van Koningsbruggen, M., & Battelli, L. (2018). Modulating the excitability of the visual cortex using a stimulation priming paradigm. *Neuropsychologia*, *119*(June), 165–171. https://doi.org/10.1016/j.neuropsychologia.2018.08.009

Herpich, F., Melnick, M. D., Agosta, S., Huxlin, K., Tadin, D., & Battelli, L. (2018). Boosting learning efficacy with non-invasive brain stimulation in intact and brain-damaged humans. *BioRxiv*, 500215. https://doi.org/10.1101/500215

Herrmann, C. S., Rach, S., Neuling, T., & Strüber, D. (2013). Transcranial alternating current stimulation: a review of the underlying mechanisms and modulation of cognitive processes. *Frontiers in Human Neuroscience*, *7*(June), 1–13. https://doi.org/10.3389/fnhum.2013.00279

Higgins, E., & George, M. (2008). *Brain Stimulation Therapies for Clinicians*. Washington, DC: American Psychiatric Press.

Horton, N. J., & Lipsitz, S. R. (1999). Review of software to fit generalized estimating equation regression models. *American Statistician*, *53*(2), 160–169. https://doi.org/10.2307/2685737

Horvath, J.C., Carter, O., & Forte, J. D. (2014). Transcranial direct current stimulation: five important issues we aren't discussing (but probably should be). *Frontiers in Systems Neuroscience*, *8*(January), 1–8. https://doi.org/10.3389/fnsys.2014.00002

Horvath, J.C, Forte, J. D., & Carter, O. (2015). Evidence that transcranial direct current stimulation (tDCS) generates little-to-no reliable neurophysiologic effect beyond MEP amplitude modulation in healthy human subjects: A systematic review. *Neuropsychologia*, *66*, 213–236. https://doi.org/10.1016/j.neuropsychologia.2014.11.021

Horvath, J.C. (2015). New quantitative analyses following price & Hamilton's critique do not change original findings of Horvath et al. *Brain Stimulation*, *8*(3), 665–666. https://doi.org/10.1016/j.brs.2015.05.001

Horvath, J.C., Forte, J. D., & Carter, O. (2015). Quantitative review finds no evidence of cognitive effects in healthy populations from single-session transcranial direct current stimulation (tDCS). *Brain Stimulation*, *8*(3), 535–550. https://doi.org/10.1016/j.brs.2015.01.400

Hubel, D. H., & Wiesel, T. N. (1968a). Receptive fields and functional architecture of monkey striate cortex. *Journal of Physiology*, *195*, 215–243.

https://doi.org/papers://47831562-1F78-4B52-B52E-78BF7F97A700/Paper/p352

Hubel, D. H., & Wiesel, T. N. (1968b). Receptive fields and functional architecture of monkey striate cortex. *The Journal of Physiology*, *195*(1), 215–243. https://doi.org/10.1113/jphysiol.1968.sp008455

Inukai, Y., Saito, K., Sasaki, R., Tsuiki, S., Miyaguchi, S., Kojima, S., … Onishi, H. (2016). Comparison of three non-invasive transcranial electrical stimulation methods for increasing cortical excitability. *Frontiers in Human Neuroscience*, *10*(December), 1–7. https://doi.org/10.3389/fnhum.2016.00668

Jacobson, L., Koslowsky, M., & Lavidor, M. (2012). TDCS polarity effects in motor and cognitive domains: A meta-analytical review. *Experimental Brain Research*, *216*(1), 1–10. https://doi.org/10.1007/s00221-011-2891-9

Joffe, K. M., Raymond, J. E., & Chrichton, A. (1997). Motion coherence perimetry in glaucoma and suspected glaucoma. *Vision Research*, *37*(7), 955–964. https://doi.org/10.1016/S0042-6989(96)00221-0

Kanai, R., Chaieb, L., Antal, A., Walsh, V., & Paulus, W. (2008). Frequency-dependent electrical stimulation of the visual cortex. *Current Biology*, *18*(23), 1839–1843. https://doi.org/10.1016/j.cub.2008.10.027

Kanai, R., Paulus, W., & Walsh, V. (2010). Transcranial alternating current stimulation (tACS) modulates cortical excitability as assessed by TMS-induced phosphene thresholds. *Clinical Neurophysiology*, *121*(9), 1551–1554. https://doi.org/10.1016/j.clinph.2010.03.022

Kandel, E. R., Schwartz, J. H., & Jessell, T. M. (2000). *Principles of neural science*. New York: McGraw-Hill, Health Professions Division.

Kar, K., & Krekelberg, B. (2014). Transcranial alternating current stimulation attenuates visual motion adaptation. *Journal of Neuroscience*, *34*(21), 7334–7340. https://doi.org/10.1523/JNEUROSCI.5248-13.2014

Karolis, V. R., Grinyaev, M., Epure, A., Tsoy, V., Du Rietz, E., Banissy, M. J., … Kovas, Y. (2018). Probing the architecture of visual number sense with parietal tRNS. *Cortex*, 1–13. https://doi.org/10.1016/j.cortex.2018.08.030

Kim, T., Soto, F., & Kerschensteiner, D. (2015). An excitatory amacrine cell detects object motion and provides feature-selective input to ganglion cells in the mouse retina. *ELife*, *4*(MAY), 1–15. https://doi.org/10.7554/eLife.08025

Kitajo, K, Doesburg, S. M., Yamanaka, K., Nozaki, D., Ward, L. M., & Yamamoto, Y. (2007). Noise-induced large-scale phase synchronization of human-brain activity associated with behavioural stochastic resonance. *Europhysics Letters (EPL)*, *80*(4), 40009. https://doi.org/10.1209/0295-5075/80/40009

Kitajo, K., Nozaki, D., Ward, L. M., & Yamamoto, Y. (2003). Behavioral stochastic resonance within the human brain. *Physical Review Letters*, *90*(21), 4. https://doi.org/10.1103/PhysRevLett.90.218103

Kleiner, M., Brainard, D., Pelli, D., Ingling, A., Murray, R., & Broussard, C. (2007). What's new in psychtoolbox-3. *Perception*, *36*(14), 1–16. https://doi.org/10.1068/v070821

Klimesch, W., Sauseng, P., & Hanslmayr, S. (2007). EEG alpha oscillations: The inhibition–timing hypothesis. *Brain Research Reviews*, *53*(1), 63–88.

https://doi.org/10.1016/j.brainresrev.2006.06.003

Kraft, A., Roehmel, J., Olma, M. C., Schmidt, S., Irlbacher, K., & Brandt, S. A. (2010). Transcranial direct current stimulation a V ects visual perception measured by threshold perimetry. *Experimental Brain Research*, *207*(3–4), 283–290. https://doi.org/10.1007/s00221-010-2453-6

Kremláček, J., Kuba, M., Kubová, Z., Langrová, J., Vít, F., & Szanyi, J. (2007). Within-session reproducibility of motion-onset VEPs: Effect of adaptation/habituation or fatigue on N2 peak amplitude and latency. *Documenta Ophthalmologica*, *115*(2), 95–103. https://doi.org/10.1007/s10633-007-9063-z

Kuba, M., Kubová, Z., Kremláček, J., & Langrová, J. (2007). Motion-onset VEPs: Characteristics, methods, and diagnostic use. *Vision Research*, *47*(2), 189–202. https://doi.org/10.1016/j.visres.2006.09.020

Kuba, M., Kremláček, J., Langrová, J., Kubová, Z., Szanyi, J., & Vít, F. (2012). Aging effect in pattern, motion and cognitive visual evoked potentials. *Vision Research*, *62*, 9–16. https://doi.org/10.1016/j.visres.2012.03.014

Kuba, M., & Kubova, Z. (1992). Visual evoked potentials specific for motion onset. *Documenta Ophthalmologica*, *80*(1), 83–89. https://doi.org/10.1007/BF00161234

Kubova, Z., Kuba, M., Hubacek, J., & Vit, F. (1990). Properties of visual evoked potentials to onset of movement on a television screen. *Documenta Ophthalmologica*, *75*(1), 67–72. https://doi.org/10.1007/BF00142595

Kubová, Z., Kuba, M., Spekreijse, H., & Blakemore, C. (1995). Contrast dependence of motion-onset and pattern-reversal evoked potentials. *Vision Research*, *35*(2), 197–205. https://doi.org/10.1016/0042-6989(94)00138-C

Lang, N., Siebner, H. R., Chadaide, Z., Boros, K., Nitsche, M. A., Rothwell, J. C., … Antal, A. (2007). Bidirectional modulation of primary visual cortex excitability: a combined tDCS and rTMS Study. *Investigative Opthalmology & Visual Science*, *48*(12), 5782. https://doi.org/10.1167/iovs.07-0706

Laufs, H., Krakow, K., Sterzer, P., Eger, E., Beyerle, A., Salek-Haddadi, A., & Kleinschmidt, A. (2003). Electroencephalographic signatures of attentional and cognitive default modes in spontaneous brain activity fluctuations at rest. *Proceedings of the National Academy of Sciences*, *100*(19), 11053–11058. https://doi.org/10.1073/pnas.1831638100

Laycock, R., Crewther, D. P., Fitzgerald, P. B., & Crewther, S. G. (2007). Evidence for fast signals and later processing in human V1/V2 and V5/ MT+: a TMS study of motion perception. *Journal of Neurophysiology*, *1*, 1253–1262. https://doi.org/10.1152/jn.00416.2007.

Levi, D. M., Klein, S. A., & Aitsebaomo, P. (1984). Detection and discrimination of the direction of motion in central and peripheral vision of normal and amblyopic observers. *Vision Research*, *24*(8), 789–800. https://doi.org/https://doi.org/10.1016/0042-6989(84)90150-0

Levin, J. E., & Miller, J. P. (1996). Broadband neural encoding in the cricket cereal sensory system enhanced by stochastic resonance. *Nature*, *380*(6570), 165–168. https://doi.org/10.1038/380165a0

Levitt, H. (1971). Transformed up/down methods in psychoacoustics. *The Journal of the*

Acoustical Society of America, *49*(2B), 467–477. https://doi.org/10.1121/1.1912375

Li, C. R. (2002). Impaired detection of visual motion in schizophrenia patients. *Progress in Neuro-Psychopharmacology and Biological Psychiatry*, *26*(5), 929–934. https://doi.org/10.1016/S0278-5846(02)00207-5

Liang, K.-Y., & Zeger, S. L. (1986). Longitudinal data analysis using generalized linear models. *Biometrika*, *73*(1), 13–22. https://doi.org/10.1093/biomet/73.1.13

Lisman, J. E. (2001). Three Ca 2+ levels affect plasticity differently: the LTP zone, the LTD zone and no man's land. *The Journal of Physiology*, *532*(2), 285–285. https://doi.org/10.1111/j.1469-7793.2001.0285f.x

Livingstone, M., & Hubel, D. (1988). Segregation of form, color, movement and depth: anatomy , physiology , and perception. *Science*, *240*(4853), 740–749. https://doi.org/10.1126/science.3283936

Logothetis, N. K., Pauls, J., Augath, M., Trinath, T., & Oeltermann, A. (2001). Neurophysiological investigation of the basis of the fMRI signal. *Nature*, *412*(6843), 150–157. https://doi.org/10.1038/35084005

Mangia, A. L., Pirini, M., & Cappello, A. (2014). Transcranial direct current stimulation and power spectral parameters: a tDCS/EEG co-registration study. *Frontiers in Human Neuroscience*, *8*(August), 1–7. https://doi.org/10.3389/fnhum.2014.00601

Manjarrez, E., Diez-Martínez, O., Méndez, I., & Flores, A. (2002). Stochastic resonance in human electroencephalographic activity elicited by mechanical tactile stimuli. *Neuroscience Letters*, *324*(3), 213–216. https://doi.org/10.1016/S0304-3940(02)00212-4

Manning, C., Tibber, M. S., Charman, T., Dakin, S. C., & Pellicano, E. (2015). Enhanced integration of motion information in children with autism. *Journal of Neuroscience*, *35*(18), 6979–6986. https://doi.org/10.1523/JNEUROSCI.4645-14.2015

Manning, C., Aagten-Murphy, D., & Pellicano, E. (2012). The development of speed discrimination abilities. *Vision Research*, *70*, 27–33. https://doi.org/10.1016/j.visres.2012.08.004

Manning, C., Dakin, S. C., Tibber, M. S., & Pellicano, E. (2014). Averaging, not internal noise, limits the development of coherent motion processing. *Developmental Cognitive Neuroscience*, *10*(August), 44–56. https://doi.org/10.1016/j.dcn.2014.07.004

Mantini, D., Perrucci, M. G., Del Gratta, C., Romani, G. L., & Corbetta, M. (2007). Electrophysiological signatures of resting state networks in the human brain. *Proceedings of the National Academy of Sciences*, *104*(32), 13170–13175. https://doi.org/10.2994/SAJH-D-13-00033.1

Mareschal, I., Bex, P. J., & Dakin, S. C. (2008). Local motion processing limits fine direction discrmination in the periphery. *Vision Research*, *48*(16), 1719–1725. https://doi.org/doi:10.1016/j.visres.2008.05.003

Martin, T., Huxlin, K. R., & Kavcic, V. (2010). Motion-onset visual evoked potentials predict performance during a global direction discrimination task. *Neuropsychologia*, *48*(12), 3563–3572. https://doi.org/10.1016/j.neuropsychologia.2010.08.005

Martinez-Conde, S., Macknik, S. L., & Hubel, D. H. (2004). The role of fixational eye

movements in visual perception. *Nature Reviews Neuroscience*, *5*(3), 229–240. https://doi.org/10.1038/nrn1348

Mather, G., Pavan, A., Campana, G., & Casco, C. (2008). The motion after-effect reloaded. *Trends in Cognitive Neuroscience*, *12*(12), 481–487. https://doi.org/10.1016/j.tics.2008.09.002.The

Maurer, K., & Dierks, T. (1991). *Atlas of Brain Mapping*. Berlin, Heidelberg: Springer Berlin Heidelberg. https://doi.org/10.1007/978-3-642-76043-3

McDonnell, M. D., & Abbott, D. (2009). What is stochastic resonance? definitions, misconceptions, debates, and its relevance to biology. *PLoS Computational Biology*, *5*(5), e1000348. https://doi.org/10.1371/journal.pcbi.1000348

Meese, T. S., & Harris, M. G. (2001). Broad direction bandwidths for complex motion mechanisms. *Vision Research*, *41*(15), 1901–1914. https://doi.org/10.1016/S0042-6989(01)00083-9

Méndez-Balbuena, I., Huidobro, N., Silva, M., Flores, A., Trenado, C., Quintanar, L., … Manjarrez, E. (2015). Effect of mechanical tactile noise on amplitude of visual evoked potentials: multisensory stochastic resonance. *Journal of Neurophysiology*, *114*(4), 2132–2143. https://doi.org/10.1152/jn.00457.2015

Merigan, W., Byrne, C., & Maunsell, J. (1991). Does primate motion perception depend on the magnocellular pathway? *The Journal of Neuroscience*, *11*(11), 3422–3429. https://doi.org/10.1523/JNEUROSCI.11-11-03422.1991

Merton, P. A., & Morton, H. B. (1980). Stimulation of the cerebral cortex in the intact human subject. *Nature*, *285*(5762), 227–227. https://doi.org/10.1038/285227a0

Metting van Rijn, A. C., Peper, A., & Grimbergen, C. A. (1990). High-quality recording of bioelectric events. *Medical & Biological Engineering & Computing*, *28*(5), 389–397. https://doi.org/10.1007/BF02441961

Metting van Rijn, A. C., Peper, A., & Grimbergen, C. A. (1991). The isolation mode rejection ratio in bioelectric amplifiers. *IEEE Transactions on Biomedical Engineering*, *38*(11), 1154–1157. https://doi.org/10.1109/10.99079

Mikami, A., Newsome, W. T., & Wurtz, R. H. (1986). Motion selectivity in macaque visual cortex. I. Mechanisms of direction and speed selectivity in extrastriate area MT. *Journal of Neurophysiology*, *55*(6), 1308–1327. https://doi.org/10.1152/jn.1986.55.6.1308

Miller, K. J., Hermes, D., Honey, C. J., Hebb, A. O., Ramsey, N. F., Knight, R. T., … Fetz, E. E. (2012). Human motor cortical activity is selectively phase-entrained on underlying rhythms. *PLoS Computational Biology*, *8*(9), e1002655. https://doi.org/10.1371/journal.pcbi.1002655

Milne, E., Swettenham, J., Hansen, P., Campbell, R., Jeffries, H., & Plaisted, K. (2002). High motion coherence thresholds in children with autism. *Journal of Child Psychology and Psychiatry*, *43*(2), 255–263. https://doi.org/10.1111/1469-7610.00018

Minami, S., & Amano, K. (2017). Illusory jitter perceived at the frequency of alpha oscillations. *Current Biology*, *27*(15), 2344-2351.e4. https://doi.org/10.1016/j.cub.2017.06.033

Miniussi, C., Harris, J. A., & Ruzzoli, M. (2013). Modelling non-invasive brain

stimulation in cognitive neuroscience. *Neuroscience and Biobehavioral Reviews*, *37*(8), 1702–1712. https://doi.org/10.1016/j.neubiorev.2013.06.014

Miniussi, C., Ruzzoli, M., & Walsh, V. (2010). The mechanism of transcranial magnetic stimulation in cognition. *Cortex*, *46*(1), 128–130. https://doi.org/10.1016/j.cortex.2009.03.004

Mitchell, D. J., McNaughton, N., Flanagan, D., & Kirk, I. J. (2008). Frontal-midline theta from the perspective of hippocampal "theta." *Progress in Neurobiology*, *86*(3), 156–185. https://doi.org/10.1016/j.pneurobio.2008.09.005

Moliadze, V, Fritzsche, G., & Antal, A. (2014). Comparing the efficacy of excitatory transcranial stimulation methods measuring motor evoked potentials. *Neural Plast*, *2014*, 837141. https://doi.org/10.1155/2014/837141

Moliadze, V., Antal, A., & Paulus, W. (2010). Electrode-distance dependent after-effects of transcranial direct and random noise stimulation with extracephalic reference electrodes. *Clinical Neurophysiology*, *121*(12), 2165–2171. https://doi.org/10.1016/j.clinph.2010.04.033

Moosmann, M., Ritter, P., Krastel, I., Brink, A., Thees, S., Blankenburg, F., … Villringer, A. (2003). Correlates of alpha rhythm in functional magnetic resonance imaging and near infrared spectroscopy. *NeuroImage*, *20*(1), 145–158. https://doi.org/10.1016/S1053-8119(03)00344-6

Moret, B., Camilleri, R., Pavan, A., & Lo Giudice, G. (2018). Differential effects of high-frequency transcranial random noise stimulation (hf-tRNS) on contrast sensitivity and visual acuity when combined with a short perceptual training in adults with amblyopia. *Neuropsychologia*, *114*(April), 125–133. https://doi.org/10.1016/j.neuropsychologia.2018.04.017

Morgan, M. J., & Ward, R. (1980). Interocular delay produces depth in subjectively moving noise patterns. *Quarterly Journal of Experimental Psychology*, *32*(3), 387–395. https://doi.org/10.1080/14640748008401833

Moss, F., Ward, L. M., & Sannita, W. G. (2004). Stochastic resonance and sensory information processing: a tutorial and review of application. *Clinical Neurophysiology*, *115*(2), 267–281. https://doi.org/10.1016/j.clinph.2003.09.014

Neuling, T., Ruhnau, P., Fuscà, M., Demarchi, G., Herrmann, C. S., & Weisz, N. (2015). Friends, not foes: Magnetoencephalography as a tool to uncover brain dynamics during transcranial alternating current stimulation. *NeuroImage*, *118*, 406–413. https://doi.org/10.1016/j.neuroimage.2015.06.026

Neuner, I., Arrubla, J., Werner, C. J., Hitz, K., Boers, F., Kawohl, W., & Shah, N. J. (2014). The Default Mode Network and EEG regional spectral power: a simultaneous fMRI-EEG study. *PLoS ONE*, *9*(2), e88214. https://doi.org/10.1371/journal.pone.0088214

Newsome, W.T., & Pare, E. B. (1988). A selective impairment of motion perception following lesions of the middle temporal visual area (MT). *The Journal of Neuroscience*, *8*(6), 2201 LP – 2211. https://doi.org/https://doi.org/10.1523/JNEUROSCI.08-06-02201.1988

Newsome, W.T., & Paré, E. B. (1988). A selective impairment of motion perception following lesions of the Middle Temporal visual area (MT). *The Journal of Neuroscience*, *8*(6), 2201–2211. https://doi.org/http

https://doi.org/10.1523/JNEUROSCI.08-06-02201.1988

Niedeggen, M., & Wist, E. R. (1998). Motion evoked brain potentials parallel the consistency of coherent motion perception in humans. *Neuroscience Letters*, *246*(2), 61–64. https://doi.org/10.1016/S0304-3940(98)00222-5

Niedeggen, M., & Wist, E. R. (1999). Characteristics of visual evoked potentials generated by motion coherence onset. *Cognitive Brain Research*, *8*(2), 95–105. https://doi.org/10.1016/S0926-6410(99)00009-9

Nitsche, M. A., Fricke, K., Henschke, U., Schlitterlau, A., Liebetanz, D., Lang, N., … Paulus, W. (2003). Pharmacological modulation of cortical excitability shifts induced by transcranial direct current stimulation in humans. *The Journal of Physiology*, *553*(1), 293–301. https://doi.org/10.1113/jphysiol.2003.049916

Nitsche, M. A., & Paulus, W. (2000). Excitability changes induced in the human motor cortex by weak transcranial direct current stimulation. *The Journal of Physiology*, *527*(3), 633–639. https://doi.org/10.1111/j.1469-7793.2000.t01-1-00633.x

Nitsche, M.A., Bikson, M., & Bestmann, S. (2015). On the use of meta-analysis in neuromodulatory non-invasive brain stimulation. *Brain Stimulation*, *8*(3), 666–667. https://doi.org/10.1016/j.brs.2015.03.008

Nitsche, M.A., Cohen, L. G., Wassermann, E. M., Priori, A., Lang, N., Antal, A., … Pascual-Leone, A. (2008). Transcranial direct current stimulation: State of the art 2008. *Brain Stimulation*, *1*(3), 206–223. https://doi.org/10.1016/j.brs.2008.06.004

Nitsche, M.A., Grundey, J., Liebetanz, D., Lang, N., Tergau, F., & Paulus, W. (2004). Catecholaminergic consolidation of motor cortical neuroplasticity in humans. *Cerebral Cortex*, *14*(11), 1240–1245. https://doi.org/10.1093/cercor/bhh085

Nitsche, M.A., Liebetanz, D., Schlitterlau, A., Henschke, U., Fricke, K., Frommann, K., … Tergau, F. (2004). GABAergic modulation of DC stimulation-induced motor cortex excitability shifts in humans. *European Journal of Neuroscience*, *19*(10), 2720–2726. https://doi.org/10.1111/j.0953-816X.2004.03398.x

Nitsche, M.A, Jaussi, W., Liebetanz, D., Lang, N., Tergau, F., & Paulus, W. (2004). Consolidation of human motor cortical neuroplasticity by D-cycloserine. *Neuropsychopharmacology*, *29*(8), 1573–1578. https://doi.org/10.1038/sj.npp.1300517

Nitsche, M.A, & Paulus, W. (2011). Transcranial direct current stimulation - update 2011. *Restorative Neurology and Neuroscience*, *29*(6), 463–492. https://doi.org/10.3233/RNN-2011-0618

Nunez, P. L., & Silberstein, R. B. (2000). On the relationship of synaptic activity to macroscopic measurements: Does co-registration of EEG with fMRI make sense? *Brain Topography*, *13*(2), 79–96. https://doi.org/10.1023/A:1026683200895

Nunez, P. L., Wingeier, B. M., & Silberstein, R. B. (2001). Spatial-temporal structures of human alpha rhythms: Theory, microcurrent sources, multiscale measurements, and global binding of local networks. *Human Brain Mapping*, *13*(3), 125–164. https://doi.org/10.1002/hbm.1030

O'Hare, L., & Hibbard, P. B. (2016). Visual processing in migraine. *Cephalalgia*, *36*(11), 1057–1076. https://doi.org/10.1177/0333102415618952

Olma, M. C., Dargie, R. a, Behrens, J. R., Kraft, A., Irlbacher, K., Fahle, M., & Brandt,

S. a. (2013). Long-term effects of serial anodal tDCS on motion perception in Subjects with occipital stroke measured in the unaffected visual hemifield. *Frontiers in Human Neuroscience*, *7*(June), 314. https://doi.org/10.3389/fnhum.2013.00314

Onorato, I., D'Alessandro, G., Di Castro, M. A., Renzi, M., Dobrowolny, G., Musarò, A., … Grassi, F. (2016). Noise enhances action potential generation in mouse sensory neurons via stochastic resonance. *PLOS ONE*, *11*(8), e0160950. https://doi.org/10.1371/journal.pone.0160950

Onton, J., Delorme, A., & Makeig, S. (2005). Frontal midline EEG dynamics during working memory. *NeuroImage*, *27*(2), 341–356. https://doi.org/10.1016/j.neuroimage.2005.04.014

Opitz, A., Falchier, A., Yan, C.-G., Yeagle, E. M., Linn, G. S., Megevand, P., … Schroeder, C. E. (2016). Spatiotemporal structure of intracranial electric fields induced by transcranial electric stimulation in humans and nonhuman primates. *Scientific Reports*, *6*(1), 31236. https://doi.org/10.1038/srep31236

Pahor, A., & Jaušovec, N. (2014). The effects of theta transcranial alternating current stimulation (tACS) on fluid intelligence. *International Journal of Psychophysiology*, *93*(3), 322–331. https://doi.org/10.1016/j.ijpsycho.2014.06.015

Pan, W. (2001). Akaike's Information Criterion in Generalized Estimating Equations. *Biometrics*, *57*(1), 120–125. https://doi.org/10.1111/j.0006-341X.2001.00120.x

Parent, A. (2004). Giovanni Aldini: from animal electricity to human brain stimulation. *The Canadian Journal of Neurological Sciences*, *31*(04), 576–584. https://doi.org/10.1017/S0317167100003851

Parkin, B. L., Bhandari, M., Glen, J. C., & Walsh, V. (2019). The physiological effects of transcranial electrical stimulation do not apply to parameters commonly used in studies of cognitive neuromodulation. *Neuropsychologia*, *128*(February), 332–339. https://doi.org/10.1016/j.neuropsychologia.2018.03.030

Pascual-Leone, A., Tarazona, F., Keenan, J., Tormos, J. M., Hamilton, R., & Catala, M. D. (1998). Transcranial magnetic stimulation and neuroplasticity. *Neuropsychologia*, *37*(2), 207–217. https://doi.org/10.1016/S0028-3932(98)00095-5

Pasqualotto, A. (2016). Transcranial random noise stimulation benefits arithmetic skills. *Neurobiology of Learning and Memory*, *133*, 7–12. https://doi.org/10.1016/j.nlm.2016.05.004

Patzwahl, D. R., & Zanker, J. M. (2000). Mechanisms of human motion perception: Combining evidence from evoked potentials, behavioural performance and computational modelling. *European Journal of Neuroscience*, *12*(1), 273–282. https://doi.org/10.1046/j.1460-9568.2000.00885.x

Pavan, A., Alexander, I., Campana, G., & Cowey, A. (2011). Detection of first- and second-order coherent motion in blindsight. *Experimental Brain Research*, *214*(2), 261–271. https://doi.org/10.1007/s00221-011-2828-3

Pelli, D G. (1990). The quantum efficiency of vision. In C. Blakemore (Ed.), *Vision: coding and efficency* (pp. 3–24). Cambridge: Cambridge University Press.

Pelli, D.G. (1997). The VideoToolbox software for visual psychophysics: transforming numbers into movies. *Spatial Vision*, *10*(4), 437–442.

https://doi.org/10.1163/156856897X00366

Pirulli, C., Fertonani, A., & Miniussi, C. (2013). The role of timing in the induction of neuromodulation in perceptual learning by transcranial electric stimulation. *Brain Stimulation*, *6*(4), 683–689. https://doi.org/10.1016/j.brs.2012.12.005

Pirulli, C., Fertonani, A., & Miniussi, C. (2014). Is neural hyperpolarization by cathodal stimulation always detrimental at the behavioral level? *Frontiers in Behavioral Neuroscience*, *8*(June), 1–10. https://doi.org/10.3389/fnbeh.2014.00226

Pobric, G., Hulleman, J., Lavidor, M., Silipo, G., Rohrig, S., Dias, E., & Javitt, D. C. (2018). Seeing the world as it is: mimicking veridical motion perception in schizophrenia using non-invasive brain stimulation in healthy participants. *Brain Topography*, *31*(5), 827–837. https://doi.org/10.1007/s10548-018-0639-6

Polat, U. (1999). Functional architecture of long-range perceptual interactions. *Spatial Vision*, *12*(2), 143–162. https://doi.org/10.1163/156856899X00094

Polat, U. (2009). Making perceptual learning practical to improve visual functions. *Vision Research*, *49*(21), 2566–2573. https://doi.org/10.1016/j.visres.2009.06.005

Popescu, T., Krause, B., Terhune, D. B., Twose, O., Page, T., Humphreys, G., & Cohen Kadosh, R. (2016). Transcranial random noise stimulation mitigates increased difficulty in an arithmetic learning task. *Neuropsychologia*, *81*, 255–264. https://doi.org/10.1016/j.neuropsychologia.2015.12.028

Prete, G., Malatesta, G., & Tommasi, L. (2017). Facial gender and hemispheric asymmetries: A hf-tRNS study. *Brain Stimulation*, *10*(6), 1145–1147. https://doi.org/10.1016/j.brs.2017.08.002

Price, A. R., & Hamilton, R. H. (2015). A re-evaluation of the cognitive effects from single-session transcranial direct current stimulation. *Brain Stimulation*, *8*(3), 663–665. https://doi.org/10.1016/j.brs.2015.03.007

Puanhvuan, D., Nojima, K., Wongsawat, Y., & Iramina, K. (2013). Effects of repetitive transcranial magnetic stimulation and transcranial direct current stimulation on posterior alpha wave. *IEEJ Transactions on Electrical and Electronic Engineering*, *8*(3), 263–268. https://doi.org/10.1002/tee.21849

Purpura, D. P., & McMurtry, J. G. (1965). Intracellular activities and evoked potential changes during polarization of motor cortex. *Journal of Neurophysiology*, *28*(1), 166–185. https://doi.org/10.1152/jn.1965.28.1.166

Raichle, M. E., MacLeod, A. M., Snyder, A. Z., Powers, W. J., Gusnard, D. A., & Shulman, G. L. (2001). A default mode of brain function. *Proceedings of the National Academy of Sciences*, *98*(2), 676–682. https://doi.org/10.1073/pnas.98.2.676

Raichle, M.E., & Snyder, A. Z. (2007). A default mode of brain function: A brief history of an evolving idea. *NeuroImage*, *37*(4), 1083–1090. https://doi.org/10.1016/j.neuroimage.2007.02.041

Ratcliff, R. (1978). A theory of memory retrieval. *Psychological Review*, *85*(2), 59–108. https://doi.org/10.1037/0033-295X.85.2.59

Ratcliff, R., & Rouder, J. N. (1998). Modeling response times for two-choice decisions. *Psychological Science*, *9*(5), 347–356. https://doi.org/10.1111/1467-9280.00067

Ratcliff, R., & Tuerlinckx, F. (2002). Estimating parameters of the diffusion model: Approaches to dealing with contaminant reaction times and parameter variability. *Psychonomic Bulletin & Review*, *9*(3), 438–481. https://doi.org/10.3758/BF03196302

Raymond, J. E. (1994). Directional anisotropy of motion sensitivity across the visual field. *Vision Research*, *34*(8), 1029–1037. https://doi.org/https://doi.org/10.1016/0042-6989(94)90007-8

Remedios, L., Mabil, P., Flores-Hernández, J., Torres-Ramírez, O., Huidobro, N., Castro, G., … Manjarrez, E. (2019). Effects of short-term random noise electrical stimulation on dissociated pyramidal neurons from the cerebral cortex. *Neuroscience*, *404*, 371–386. https://doi.org/10.1016/j.neuroscience.2019.01.035

Riani, M., & Simonotto, E. (1994). Stochastic resonance in the perceptual interpretation of ambiguous figures: A neural network model. *Phys. Rev. Lett.*, *72*(19), 3120–3123. https://doi.org/10.1103/PhysRevLett.72.3120

Rodman, H.R, & Albright, T. D. (1989). Single-unit analysis of pattern-motion selective properties in the middle temporal visual area (MT). *Experimental Brain Research.*, *75*(1), 53–64. https://doi.org/10.1007/BF00248530

Rodman, H.R, & Albright, T. D. (1987). Coding of visual stimulus velocity in area MT of the macaque. *Vision Research*, *27*(12), 2035–2048. https://doi.org/10.1016/0042-6989(87)90118-0

Romanska, A., Rezlescu, C., Susilo, T., Duchaine, B., & Banissy, M. J. (2015). High-frequency transcranial random noise stimulation enhances perception of facial identity. *Cerebral Cortex*, *25*(11), 4334–4340. https://doi.org/10.1093/cercor/bhv016

Romei, V., Thut, G., & Silvanto, J. (2016). Information-based approaches of noninvasive transcranial brain stimulation. *Trends in Neurosciences*, *39*(11), 782–795. https://doi.org/10.1016/j.tins.2016.09.001

Rufener, K. S., Geyer, U., Janitzky, K., Heinze, H. J., & Zaehle, T. (2018). Modulating auditory selective attention by non-invasive brain stimulation: Differential effects of transcutaneous vagal nerve stimulation and transcranial random noise stimulation. *European Journal of Neuroscience*, *48*(6), 2301–2309. https://doi.org/10.1111/ejn.14128

Rufener, K. S., Ruhnau, P., Heinze, H., & Zaehle, T. (2017). Transcranial random noise stimulation (tRNS) shapes the processing of rapidly changing auditory information. *Frontiers in Cellular Neuroscience*, *11*(June), 1–11. https://doi.org/10.3389/fncel.2017.00162

Ruzzoli, M., Abrahamyan, A., Clifford, C. W. G., Marzi, C. A., Miniussi, C., & Harris, J. A. (2011). The effect of TMS on visual motion sensitivity: an increase in neural noise or a decrease in signal strength? *Journal of Neurophysiology*, *106*(1), 138–143. https://doi.org/10.1152/jn.00746.2010

Saiote, C., Polanía, R., Rosenberger, K., Paulus, W., & Antal, A. (2013). High-frequency tRNS reduces BOLD activity during visuomotor learning. *PLoS ONE*, *8*(3), 1–8. https://doi.org/10.1371/journal.pone.0059669

Sarmiento, C. I., San-Juan, D., & Prasath, V. B. S. (2016). Letter to the Editor: Brief history of transcranial direct current stimulation (tDCS): from electric fishes to

microcontrollers. *Psychological Medicine*, *46*(15), 3259–3261. https://doi.org/10.1017/S0033291716001926

Scase, M. O., Braddick, O. J., & Raymond, J. E. (2000). What is noise for the motion system? *Vision Research*, *36*(95), 2579–2586. https://doi.org/10.1016/0042-6989(95)00325-8

Schoen, I., & Fromherz, P. (2008). Extracellular stimulation of mammalian neurons through repetitive activation of Na+ channels by weak capacitive currents on a silicon chip. *Journal of Neurophysiology*, *100*(1), 346–357. https://doi.org/10.1152/jn.90287.2008

Schutter, D. J. L. G., & Hortensius, R. (2010). Retinal origin of phosphenes to transcranial alternating current stimulation. *Clinical Neurophysiology*, *121*(7), 1080–1084. https://doi.org/10.1016/j.clinph.2009.10.038

Schwarzkopf, D. S., Silvanto, J., & Rees, G. (2011). Stochastic resonance effects reveal the neural mechanisms of transcranial magnetic stimulation. *Journal of Neuroscience*, *31*(9), 3143–3147. https://doi.org/10.1523/JNEUROSCI.4863-10.2011

Schwiedrzik, C. (2009). Retina or visual cortex? The site of phosphene induction by transcranial alternating current stimulation. *Frontiers in Integrative Neuroscience*, *3*(1), 1–2. https://doi.org/10.3389/neuro.07.006.2009

Silvanto, J., & Muggleton, N. G. (2008). Testing the validity of the TMS state-dependency approach: Targeting functionally distinct motion-selective neural populations in visual areas V1/V2 and V5/MT+. *NeuroImage*, *40*(4), 1841–1848. https://doi.org/10.1016/j.neuroimage.2008.02.002

Simmers, A. J., Ledgeway, T., & Hess, R. F. (2005). The influences of visibility and anomalous integration processes on the perception of global spatial form versus motion in human amblyopia. *Vision Research*, *45*(4), 449–460. https://doi.org/10.1016/j.visres.2004.08.026

Simonotto, E., Spano, F., Riani, M., Ferrari, A., Levrero, F., Pilot, A., … Moss, F. (1999). fMRI studies of visual cortical activity during noise stimulation. *Neurocomputing*, *27*, 511–516.

Simonotto, E., Riani, M., Seife, C., Roberts, M., Twitty, J., & Moss, F. (1997). Visual perception of stochastic resonance. *Physical Review Letters*, *78*(6), 1186–1189. https://doi.org/10.1103/PhysRevLett.78.1186

Snowball, A., Tachtsidis, I., Popescu, T., Thompson, J., Delazer, M., Zamarian, L., … Cohen Kadosh, R. (2013). Long-term enhancement of brain function and cognition using cognitive training and brain stimulation. *Current Biology*, *23*(11), 987–992. https://doi.org/10.1016/j.cub.2013.04.045

Spiegel, D. P., Hansen, B. C., Byblow, W. D., & Thompson, B. (2012). Anodal transcranial direct current stimulation reduces psychophysically measured surround suppression in the human visual cortex. *PLoS ONE*, *7*(5), e36220. https://doi.org/10.1371/journal.pone.0036220

Spitoni, G. F., Cimmino, R. L., Bozzacchi, C., Pizzamiglio, L., & Di Russo, F. (2013). Modulation of spontaneous alpha brain rhythms using low-intensity transcranial direct-current stimulation. *Frontiers in Human Neuroscience*, *7*(September), 1–9. https://doi.org/10.3389/fnhum.2013.00529

Stagg, C. J., Best, J. G., Stephenson, M. C., O'Shea, J., Wylezinska, M., Kincses, Z. T., … Johansen-Berg, H. (2009). Polarity-sensitive modulation of cortical neurotransmitters by transcranial stimulation. *Journal of Neuroscience*, *29*(16), 5202–5206. https://doi.org/10.1523/JNEUROSCI.4432-08.2009

Stein, J. (2001). The magnocellular theory of developmental dyslexia. *Dyslexia*, *7*(1), 12–36. https://doi.org/10.1002/dys.186

Steinberg, H. (2013). Letter to the Editor: Transcranial direct current stimulation (tDCS) has a history reaching back to the 19th century. *Psychological Medicine*, *43*(03), 669–671. https://doi.org/10.1017/S0033291712002929

Stigliani, A., Jeska, B., & Grill-Spector, K. (2017). Encoding model of temporal processing in human visual cortex. *Proceedings of the National Academy of Sciences*. Retrieved from http://www.pnas.org/content/early/2017/12/04/1704877114.abstract

Talcott, J. B., Hansen, P. C., Assoku, E. L., & Stein, J. F. (2000). Visual motion sensitivity in dyslexia: evidence for temporal and energy integration deficits. *Neuropsychologia*, *38*(7), 935–943. https://doi.org/10.1016/S0028-3932(00)00020-8

Tavakoli, A. V, & Yun, K. (2017). Transcranial alternating current stimulation (tACS) mechanisms and protocols. *Frontiers in Cellular Neuroscience*, *11*(September), 1–10. https://doi.org/10.3389/fncel.2017.00214

Team, R. C. (2013). R: A Language and Environment for Statistical Computing. Vienna, Austria: R Foundation for Statistical Computing. Retrieved from http://www.r-project.org

Terney, D., Chaieb, L., Moliadze, V., Antal, A., & Paulus, W. (2008). Increasing human brain excitability by transcranial high-frequency random noise stimulation. *Journal of Neuroscience*, *28*(52), 14147–14155. https://doi.org/10.1523/JNEUROSCI.4248-08.2008

Thompson, B., Aaen-Stockdale, C., Koski, L., & Hess, R. F. (2009). A double dissociation between striate and extrastriate visual cortex for pattern motion perception revealed using rTMS. *Human Brain Mapping*, *30*(10), 3115–3126. https://doi.org/10.1002/hbm.20736

Tibber, M. S., Anderson, E. J., Bobin, T., Carlin, P., Shergill, S. S., & Dakin, S. C. (2015). Local and global limits on visual processing in schizophrenia. *PLoS ONE*, *10*(2), 1–17. https://doi.org/10.1371/journal.pone.0117951

Tibber, M. S., Kelly, M. G., Jansari, A., Dakin, S. C., & Shepherd, A. J. (2014). An inability to exclude visual noise in migraine. *Investigative Ophthalmology and Visual Science*, *55*(4), 2539–2546. https://doi.org/10.1167/iovs.14-13877

Treviño, M., De la Torre-Valdovinos, B., & Manjarrez, E. (2016). Noise improves visual motion discrimination via a stochastic resonance-like phenomenon. *Frontiers in Human Neuroscience*, *10*(November), 572. https://doi.org/10.3389/fnhum.2016.00572

Tyler, S. C., Contò, F., & Battelli, L. (2018). Rapid improvement on a temporal attention task within a single session of high-frequency transcranial random noise stimulation. *Journal of Cognitive Neuroscience*, *30*(5), 656–666. https://doi.org/10.1162/jocn_a_01235

van der Groen, O., Tang, M. F., Wenderoth, N., & Mattingley, J. B. (2018). Stochastic resonance enhances the rate of evidence accumulation during combined brain stimulation and perceptual decision- making. *PLoS Computational Biology*, *14*(7), 1–17. https://doi.org/10.1371/journal.pcbi.1006301

van der Groen, O., & Wenderoth, N. (2016). Transcranial random noise stimulation of visual cortex: stochastic resonance enhances central mechanisms of perception. *Journal of Neuroscience*, *36*(19), 5289–5298. https://doi.org/10.1523/JNEUROSCI.4519-15.2016

Van Doren, J., Langguth, B., & Schecklmann, M. (2014). Electroencephalographic effects of transcranial random noise stimulation in the auditory cortex. *Brain Stimulation*, *7*(6), 807–812. https://doi.org/10.1016/j.brs.2014.08.007

van Koningsbruggen, M. G., Ficarella, S. C., Battelli, L., & Hickey, C. (2016). Transcranial random-noise stimulation of visual cortex potentiates value-driven attentional capture. *Social Cognitive and Affective Neuroscience*, *11*(9), 1481–1488. https://doi.org/10.1093/scan/nsw056

Veniero, D., Vossen, A., Gross, J., & Thut, G. (2015). Lasting EEG/MEG aftereffects of rhythmic transcranial brain stimulation: level of control over oscillatory network activity. *Frontiers in Cellular Neuroscience*, *9*(December). https://doi.org/10.3389/fncel.2015.00477

Vossen, A., Gross, J., & Thut, G. (2015). Alpha Power Increase After Transcranial Alternating Current Stimulation at Alpha Frequency (α-tACS) Reflects Plastic Changes Rather Than Entrainment. *Brain Stimulation*, *8*(3), 499–508. https://doi.org/10.1016/j.brs.2014.12.004

Wach, C., Krause, V., Moliadze, V., Paulus, W., Schnitzler, A., & Pollok, B. (2013). The effect of 10 Hz transcranial alternating current stimulation (tACS) on corticomuscular coherence. *Frontiers in Human Neuroscience*, *7*(August), 1–10. https://doi.org/10.3389/fnhum.2013.00511

Ward, L. M. (2009). Physics of neural synchronisation mediated by stochastic resonance. *Contemporary Physics*, *50*(5), 563–574. https://doi.org/10.1080/00107510902879246

Warren, P. A., & Rushton, S. K. (2009). Optic flow processing for the assessment of object movement during ego movement. *Current Biology*, *19*(18), 1555–1560. https://doi.org/10.1016/j.cub.2009.07.057

Wobbrock, J., Findlater, L., Gergle, D., & Higgins, J. (2011). The aligned rank transform for nonparametric factorial analyses using only ANOVA procedures. In *Proceedings of the SIGCHI Conference on Human Factors in Computing Systems* (pp. 143–146). Vancouver, BC, Canada: ACM. https://doi.org/10.1145/1978942.1978963

Zaehle, T., Rach, S., & Herrmann, C. S. (2010). Transcranial alternating current stimulation enhances individual alpha activity in human EEG. *PLoS ONE*, *5*(11), e13766. https://doi.org/10.1371/journal.pone.0013766

Zaehle, T., Sandmann, P., Thorne, J. D., Jäncke, L., & Herrmann, C. S. (2011). Transcranial direct current stimulation of the prefrontal cortex modulates working memory performance: combined behavioural and electrophysiological evidence. *BMC Neuroscience*, *12*(1), 2. https://doi.org/10.1186/1471-2202-12-2

Zalar, B., Martin, T., & Kavcic, V. (2015). Cortical con figuration by stimulus onset

visual evoked potentials (SO-VEPs) predicts performance on a motion direction discrimination task. *International Journal of Psychophysiology*, *96*(3), 125–133. https://doi.org/10.1016/j.ijpsycho.2015.04.004

Zama, T., & Kitajo, K. (2019). EEG recording during online modulation of brain activity by transcranial random noise stimulation. *Brain Stimulation*, *12*(2), 490–491. https://doi.org/10.1016/j.brs.2018.12.604

Zeng, F. G., Fu, Q. J., & Morse, R. (2000). Human hearing enhanced by noise. *Brain Research*, *869*(1–2), 251–255. https://doi.org/10.1016/S0006-8993(00)02475-6

Zito, G. A., Senti, T., Cazzoli, D., Müri, R. M., Mosimann, U. P., Nyffeler, T., & Nef, T. (2015). Cathodal HD-tDCS on the right V5 improves motion perception in humans. *Frontiers in Behavioral Neuroscience*, *9*(September), 257. https://doi.org/10.3389/fnbeh.2015.00257